Sorting into Exposure: Inequality and Welfare Effects of Urban Fracking in Dynamic Equilibrium*

Kyung Tae Cho†

November 3, 2026

Abstract

Urban fracking creates a local environmental disamenity, but its welfare consequences ultimately depend on how residents sort across neighborhoods, how rents and neighborhood composition adjust, and how residents value those changes over time. I study these forces in Tarrant County, Texas, using a dynamic residential sorting equilibrium model. Fracking restrictions reduce environmental exposure but generate heterogeneous welfare effects across demographic groups through equilibrium adjustments in rents and neighborhood composition and changes in expected future neighborhood values. A targeted ban in neighborhoods with high concentrations of poor Hispanic residents raises rents and induces poor Hispanic residents to move out, thereby leaving the policy's intended beneficiaries worse off. Tightening well-entry along the profitability margin benefits every demographic group in a myopic residential sorting model but makes some minority groups worse off when residents are forward-looking. Methodologically, I develop tractable procedures for estimating dynamic residential sorting and solving equilibrium counterfactuals using only aggregate location shares and moving probabilities, both commonly available in conventional census data.

Keywords: Urban Fracking, Residential Sorting, Environmental Justice, Dynamic Discrete Choice Model

*I am deeply indebted to my advisor, Steve Puller, for his help and support. This project also greatly benefitted from the constructive feedback and assistance of Anna Ziff, Fernando Luco, Ben Klopack, Eric Lewis, Emily Cook, and participants of 2026 MEG Annual Meeting, 2025 SEA Annual Meeting, CU Environmental Economics Workshop, and PLIO conferences at Texas A&M University. All errors are my own.

†Ph.D. Student, Department of Economics, Texas A&M University. *email: ktcho0622@tamu.edu*

1 Introduction

Advances in horizontal drilling and hydraulic fracturing have brought oil and gas extraction into suburban and urban neighborhoods, placing wells in close proximity to large and demographically diverse populations. Because many of the environmental and health risks associated with shale gas development are concentrated near well sites, this expansion raises both welfare and distributional concerns (Adgate, Goldstein, & McKenzie, 2014; Clough, 2018). Even if households view nearby wells as a disamenity, however, the welfare consequences of urban fracking and its distributional implications are not obvious. A well that makes a neighborhood less desirable can reduce local housing demand and, in turn, housing costs (Balthrop & Hawley, 2017). Lower housing costs therefore provide a compensating benefit whose value can differ across households. Those with a high willingness to pay to avoid well exposure may remain worse off, while others may value the housing cost reduction enough to offset the environmental loss. Indeed, households can sort into more polluted neighborhoods even when they dislike pollution if their willingness to pay to avoid it is sufficiently low (Depro, Timmins, & O'Neil, 2015). The central puzzle is therefore whether the same environmental disamenity can reduce welfare for some demographic groups while increasing it for others once the housing market adjusts.

Answering this question requires more than measuring the capitalization of well exposure into housing costs. When households relocate, they change demand across neighborhoods and reshape neighborhood composition, which can in turn affect subsequent residential choices when households exhibit socio-demographic homophily (Bayer, Ferreira, & McMillan, 2007). These equilibrium responses can also evolve over time. With moving costs, choosing a neighborhood today affects the costs of relocating tomorrow, so households evaluate current locations partly through their expectations about future neighborhood conditions (Bayer, McMillan, Murphy, & Timmins, 2016). A well can therefore affect welfare through its direct environmental cost, the equilibrium response of housing costs and neighborhood composition, and the future neighborhood values households expect when making location choices. Evaluating who gains and loses from urban fracking and from policies that regulate it therefore calls for a dynamic equilibrium model of residential sorting.

I study this question in Tarrant County, Texas, where the Barnett Shale boom brought shale gas development into densely populated suburban and urban neighborhoods (Fry, 2013; Fry,

Brannstrom, & Sakinejad, 2017). There are more than 4,000 wells[1] in this urban county of roughly two million residents, where drilling is widespread and extends even into densely populated urban areas. Using aggregate census data and well-level records from the Railroad Commission of Texas, I first document how neighborhood characteristics, such as median rent and racial and ethnic composition, evolve in the years around a tract's first exposure to a shale gas well within one mile of its population-weighted centroid. I find that after first exposure, median rent and the White share are lower, the Hispanic share is higher, and the Black share changes little relative to the pre-exposure baseline. These descriptive patterns are consistent with differential residential sorting across groups and adjustments in housing costs around nearby well development. The decline in the White share and the increase in the Hispanic share appear among both poor and non-poor households but are much more pronounced among non-poor residents, indicating that the relevant heterogeneity may run along income as well as race and ethnicity. Together, these facts motivate a structural analysis of how the housing market responds in equilibrium to urban shale gas development.

To evaluate the welfare consequences of these adjustments, I estimate a dynamic residential sorting equilibrium model for demographic groups defined by race, ethnicity, and poverty status. Households choose among neighborhoods based on housing costs, well exposure, racial composition, and other local characteristics, while housing costs and neighborhood composition adjust endogenously as households re-sort across locations. Moving costs make these choices forward-looking: a household's destination today becomes its origin tomorrow, so households evaluate current locations partly through their expectations about future neighborhood values. The estimates reveal substantial heterogeneity in households' aversion to nearby wells. At the aggregate racial level, White households exhibit the strongest aversion, while within each racial and ethnic group, non-poor households are consistently more averse to well exposure than poor households.

Building on the model estimates, I first consider a broad counterfactual that bans all wells located within Fort Worth to characterize the overall welfare consequences of urban fracking.[2] The welfare effects divide sharply along both racial and economic lines: White households and poor

[1] According to records from the Railroad Commission of Texas, I identify 4,052 horizontal gas wells with exact surface coordinates and validated well-completion dates.

[2] This counterfactual is also motivated by actual attempts to restrict urban drilling. In 2014, the neighboring city of Denton passed a voter-initiated ban on hydraulic fracturing, which the Texas legislature preempted the following year through House Bill 40. Fort Worth is the largest city in Tarrant County and concentrates a substantial share of the county's urban wells, making a city-wide restriction both quantitatively meaningful and administratively coherent as a unit of policy.

Black and Hispanic households gain from the ban, while non-poor Hispanic households lose and non-poor Black households experience little net welfare change. Decomposing these effects helps explain why the same reduction in well exposure can generate different welfare consequences across groups. Ceteris paribus, reduced well exposure raises contemporaneous utility for every group. The ban, however, also changes equilibrium rents and neighborhood composition and, because households are forward-looking, their expectations about how these outcomes evolve in future equilibria. For non-poor Black and Hispanic households, the expected future equilibrium changes induced by the ban are less favorable from their perspective, offsetting part of the contemporaneous gain from reduced well exposure. For non-poor Hispanic households, this adverse effect is large enough to reverse the sign of the overall welfare effect.

Next, motivated by environmental justice concerns about disadvantaged communities (Banzhaf, Ma, & Timmins, 2019), I examine whether targeted environmental improvements necessarily benefit their intended residents by banning wells within one mile of census tracts with the highest concentrations of poor Hispanic residents. The policy raises rents in most targeted neighborhoods and induces substantial residential re-sorting, with poor households of all three racial and ethnic groups moving out while non-poor households move in. Poor Hispanic residents experience the largest outflow from the targeted neighborhoods and, among those initially living there, lose welfare despite the reduction in well exposure. The counterfactual therefore illustrates how an environmental improvement targeted at disadvantaged neighborhoods can alter housing costs and neighborhood composition in ways that undermine its intended distributional benefits, consistent with broader concerns about environmental gentrification (Borsky, Fesselmeyer, & Vogelsang, 2024).

Granted, one would expect the first two counterfactuals to impose direct losses on well operators, since they prevent wells regardless of their value. The final counterfactual takes operator profits into account. In fact, more than half of the wells in my sample fail to recover their drilling and operating costs as of 2021.[3] Evaluated ex post, preventing these wells would have spared residents the environmental disamenity and operators their realized losses. Instruments that raise the cost

[3]This does not necessarily imply the irrationality of the well operators. Uncertainty about future market conditions and geological productivity can generate a gap between expected and realized profitability. Learning about subsurface geological quality is an important feature of shale drilling decisions (Agerton, 2020). Contractual incentives embedded in mineral leases can also affect drilling decisions (Herrnstadt, Kellogg, & Lewis, 2024).

of entry, such as removing production tax preferences[4] or imposing fees per well,[5] operate on this margin by deterring the wells with the lowest expected profitability first. I therefore progressively remove under-performing wells, beginning with those generating the largest realized losses, as an approximation to a progressively tighter entry policy,[6] and compare the dynamic model with a separately estimated myopic sorting model. In the myopic model, every group gains and the policy is, ex post, a Pareto improvement among operators and all residents. In the dynamic model, non-poor Black and Hispanic households lose because the expected future equilibrium changes induced by the policy outweigh the contemporaneous benefit of reduced well exposure. Even a policy with no direct losers, and one that targets industry rather than residents, thus creates losers among residents once they are forward-looking.

Methodologically, the paper develops two tools that make this analysis feasible with aggregate data and a high-dimensional state space. First, I estimate dynamic residential sorting using only aggregate location shares and aggregate non-mover rates, obtained from conventional census data. Because these inputs are publicly available for essentially every US neighborhood and from the censuses of many other countries, the method can be applied by any researcher to a wide range of settings. Building on the aggregate-share inversion in Depro, Timmins, and O'Neil (2015) and the choice-specific-value approach of Bayer et al. (2016), I recover choice-specific values and moving costs without observing household-level migration histories and use their estimated transition to recover flow-utility parameters. This avoids solving the dynamic program over the full state space during estimation.

Second, I develop a tractable procedure for dynamic equilibrium counterfactuals. Recent studies of dynamic residential sorting, such as Almagro and Domínguez-Iino (2025) and Davis, Gregory, Hartley, and Tan (2021), estimate preferences with conditional-choice-probability (CCP) methods (Hotz & Miller, 1993; Arcidiacono & Miller, 2011) and their variants, which reduce the need to specify how the full state space evolves during estimation. Counterfactual analysis, however, still requires a rule for how households form expectations when a policy changes endogenous neighbor-

[4]Texas grants a reduced production tax rate to qualifying high cost gas wells, including Barnett Shale wells, under Section 201.057 of the Texas Tax Code. Thomas, Collins, Etienne, and Mugabe (2024) discuss how state tax policies affect extraction incentives.

[5]Pennsylvania's impact fee under Act 13 is an example. Black, McCoy, and Weber (2018) find that it significantly reduced acreage leased for shale development.

[6]Section 8.4 discusses the connection between expected and realized profitability.

hood outcomes such as rents and demographic composition. My approach provides such a rule by carrying the estimated transition of choice-specific values into the counterfactual. Rather than conducting conventional value function iteration over the full state space (Rust, 1987), I solve directly for the fixed point in the vector of counterfactual choice-specific values. The key restriction is that the estimated parameters governing the transition of choice-specific values are invariant to the policy, while the expected future values themselves adjust as counterfactual rents and neighborhood composition change. This provides a tractable way to update households' expectations while solving for the new equilibrium.

This paper contributes to three literatures. First, I contribute to the literature on the local consequences of unconventional oil and gas development. Existing work has established that fracking affects nearby housing values (Balthrop & Hawley, 2017; Muehlenbachs, Spiller, & Timmins, 2015), reshapes local labor markets (Bartik, Currie, Greenstone, & Knittel, 2019; Maniloff & Mastromonaco, 2017; Black, Boslett, Hill, Ma, & McCoy, 2021; Feyrer, Mansur, & Sacerdote, 2017), and carries health risks concentrated close to well sites (Adgate et al., 2014; McKenzie, Witter, Newman, & Adgate, 2012; Hays, McCawley, & Shonkoff, 2017). I build on this literature by asking how heterogeneous urban residents value these localized disamenities and how residential sorting in response to them reshapes rents and neighborhood composition. This shifts the focus from the local price or health effects of a well to its welfare consequences and how those consequences are distributed across demographic groups.

The second is a growing literature of environmental justice, which documents that minority and low-income households disproportionately bear environmental burdens (Banzhaf et al., 2019; Cain, Hernandez Cortes, Timmins, & Weber, 2024), including proximity to fracking (Zwickl, 2019; Timmins & Vissing, 2022). A recurring theme is that residential mobility itself shapes the observed correlation between race, income, and exposure (Depro, Timmins, & O'Neil, 2015; Christensen & Timmins, 2022), and that place-based interventions can redistribute welfare in unintended ways. Heat-mitigation policy can leave poorer and minority households worse off (Borsky et al., 2024), and public housing demolition raised welfare of White households while lowering that of low-income minority households (Almagro, Chyn, & Stuart, 2023). My findings add to this theme: the distributional consequences of well removal is itself an equilibrium outcome, so interventions meant to help minority neighborhoods can leave their intended beneficiaries worse off.

Third, I contribute to the literature on dynamic discrete choice and residential sorting. Existing dynamic residential sorting models, including Bayer et al. (2016); Almagro and Domínguez-Iino (2025); Davis et al. (2021), use individual-level residential histories to study forward-looking location choices. Heblich, Trew, and Zylberberg (2020) also estimate dynamic residential sorting using aggregate data, modeling moving frictions through an exogenous relocation-opportunity shock. In my framework, moving frictions instead take the form of moving costs, with the decision to relocate arising endogenously from households' location choices in each period. I also provide a tractable procedure for carrying the estimated dynamic model into equilibrium counterfactuals in which rents, neighborhood composition, and households' expectations adjust endogenously.

The rest of the paper is organized as follows. Section 2 provides institutional background on urban fracking in Tarrant County, and Section 3 describes the data. Section 4 presents the descriptive evidence that motivates the structural analysis. Section 5 introduces the dynamic residential sorting equilibrium model, and Section 6 describes its estimation using aggregate census data. Section 7 presents the model estimates and discusses their implications. Section 8 develops the counterfactual equilibrium procedure and applies it to three policy exercises. Section 9 concludes.

2 Background on Urban Fracking in Tarrant County

While the paper centers on fracking, the framework applies more broadly to settings in which a new neighborhood disamenity enters an urban housing market, altering the trade-offs residents face between housing costs and local characteristics. Tarrant County, Texas, provides a particularly useful setting for studying these forces. Horizontal drilling brought a highly localized environmental disamenity into an already developed and demographically heterogeneous urban area, with wells appearing near homes, schools, parks, and other developed land. Because drilling expanded gradually over time, residents choosing where to live faced not only current well exposure but also changes in future neighborhood conditions. The setting therefore allows me to study how residents sort in response to a localized environmental change and how those responses affect rents, neighborhood composition, and welfare when residents are forward-looking.

The institutional setting also helps clarify several assumptions used in the analysis. I treat nearby wells as a tract-level environmental disamenity rather than as a source of compensating

income to nearby residents. This interpretation does not require drilling to have no economic benefits. Instead, it requires that mineral payments and drilling employment provide little reason for a resident to choose a particular tract because it is close to a well. Residents also have limited control over whether nearby minerals are developed, while residential construction can continue around existing wells and additional wells can later be added to the same pad. Finally, subsurface variation in the Barnett Shale affects the cost of drilling without directly changing the surface characteristics over which residents sort. The remainder of this section summarizes these features. Appendix E provides the institutional details and supporting evidence.

Urban drilling and local environmental disamenities. Horizontal drilling and hydraulic fracturing sharply reduced the surface footprint required to extract natural gas. A single well pad can reach a wide subsurface area, allowing gas beneath developed neighborhoods to be extracted without the dense grid of surface wells required by conventional vertical drilling. Tarrant County, home to more than two million residents and forming a major part of the Dallas–Fort Worth metropolitan area, sits atop the Barnett Shale, one of the major shale-gas fields developed during the U.S. shale boom. More than 4,000 horizontal gas wells were drilled across the county, including in densely developed neighborhoods near homes, schools, parks, and other urban land uses. Nearly one million residents lived within half a mile of oil and gas activity, illustrating how extensively drilling became embedded in the urban landscape.

This proximity also made the environmental and quality-of-life effects of drilling salient to nearby residents. Previous studies document concerns associated with air pollution, noise, induced seismicity, and risks to groundwater, many of which are concentrated near well sites (Adgate et al., 2014; Hays et al., 2017; Black et al., 2021). These concerns were also visible in local political activities. Residents and community organizations repeatedly sought tighter restrictions on urban drilling, including campaigns against new well permits in Arlington and efforts to strengthen Fort Worth's gas-well ordinance, and the neighboring city of Denton went further and adopted a voter-initiated fracking ban in 2014 before the state legislature preempted it the following year.[7] Taken together, the localized nature of these effects and the public response to them support treating nearby well exposure as a neighborhood disamenity over which residents may sort.

[7]Section 8.2 discusses these local efforts in the context of a counterfactual analysis on a city-wide fracking ban.

Mineral income and employment. A potential concern with interpreting residential responses to nearby drilling as responses to an environmental disamenity is that drilling can also generate income. In Tarrant County, however, the main economic benefits of drilling are unlikely to create meaningful residential demand for proximity to an individual well. Mineral payments accrue to mineral owners rather than automatically to the residents living near a surface well. Mineral rights may be severed from surface ownership, renters do not receive mineral rights through their tenancy, and the small residential parcels typical of an urban area imply small fractional interests for many owners. Moreover, royalty payments depend on ownership of the minerals being produced rather than simply on residence near the surface location of a well.[8]

A second potential channel is local labor demand. Existing studies find that shale development can raise employment and income enough to affect migration, particularly at the county or regional level (Bartik et al., 2019; Feyrer et al., 2017). These effects, however, do not necessarily create demand for residential proximity to an individual well. Employment is concentrated in the labor-intensive drilling and completion phase, which typically lasts only a few weeks per well, whereas a producing well can operate for decades with relatively little continuing labor.[9] The employment channel therefore operates at a broader geographic scale than the census-tract-level residential proximity to individual wells studied here.

This distinction is especially relevant in Tarrant County, which is part of the large and diversified Dallas–Fort Worth labor market. In the 2021 American Community Survey, agriculture, forestry, fishing, hunting, and mining together employed only 5,793 of Tarrant County's 1,061,812 civilian workers, or about 0.5 percent.[10] Even substantial employment effects from shale development at the regional level would therefore provide little reason for a resident to choose one Tarrant County tract over another because of its proximity to a well. Together with the limited connection between residential location and mineral income described above, these facts support interpreting nearby well exposure primarily as a tract-level environmental disamenity rather than as a source

[8]The supporting evidence is reported in Appendix E.2. In the Tarrant Appraisal District mineral roll, royalty interests are generally small, and a substantial share of nearby residents either rent or do not hold the relevant mineral interest. The appendix also compares Tarrant County with Midland County, where mineral ownership plays a much larger economic role.

[9]Completion of a shale well, including hydraulic fracturing, typically takes one to five weeks. Once a well enters production, lease operators monitor multiple wells along a route rather than remaining at a single site.

[10]The ACS category is broader than oil and gas extraction and includes agriculture, forestry, fishing, and hunting. The 0.5 percent figure therefore provides an upper bound on the employment share attributable to mining, including oil and gas extraction. Source: U.S. Census Bureau, 2021 American Community Survey.

of compensating income tied to residential location.

Well placement and residential development. Residents also have limited direct control over whether nearby drilling occurs. Texas law gives the mineral estate substantial authority to develop subsurface resources, so objection by an individual surface owner does not by itself prevent a mineral lessee from developing the minerals. An individual mineral owner who refuses to lease likewise need not be able to prevent development of the surrounding unit. State and municipal rules regulate where and how drilling can occur, but they did not exclude drilling from developed urban areas during the period studied here. Appendix E.3 describes the relevant state permitting rules, mineral-estate law, pooling provisions, and municipal drilling ordinances.

Regulation was also asymmetric between new wells and new housing near existing wells. Municipal rules generally require larger setbacks when a new well was drilled near an existing protected use than when new housing was subsequently built near an existing well.[11] Residential development therefore continued around established well sites during the Barnett boom (Fry et al., 2017). This feature matters for the analysis in two ways. First, the presence of a well did not mechanically remove nearby housing from the residential choice set or prevent housing supply from adjusting. Second, operators could add wells to an existing pad after nearby housing had been developed. Residents could therefore choose where to live, but they did not directly choose the path of future drilling around that location. This provides an institutional basis for treating well exposure as a neighborhood characteristic over which residents sort and for allowing future neighborhood values to matter when residents are forward-looking.

Geology and drilling costs. The Barnett Shale also provides useful variation in the cost of drilling. Subsurface characteristics vary across Tarrant County and affect the cost and productivity of reaching the formation, even across neighborhoods within the same urban housing market. These geological characteristics are distinct from the surface amenities that residents observe when choosing where to live. I use this variation later in the estimation to isolate changes in well exposure that arise from the cost side of drilling rather than from residential demand or other surface

[11] For example, Fort Worth require a new well to be at least 600 feet from a protected use, while a new habitable structure can be built 200 feet from an existing wellbore, and as close as 125 feet from a permitted multi-well pad site on lots platted before 2009. Arlington similarly require a 600-foot setback for new wells but only 300 feet for new residential development near an existing well.

neighborhood characteristics. Section 3 describes the geological measures, and Section **??** explains how they enter the empirical strategy.

The evolution of drilling. Drilling in Tarrant County spanned more than a decade and followed a pronounced boom-and-bust cycle. Figure 1 summarizes the scale and timing of the Barnett boom together with the economic conditions facing well operators. Completions rose from only a handful of wells in the early 2000s to nearly 800 in 2008 and remained high for several years before falling sharply after 2012. Natural gas prices also rose sharply during the boom before falling after 2008, while drilling costs increased and remained elevated.

The boom also left behind a large number of wells that did not recover their drilling and operation costs. Natural gas prices fell sharply after 2008 while drilling costs remained elevated, and the average operator value of later completion cohorts fell to around zero or below. Among the 4,014 wells for which I construct operator value, 63 percent did not recover their drilling costs through 2021.[12] Wells that failed to recover their drilling costs therefore constituted a substantial share of drilling in the county. Section 8.4 examines the welfare effects of deterring these wells.

3 Data

The empirical strategy requires three things: neighborhood-level demographic composition observed repeatedly over the boom, a measure of each neighborhood's exposure to drilling, and variation in drilling costs that is unrelated to residential amenities. Publicly available census data provide the first, well records from the state regulator provide the second, and the geology of the Barnett Shale provides the third. This section describes these sources, along with two datasets I construct for the counterfactual analysis: an operator-level valuation of every well and a corpus of digitized mineral leases. Appendix F provides construction details.

3.1 Neighborhood Panel

Census data. Neighborhood demographics and housing characteristics come from the 2000 Decennial Census and the 2005–2009, 2012–2016, and 2018–2022 five-year American Community Sur-

[12] Operator value is the discounted value of observed production net of drilling and operating costs. Section 3.2 describes its construction. Because some wells were still producing at the end of the sample, values measured through 2021 need not equal their eventual lifetime values.

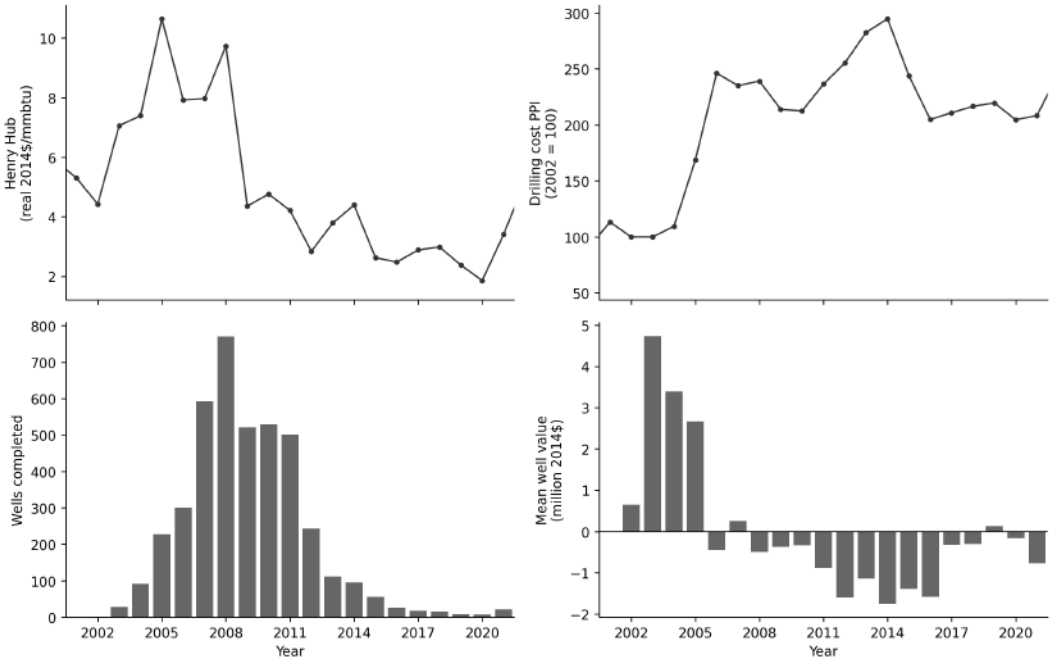


Figure 1: Drilling activity and well economics in Tarrant County, 2001–2021

Notes: Completions are horizontal gas wells in Tarrant County by RRC validated well date. Henry Hub is the annual mean of the monthly spot price, deflated to 2014 dollars using the CPI-U. Drilling cost is the annual mean of the BLS producer price index for drilling oil and gas wells, rebased to 2002. Mean well value is the average operator value among valued wells completed in each year, based on cash flows observed through 2021 and expressed in real 2014 dollars.

vey (ACS), distributed by NHGIS.[13] The four periods bracket the Barnett boom: 2000 predates the first urban horizontal well, 2007 and 2014 span the drilling peak, and 2021 captures the aftermath. I harmonize all periods to 2020 census tract boundaries with the NHGIS geographic crosswalk and keep tracts with complete observations in every period, yielding a balanced panel of 390 tracts. These data supply the two objects the model is estimated on: the population of each of six demographic groups in each tract, formed by interacting race and ethnicity (non-Hispanic White, non-Hispanic Black, and Hispanic) with poverty status, which measures group-specific choice shares; and median gross rent, the equilibrium price. Median rooms, structure year, and owner-occupied units enter as observed tract characteristics. The small tracts of an urban county limit the threat of ecological fallacy at this level of aggregation (Banzhaf et al., 2019).

Wells. Well records come from the Railroad Commission of Texas (RRC), which reports the permit date and surface coordinates of each wellbore: 6,055 horizontal wells in Tarrant County, of

[13] One-year ACS estimates are available only at the county level. I use the five-year releases and treat the 2005–2009 sample as representing 2007, the 2012–2016 sample as 2014, and the 2018–2022 sample as 2021.

which 5,391 are gas wells. The amenity of interest counts, for each tract and period, the horizontal gas wells permitted before that period and located within one mile of the tract's population-weighted centroid.[14]

Geology. Cost variation comes from the geology of the shale itself. Montgomery, Jarvie, Bowker, and Pollastro (2005) and Pollastro, Jarvie, Hill, and Adams (2007) survey the depth, thickness, and thermal maturity of the Barnett formation, measured independently of drilling activity in the area; I georeference their isopach maps, interpolate them, and average each characteristic within tract boundaries (Appendix F.1). Depth is the instrument-relevant variable: it ranges from 6,149 to 8,317 feet across the county, and deeper shale raises drilling cost without directly affecting life above ground. Thickness and thermal maturity display little economically meaningful variation and are not used.

Other neighborhood characteristics. Violent crime rates come from the annual *Crime in Texas* reports of the Texas Department of Public Safety, the state's Uniform Crime Reporting program. I sum the four violent index offenses (murder, rape, robbery, and aggravated assault) per 100,000 residents at the city-level, the finest geography reported, and assign each tract the rate of the city containing it.[15] Land-use composition comes from zoning data of the North Central Texas Council of Governments, from which I construct the share of tract land in residential, commercial, and industrial use. Both enter as controls in the flow utility.

Table 1 reports summary statistics. Two features of the panel matter for what follows. First, exposure is pervasive rather than concentrated: 46 percent of tract-years have at least one well within a mile, and the average tract-year has five, so drilling is a county-wide urban phenomenon rather than a fringe land use. Second, every demographic group is well represented in the county, with tract-level populations of each group ranging from zero to several thousand; the sorting patterns the model exploits are movements of sizable populations across tracts, not thin cells.

[14] Population-weighted centroids are published by the Census Bureau. Anchoring exposure at the population center rather than the geometric centroid measures proximity to where residents live. A fixed radius is preferred to a within-boundary count because drilling externalities such as truck traffic, noise, and flaring extend past tract lines.

[15] There are 41 cities in Tarrant County; tracts in unincorporated areas receive the rate reported by the Tarrant County Sheriff's Office. Some small affluent cities record no violent index crime at all: Westover Hills, with a population under 700 and its own police department, records zero violent offenses in every sample period.

Table 1: Summary Statistics: Neighborhood Panel

	Mean	Std. Dev.	P10	P90
Census				
Median gross rent (USD)	1,046	394	603	1,588
Median rooms	5.3	1.1	3.9	6.6
Median structure year	1978	16	1956	1998
Owner-occupied units	873	512	208	1,581
Total population	3,813	1,443	2,052	5,711
White	2,054	1,331	353	3,900
Black	629	704	32	1,619
Hispanic	1,129	998	217	2,520
White, poor	149	134	24	304
White, non-poor	1,869	1,282	263	3,683
Black, poor	129	211	0	393
Black, non-poor	500	563	25	1,307
Hispanic, poor	220	307	0	634
Hispanic, non-poor	900	767	193	1,931
Wells				
Wells within 1 mile	5.0	8.1	0	16
Any well within 1 mile	0.46	0.50	0	1
Geology				
Shale depth (ft)	7,259	450	6,639	7,788
Shale thickness (ft)	347	56	284	428
Thermal maturity (Ro)	1.46	0.18	1.23	1.74
Other				
Violent crime rate	483	193	179	707
Residential land share	0.39	0.17	0.13	0.60
Commercial land share	0.05	0.06	0.00	0.13
Industrial land share	0.04	0.07	0.00	0.12

Notes: N = 1,560 (390 tracts × 4 periods: 2000, 2007, 2014, 2021). P10 and P90 are the 10th and 90th percentiles. Poverty status is determined for a subset of the population that excludes the institutionalized and those in group quarters, so the poor and non-poor counts may not sum exactly to group totals. "Wells within 1 mile" is the number of horizontal gas wells permitted before the period and located within one mile of the tract's population-weighted centroid; "Any well within 1 mile" is an indicator for a positive count. Poor and non-poor refer to population below and above the federal poverty line. Population counts are non-integer in the underlying data because harmonization to 2020 tract boundaries interpolates across boundary changes; the table reports rounded values while the analysis uses unrounded ones. The violent crime rate is the sum of murder, rape, robbery, and aggravated assault offenses per 100,000 residents of the city containing the tract.

3.2 Operator Value of Wells

Following Gülen, Browning, Ikonnikova, and Tinker (2013), I compute each well's discounted profit, net of fixed drilling cost, from its observed production, using the valuation methods standard in petroleum engineering and the cost and price assumptions specific to Barnett Shale wells . Of the 5,147 horizontal gas wells with surface locations, 4,014 are valued; 63 percent fail to recover their costs by this measure. Appendix F.2 details the construction and reports the distribution of well values.

Royalties are paid at realized rather than assumed rates, which I recover from the lease contracts themselves. Mineral leases in Tarrant County are recorded with the county clerk, and the *New York Times* digitized 84,250 of these documents in the course of its reporting on the Barnett Shale[16]. I process the full corpus with optical character recognition, obtaining a royalty rate for 83 percent of documents, and assign leases to census tracts to form tract-level mean realized rates; each wellbore's royalty rate is then the average over the tracts its lateral crosses.[17] Appendix F.3 reports extraction details.

4 Stylized Facts

This section documents how the demographic composition and median rent of a census tract evolve after the tract is first exposed to nearby shale gas development. Two facts emerge. First, in exposed tracts the white population share falls steadily while the Hispanic share rises, and median rent declines. Second, these compositional shifts are concentrated among non-poor households: the non-poor white share falls, and it is the non-poor Hispanic share, not the poor Hispanic share, that rises most. Together, these two facts motivate a sorting model with preferences over well proximity that are heterogeneous across both race and poverty status.

The welfare consequences of shale gas development depend on the joint behavior of composition and rent. New shale gas development can add up to a local disamenity, but its welfare cost to any resident is mitigated if housing costs adjust downward in equilibrium. If willingness to pay to avoid

[16]Timmins and Vissing (2022) use the same raw data to analyze the environmental justice in mineral lease negotiation process.

[17]Lease documents record royalty terms but not signing bonuses, which by convention are negotiated outside the recorded memorandum. Timmins and Vissing (2022) face the same limitation.

well proximity differs across groups, the equilibrium rent decline overcompensates some groups and undercompensates others, and the demographic composition of exposed tracts shifts toward the groups with the weakest aversion. If residents additionally hold preferences over the racial and ethnic composition of their neighborhood, this compositional change is itself welfare relevant, since the induced change in neighbors changes the value of a location even for households that never move. The descriptive exercise below is designed to detect these compositional and price responses in the raw data before imposing the structure of the model.[18]

I describe how outcomes evolve around a tract's first exposure with a specification that takes the similar form of an event study. For an outcome Y_{jt}, I estimate

$$Y_{jt} = \alpha + \sum_{k \in \{-2,-1,0,1,2\}} \beta_k D_{jk} + X_{jt}\beta_X + \phi_c + \phi_t + \epsilon_{jt}, \tag{1}$$

where D_{jk} is a dummy equal to one if period t is k periods from the first period in which any well is present within one mile of tract j's population-weighted centroid, and zero otherwise.[19] The terms ϕ_c and ϕ_t are city and time fixed effects.[20] X_{jt} contains the controls that enter the flow utility of the structural model: the commercial and residential land-use shares, the median number of rooms, the median year of structure construction, the count of owner-occupied housing units, and the violent crime rate. The tract poverty rate is excluded from X_{jt} because the subgroup outcomes below partition the population by poverty status, so conditioning on the aggregate poverty rate would condition on a variable mechanically related to those outcomes. I estimate equation 1 separately for each outcome and cluster standard errors at the tract-level. The 72 tracts that never record a positive one-mile well count serve as the comparison group.

[18]The facts of interest are comparisons across groups rather than levels. The same specification, sample, and exposure definition underlie every outcome, so a confounder that affects exposed tracts without favoring particular groups shifts the estimated paths together and leaves the cross-group ordering intact. Generating the ordering spuriously would require selection correlated with the future settlement of specific subgroups, which the conditioning exercises reported below weigh against. The model takes from these contrasts only their qualitative content, with magnitudes estimated within the structural framework.

[19]Dating exposure by the population-weighted one-mile radius, rather than by the first well drilled within the tract's own boundary, keeps the definition of exposure in this section identical to the one-mile well count used as the measure of exposure throughout the paper. A tract can therefore be exposed before any well is drilled inside its own boundary, if a well in a neighboring tract falls within one mile of the population-weighted centroid.

[20]Establishing a causal effect in an event study or difference-in-differences framework would ordinarily call for census tract fixed effects, which absorb time-invariant differences across tracts. With four periods and exposure concentrated in two cohorts, tract fixed effects absorb most of the variation in the outcomes, and the purpose of this exercise is descriptive rather than causal.

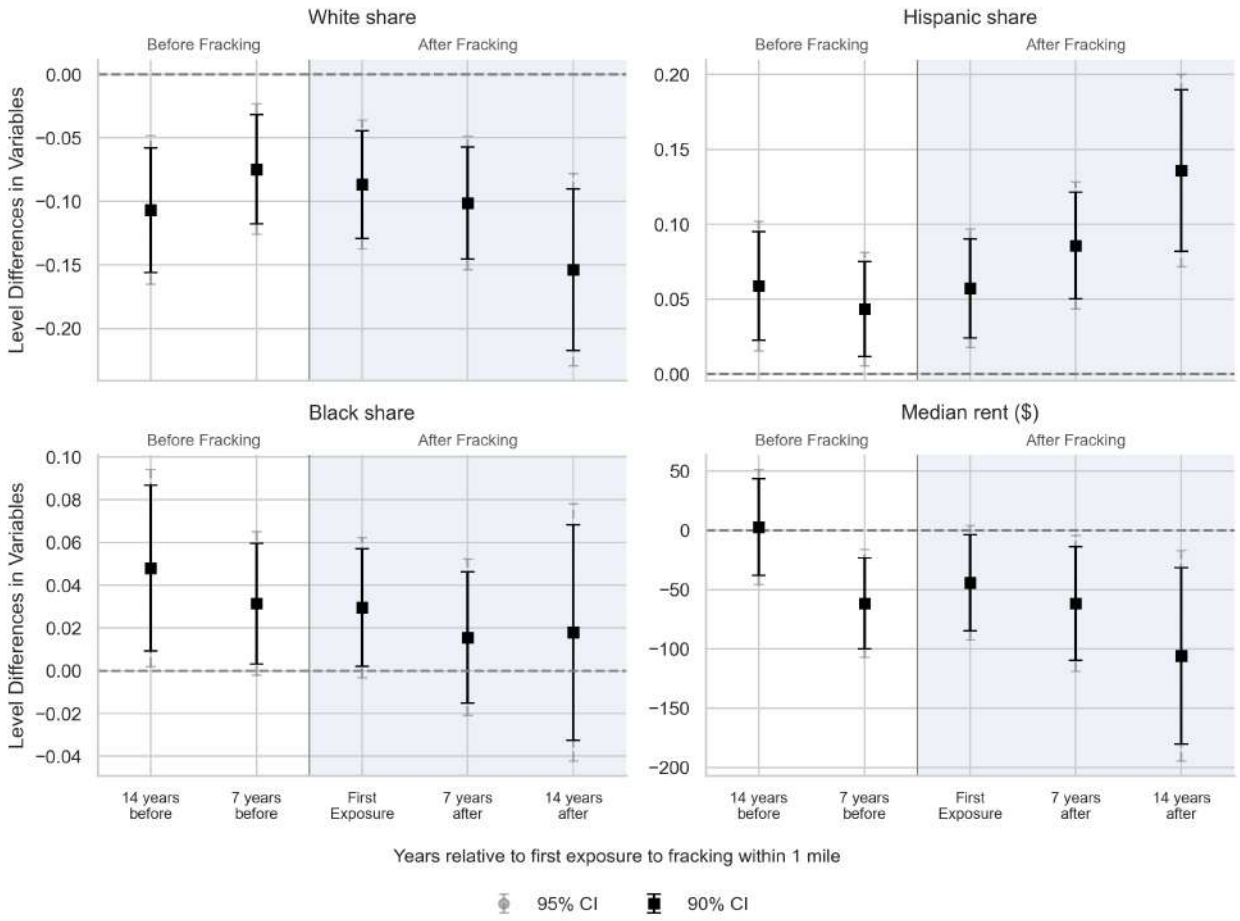


Figure 2: Population shares and median rent around first well exposure

Notes: Each panel plots the coefficients $\hat{\beta}_k$ from equation 1 for the outcome named in the panel title. All regressions include city and year fixed effects and the control set described in the text. Standard errors are clustered at the tract-level; black bars show 90 percent and gray dashed bars 95 percent confidence intervals. The $k = -2$ coefficient is identified from the 2014 exposure cohort and the $k = 2$ coefficient from the 2007 cohort.

The white share of exposed tracts declines steadily after first exposure, and the Hispanic share rises. Figure 2 shows the white share falling to 15.4 percentage points below the reference-period gap by $k = 2$ and the Hispanic share rising by 13.6 percentage points at the same horizon. The Black share shows no movement at any horizon, and median rent falls after exposure, with the gap reaching roughly 106 dollars by $k = 2$.[21]

The aggregate shifts come almost entirely from non-poor households. Figure 3 repeats the exercise for the six race-by-poverty population shares, poor and non-poor white, Black, and Hispanic

[21]The Hispanic share increase is the most robust of these paths: it survives tract fixed effects, growing to 5.7 percentage points at $k = 2$, whereas tract fixed effects attenuate the white share decline and reverse the sign of the rent path, indicating that part of those patterns reflects persistent level differences between exposed and unexposed tracts.

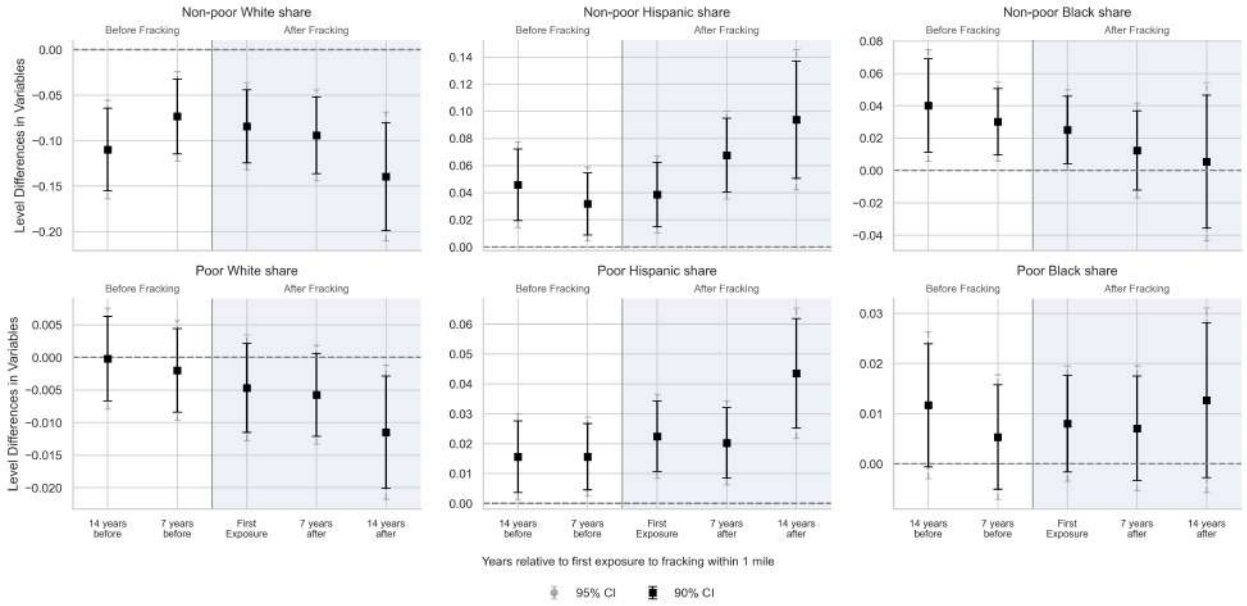


Figure 3: Race-by-poverty population shares around first well exposure

Notes: Each panel plots the coefficients $\hat{\beta}_k$ from equation 1 for the population share of the subgroup named in the panel title, with $k = -1$ as the omitted reference period. The specification, control set, fixed effects, clustering, and confidence interval conventions are identical to Figure 2. Subgroup shares use total tract population as the denominator.

residents, using the identical specification and control set. The white share decline is concentrated among non-poor white residents, whose share falls by 13.9 percentage points at $k = 2$, against 1.1 percentage points for poor white residents. The non-poor Hispanic share rises by 9.4 percentage points at $k = 2$, more than twice the increase for poor Hispanic households, and neither Black subgroup responds at any horizon.[22]

These paths are descriptive rather than causal. Wells were not randomly sited, the pre-period coefficients are not zero, and the outcomes are population shares that capture net compositional change rather than migration flows.[23]

In fact, identifying causal effect of well exposure is in any case untenable using a conventional quasi-experimental design in this setting, because well exposure violates the Stable Unit Treatment Value Assumption (SUTVA). In a discrete choice framework, a resident selects the tract that

[22]The ordering of the poor and non-poor Hispanic responses also holds when the comparison group is restricted to not-yet-exposed tracts, and the subgroup coefficients are essentially unchanged by conditioning on the growth of tract housing units or on a composite index of suburban character built from density, lot size, tenure, land use, and centrality.

[23]Exposure timing consists of two cohorts, 83 tracts first exposed in 2007 and 235 in 2014, so the $k = -2$ coefficient is identified solely from the 2014 cohort observed in 2000 and the $k = 2$ coefficient solely from the 2007 cohort observed in 2021.

maximizes lifetime utility, so when a well is drilled in one tract, demand lost from that tract is reallocated across the remaining tracts in the choice set, and equilibrium rent and demographic composition adjust in exposed and unexposed tracts alike.[24] The comparison group is therefore itself affected by nearby well entry. Recovering welfare-consistent counterfactuals requires an explicit equilibrium model of residential sorting.

5 Model

This section develops a dynamic residential sorting equilibrium model of the local housing market. Residents choose among neighborhoods by weighing current housing costs and neighborhood amenities against moving costs and expected future neighborhood values. The demand side builds on Bayer et al. (2016) and Depro, Timmins, and O'Neil (2015). The source of dynamics is the presence of moving costs: because a resident's current destination becomes her origin in the next period, the location chosen today affects the costs of subsequent relocation and therefore carries future consequences.[25] Residents consequently choose locations to maximize expected lifetime utility rather than current-period utility alone, under beliefs about how much neighborhood value will change in the future.

The residents are distinguished by discrete type $g \in \mathcal{G}$. In the main specification, $\mathcal{G}$ consists of six groups defined by the interaction of race and ethnicity (non-Hispanic White, non-Hispanic Black, and Hispanic) with poverty status (poor and non-poor).[26] In each period t, an infinitely lived resident i of type g chooses among J neighborhoods in Tarrant County and an outside option $J+1$. Thus, the choice set is $\mathcal{J} \equiv \{1, ..., J, J+1\}$. The outside option represents leaving the local housing market and is treated as a terminal action for incumbent residents, while new residents may enter Tarrant County from outside the modeled market in subsequent periods.

At the beginning of each period t, type g residents observe the common state, which I denote by

[24] For example, when demand falls in a tract with a well, unexposed tracts are substitutes in equilibrium, so demand there rises and rents adjust upward. Population composition in unexposed tracts is subject to the same equilibrium spillover. I examine these spillovers in detail in the counterfactual analysis.

[25] This form of state dependence induced by moving costs is often described as a "lock-in effect"; see Yeo and Miller (2018) and Shcherbakov (2016) for similar motivation for introducing dynamics into a model.

[26] I treat demographic type as fixed over the model horizon. This means that the model abstracts from transitions between poor and non-poor status. For comparison, I also estimate an aggregate specification with three racial and ethnic groups that does not distinguish residents by poverty status.

$\Omega_{gt} \equiv \{p_t, X_t, \xi_t, sc_{gt}\}$. Here, p_t is the vector of housing costs across neighborhoods,[27] X_t collects well exposure w_t, racial composition r_t, and other observable neighborhood characteristics including median housing characteristics, crime, and land use. ξ_t collects neighborhood amenities that are observed by residents but unobserved by the econometrician, and sc_{gt} denotes the group and time specific moving cost. In addition to Ω_{gt}, resident i enters the period with current location d_{it} and receives location-specific idiosyncratic preference shocks ϵ_{igt}. Thus, the relevant state for a type g resident is given by $(\Omega_{gt}, d_{it}, \epsilon_{igt})$.

Then, resident i's flow utility in group g at time t from choosing location j can be expressed as

$$u_{ijgt} = f(p_{jt}, X_{jt}, \xi_{jt}; \theta_g) - sc_{gt}\mathbb{1}(d_{it} \neq j) + \epsilon_{ijgt} \tag{2}$$

where θ_g denotes group-specific utility parameters and $\mathbb{1}(d_{it} \neq j)$ equals one if resident i moves from her current location to another and zero otherwise. The term $f(p_{jt}, X_{jt}, \xi_{jt}; \theta_g)$ denotes the per-period utility common to all residents in group g. From now on, I drop the subscript g for notational simplicity. For the same purpose, I use $f_j(\Omega_t)$ as shorthand for $f(p_{jt}, X_{jt}, \xi_{jt}; \theta)$ although moving cost sc_t included in Ω_t enters utility separately.

The resident's goal is to maximize her lifetime expected utility by choosing an optimal sequence of locations $j^* = \{j^*_{ir}\}_{r=t}^{\infty}$ that solves

$$j^* \in \arg\max_{\{j_{ir}\}_{r=t}^{\infty}} E\left[\sum_{r=t}^{\infty} \beta^{r-t} u_{ij_{ir}r}(\cdot) \,\middle|\, \Omega_t, d_{it}, \epsilon_{it}\right]. \tag{3}$$

Following Rust (1987), I impose the following standard simplifying assumptions from the dynamic discrete choice literature. First, I assume that the evolution of Ω_t follows a Markov process. Also, I assume that individual-specific idiosyncratic preference shocks follow an i.i.d. Type I extreme value distribution. Finally, I impose the conditional independence assumption that, conditional on Ω_t, the current idiosyncratic preference shocks have no predictive power for the evolution of Ω_{t+1}. Together with the i.i.d. assumption on the preference shocks, this implies that the Markov transition density can be decomposed as

[27] I express housing costs in rental-equivalent terms. For homeowners, this corresponds to treating housing value as the discounted value of the rental services generated by the property, as in Almagro and Domínguez-Iino (2025), and Almagro et al. (2023).

$$\Gamma(\Omega_{t+1}, \epsilon_{t+1}|\Omega_t, \epsilon_t) = \Gamma_\Omega(\Omega_{t+1}|\Omega_t)\Gamma_\epsilon(\epsilon_{t+1}). \tag{4}$$

Given the existence of the optimal decision rule j^* and the Markov structure of the problem, I can express the value function $V(\cdot)$ as the following Bellman equation:

$$V(\Omega_t, d_{it}, \epsilon_{it}) = \max \left\{ \begin{array}{c} \max\limits_{j \in \{1,\ldots,J\}} \left\{ f_j(\Omega_t) - sc_t \mathbb{1}(d_{it} \neq j) + \epsilon_{ijt} + \beta E[EV(j, \Omega_{t+1}) \mid \Omega_t] \right\}, \\ \\ f_{J+1}(\Omega_t) - sc_t \mathbb{1}(d_{it} \neq J+1) + \epsilon_{i,J+1,t} \end{array} \right\}. \tag{5}$$

where $EV(j, \Omega_t) = \int V(\Omega_t, j, \epsilon_{it}) d\Gamma_\epsilon(\epsilon_{it})$ denotes the expected value function. For the terminal outside option, there is no subsequent residential choice within the modeled market. Note that equation 5 nests both staying and moving decisions. If the resident chooses her current location, $j = d_{it}$, she incurs no moving cost. If she chooses another location, she incurs sc_t. Thus, she would move only if the total value from the best alternative location, net of moving cost, exceeds the total value from her current location.

Now, I define choice-specific value function associated with an inside location j as

$$CV_{jt} = f_j(\Omega_t) + \beta E[EV(j, \Omega_{t+1})|\Omega_t]. \tag{6}$$

For the terminal outside option, there is no continuation value. I normalize its per-period utility to zero, so that $CV_{J+1,t} = 0$. Also, following the result from Rust (1987), the expected value function in equation 5 can be expressed as

$$EV(d_{it}, \Omega_t) = \ln \left(exp(CV_{d_{it},t}(\Omega_t)) + \sum_{j \in \mathcal{J} \setminus \{d_{it}\}} exp(CV_{jt}(\Omega_t) - sc_t) \right) + \gamma \tag{7}$$

where γ stands for the Euler constant.

Now, I specify how to specify pairwise moving probability from a location k to location j. Let $d_{it} = k$; resident i is living in location k. The pairwise moving probability is defined as the

probability of j bringing the largest value to resident i as

$$P_{jkt} \equiv Pr(CV_{jt} - sc_t * \mathbb{1}(j \neq k) + \epsilon_{ijt} \geq CV_{lt} - sc_t * \mathbb{1}(l \neq k) + \epsilon_{ilt}, \ \forall l) \tag{8}$$

With i.i.d type 1 extreme value distribution of ϵ_{it}, the probability of resident i currently living at k choosing location j is

$$P_{jkt} = \frac{exp(CV_{jt} - CV_{kt} - sc_t * \mathbb{1}(j \neq k))}{\sum_{l=1}^{J+1} exp(CV_{lt} - CV_{kt} - sc_t * \mathbb{1}(l \neq k)))}, \tag{9}$$

which is the familiar logit formula in the discrete choice model literature[28]. Note that since probability is common across individuals, P_{jkt} can also be interpreted as the share of individuals who decide to move on to j from k. Then, by construction, the share of non-movers in location k is derived as

$$P_{kkt} = \frac{1}{\sum_{l=1}^{J+1} exp(CV_{lt} - CV_{kt} - sc_t * \mathbb{1}(l \neq k)))}. \tag{10}$$

Reintroducing the group-specific subscript g, and letting N_{jgt} denote the number of group g resident at tract j at period t, one can define total residential demand for tract j, N_{jt+1} as

$$N_{jt+1} = \sum_{g \in \mathcal{G}} \sum_{k \in \mathcal{J}} N_{kgt} \times P_{jkgt} \tag{11}$$

where P_{jkgt} is the probability that a group g resident residing at location k in period t chooses tract j for period $t+1$, as defined in equation 9. For $k = J+1$, $N_{J+1,g,t}$ represents the mass of potential entrants from outside the market.

Similar to (Almagro et al., 2023), I close the model by introducing a simple housing supply function $S_{jt+1}(p_{jt})$ with calibrated supply elasticity φ, as

$$S_{jt+1}(p_{jt}) = \lambda_{jt} p_{jt}^{\varphi}. \tag{12}$$

Let λ_{jt} denote a census tract–by–time-specific factor that captures supply-side determinants affecting equilibrium price responses, such as land availability. In practice, supply-side parameters are calibrated using estimates from (Baum-Snow & Han, 2024), which provides housing supply elastic-

[28]Note that $Pr(CV_{jt} - sc_t * \mathbb{1}(j \neq k) + \epsilon_{ijt} \geq CV_{lt} - sc_t * \mathbb{1}(l \neq k) + \epsilon_{ilt}, \ \forall l) = Pr(CV_{jt} - CV_{kt} - sc_t * \mathbb{1}(j \neq k) + \epsilon_{ijt} \geq CV_{lt} - CV_{kt} - sc_t * \mathbb{1}(l \neq k) + \epsilon_{ilt}, \ \forall l)$.

ities across a wide range of U.S. metropolitan areas. Note that the supply function is formulated with an intertemporal structure to align with the timing of adjustments on the demand side.

Given that the research question focuses on how changes in locational attributes affect residential demand, incorporating a parsimonious supply-side structure within the equilibrium framework enables me to compute tract-level price changes induced by demand shifts, without introducing excessive complexity into the analysis. Conditional on residents' beliefs about future neighborhood values,[29] the locational characteristics of each census tract j, denoted by X_{jt} and ξ_{jt}, and all model parameters, solving for the housing market equilibrium reduces to finding a vector of prices p_t^* such that the residential choices implied by the dynamic demand model generate demand that equals housing supply in every tract. That is, p_t^* simultaneously satisfies

$$N_{j,t+1}(p_t^*|\cdot) = S_{j,t+1}(p_t^*), \qquad \forall j. \tag{13}$$

6 Estimation of the Structural Model

In this section, I describe how to estimate preference parameters θ_g for each group from the dynamic model discussed in the previous section. The novelty is that by combining the estimation methods of Depro, Timmins, and O'Neil (2015) and Bayer et al. (2016), the estimation only requires aggregate-level market share data and the ratio of total movers, which are readily available using aggregate census data.[30] Also, the estimation is free from the curse of dimensionality[31] since I bypass value function iteration for solving the dynamic model by following the framework of Bayer et al. (2016). Given minimal data requirements, low computational cost, and traceability, I believe that the new framework provides a practical alternative for estimating various classes of dynamic discrete choice models, not limited to modeling residential sorting.

The final goal is to back out utility parameters θ_g for each group g, based on aggregate census data. To achieve this, the estimation consists of three steps. The first step is to back out choice-

[29] Section 6.2 describes how these beliefs are estimated. Section 8.1 describes how counterfactual equilibria are computed under the beliefs estimated in Section 6.2.

[30] While (Heblich et al., 2020) also constructs a dynamic model of residential sorting based on aggregate-level data, the model does not endogenize the decision to move, as it assumes an exogenous probability of moving. The framework suggested in this paper, in contrast, fully endogenizes the decision to move by introducing moving costs.

[31] The curse of dimensionality in the dynamic structural model implies that the computational cost of estimation of a dynamic structural model explodes exponentially as the dimension grows linearly, making the estimation often infeasible. See Aguirregabiria, Collard-Wexler, and Ryan (2021) for a detailed discussion of this issue.

specific values for each location j (CV_{jt}), and moving cost (sc_{gt}), for each group g, using aggregate-level market shares derived from aggregate-level census data. The second step is to calculate per-period mean utilities ($f(\Omega_t; \theta_g)$) from choice-specific values derived from step 1. The last step is to estimate utility parameters θ_g from per-period utilities. I describe each step in detail in the remaining part of this section.

6.1 Estimation Step 1: choice-specific values

In this section, I describe how to calculate choice-specific values associated with each j location. This step is a dynamic counterpart of a similar estimation procedure for a static model suggested in (Depro, Timmins, & O'Neil, 2015). Suppose that we observe the number of group g residents at each census tract j at time t, denoted as N_{jgt}. Then, the group-specific market share of census tract j is

$$S_{jgt} = \frac{N_{jgt}}{N_{gt}}, \tag{14}$$

where N_{gt} is the total population of group g residents, including the outside option $J+1$.[32] Given the census tract-level natural rate of population change (often referred to as the rate of natural increase) ρ_{jgt}, the following $(J+1) \times 1$ system of equations should hold

$$S_{jg,t+1} = \sum_{l=1}^{J+1} P_{jlgt} \frac{\rho_{lgt} * N_{lgt}}{\rho_{gt} * N_{gt}} \quad \forall\, j \in \{1, ..., J+1\} \tag{15}$$

where ρ_{gt} is the overall natural rate of population change in the entire area[34] and P_{jlgt} is given by equation 9. It is useful to re-write equation 15 as

$$S_{jg,t+1} = \sum_{l=1}^{J+1} \left(\frac{exp(CV_{jgt} - CV_{lgt} - sc_{gt} * \mathbb{1}(j \neq l))}{\sum_{n=1}^{J+1} exp(CV_{ngt} - CV_{lgt} - sc_{gt} * \mathbb{1}(n \neq l)))} \right) \frac{\rho_{lgt} * N_{lgt}}{\rho_{gt} * N_{gt}} \quad \forall\, j \in \{1, ..., J+1\} \tag{16}$$

[32] There is no absolute rule for determining the total market size when using aggregate share data, and hence no unique way to determine the number of residents at the outside location $J+1$ (Nevo, 2000). In this paper, I set the total population for each group to the observed maximum population in Tarrant County for each group plus 10,000.[33] In other words, $N_{gt} = max_\tau \{\sum_{j=1}^{J} N_{\tau gt}\}_{\tau=1}^{T} + 10,000$. Accordingly, the number of group g residents residing in the outside location $J+1$ is determined as $N_{J+1,gt} = N_{gt} - \sum_{j=1}^{J} N_{jgt}$.

[34] As census tract-level vital statistics in Tarrant County is unavailable, I assume $\rho_{jgt} = \rho_{gt}$. As the terms cancel each other out in equation 15, the equation reduces to $S_{jg,t+1} = \sum_{l=1}^{J+1} P_{jlgt} \frac{N_{lgt}}{N_{gt}} \quad \forall\, j \in \{1, ..., J+1\}$.

The process of estimating CV_{jgt} for each j and sc_{gt} consists of an inner loop and an outer loop. The inner loop finds the solution to equation 16 for a given guess of sc_{gt}. Given a value of sc_{gt} and a normalization[35] on $CV_{gt} \equiv \{CV_{jgt}\}_{j=1}^{J+1}$, equation 16 leads to a contraction mapping in CV_{gt}, as shown in Berry (1994). Thus, one can calculate the exact value of CV_{gt} by the following contraction mapping exercise.

First, I set an initial guess for CV_{gt}, denoted by CV_{gt}^0. For all locations j, I use this guess, together with the observed distribution of group g residents in period t, $\bar{S}_{jgt}$, to calculate the predicted share of group g residents in period $t+1$, denoted by $\widetilde{S}_{jg,t+1}$, using equation 16. I then update the guess for CV_{gt} following Berry (1994):

$$CV_{gt}^{m+1} = CV_{gt}^{m} + \ln \bar{S}_{g,t+1} - \ln \widetilde{S}_{g,t+1}^{m}, \tag{17}$$

where m indexes the iteration and $m = 0$ denotes the initial guess. I repeat this process until CV_{gt}^m converges to $\widehat{CV}_{gt}$, which is declared when $||CV_{gt}^{m+1} - CV_{gt}^{m}|| < \epsilon$, where ϵ denotes a desired tolerance level.[36]

The outer loop pins down sc_{gt} using the non-mover probability $\widehat{P}_{jjgt}$ implied by equation 10 and $\widehat{CV}_{gt}$ obtained from the inner loop. The ACS and decennial census data provide information on the share of residents who did not move between periods t and $t+1$ for each racial/ethnic group g.[37] Let $Non_Movers_{g,t+1}$ denote the observed number of group g residents in period $t+1$ who did not move over the preceding period. I then search for the value $\widehat{sc}_{gt}$ that satisfies

$$\frac{Non_Movers_{g,t+1}}{\sum_{j=1}^{J} N_{jg,t+1}} = \sum_{j=1}^{J} \widehat{P}_{jjgt}(\widehat{sc}_{gt}) \frac{N_{jgt}}{\sum_{l=1}^{J} N_{lgt}}. \tag{18}$$

Equation 18 states that the predicted share of residents who remain in their current location between periods t and $t+1$ should equal the corresponding observed share of non-movers.[38] I use the df-sane method (Cruz, Martínez, & Raydan, 2006) to solve for $\widehat{sc}_{gt}$, updating $\widehat{CV}_{gt}$ through

[35] I normalize $\{CV_{jgt}\}_{j=1}^{J+1}$ such that $CV_{J+1,gt} = 0$. This is equivalent to setting the per-period utility of the outside option to zero, as there is no continuation value following the terminal exit. Note that the solution to equation 16 is unique up to the addition of a scalar.

[36] I set the tolerance level to $\epsilon = 10^{-13}$.

[37] The ACS provides annual non-moving probabilities. I combine these annual probabilities over the years between periods t and $t+1$ to construct the non-moving probability corresponding to one model period.

[38] Equation 18 uses only residents living inside the modeled market, since the observed non-moving rate is defined for current residents of Tarrant County.

the inner loop for each guess of sc_{gt}.

6.2 Estimation Step 2: Per-period Mean Utilities

In this section, I describe how to separate per-period mean utility flows $f(p_{jt}, X_{jt}, \xi_{jt}; \theta_g)$. I drop the subscript g for notational simplicity, while the following process is repeated independently for each g.

Note that combining equations 6 and 7, per-period utility can be expressed as

$$f_{jt}(\Omega_t) = CV_{j,t} - \beta E\left[ln\left(exp(CV_j(\Omega_{t+1})) + \sum_{l \in \mathcal{J}\setminus\{j\}} exp(CV_l(\Omega_{t+1}) - sc)\right) + \gamma|\Omega_t\right]. \quad (19)$$

Thus, to recover per-period mean utility flow from choice-specific values, one should calculate the discounted expectation of expected value, which typically requires specifying the conditional transition probabilities of the state variables as in Rust (1987).

Alternatively, following Bayer et al. (2016), I assume that residents directly predict the future choice-specific values of inside locations $\{CV_{j,t+1}\}_{j=1}^{J}$ given the current value of $\{CV_{jt}\}_{j=1}^{J}$, and Ω_t. Given this assumption, I estimate the transition probabilities of choice specific value functions as

$$CV_{jt} = \gamma_{0,j} + \sum_{l=1}^{L} \gamma_{1,l} CV_{j,t-1} + \sum_{l=1}^{L} X'_{j,t-1}\gamma_{2,l} + \gamma_3 t + \omega_{j,t}, \quad (20)$$

where L is the number of time-lagged variables[39] and $\omega_{j,t}$ is a mean-zero error term. I estimate equation 20 using OLS, replacing CV_{jt} with $\widehat{CV}_{jt}$ obtained from Step 1 in Section 6.1.

Note that residents do not consider individual evolution of each variable in the state space. This simplifies the analysis dramatically by bypassing the calculation of the fixed-point problem in value iteration. In particular, this facilitates the estimation of dynamic demand when the state space is large, as is often the case in settings such as residential location choice, where economic agents consider multiple characteristics of each choice option.

After I run OLS on equation 20, I randomly draw a large number of simulated residuals from the empirical distribution of $\omega_{j,t}$, creating a large number of simulated next-period choice-specific values. Then, using Equation 7, I calculate the conditional expectation of next-period expected

[39] I used $L = 1$ given the short time dimension of my data.

value $E(EV(j,\Omega_{t+1})|\Omega_t)$ using Monte Carlo simulation. To be specific, let r denote simulation draws, where $r = 1, ..., R$.[40] Then,

$$\breve{E}(EV(j,\Omega_{t+1})|\Omega_t) = \frac{1}{R}\sum_{r=1}^{R}\left[\ln\left(\exp(\widetilde{CV}_{rj,t+1}) + \sum_{l\in\mathcal{J}\setminus\{j\}}\exp(\widetilde{CV}_{rl,t+1} - sc_t)\right) + \gamma\right]. \quad (21)$$

where $\widetilde{CV}_r$ denotes the rth vector of simulated next-period choice-specific values derived from Equation 20, and $\breve{E}(\cdot)$ is the Monte Carlo expectation.[41] Now, given an appropriate value of β,[42] I recover the per-period utility as

$$\widehat{f}_{jt}(\Omega_t) = \widehat{CV}_{j,t} - \beta\breve{E}(EV(j,\Omega_{t+1})|\Omega_t), \ \forall j \in \{1, ..., J\}. \quad (22)$$

6.3 Estimation Step 3: Recovering Utility Parameters

After I calculate $\widehat{f}_{jgt}$ for all inside locations and every possible combination of time t and group g, I can estimate the utility parameters by the following process.

For estimation of utility parameters, I impose linearity of $f(p_{jt}, X_{jt}, \xi_{jt}; \theta_g)$ and model an estimable equation as

$$f_{jgt} = \theta_{g0} + \theta_{gp}p_{jt} + X'_{jgt}\theta_{gx} + \theta_{gc} + \theta_{gt} + \xi_{jt} \quad (23)$$

where θ_{g0} is a constant, θ_{gc} denotes city-specific unobservable components, θ_{gt} denotes time-specific unobservable components, p_{jt} is housing cost (rental price), and ξ_{jgt} is utility associated with unobservable characteristics of each neighborhood j. I further decompose ξ_{jgt} into two parts as

$$\xi_{jgt} = \nu_{jgt} + \iota_{jgt} \quad (24)$$

where ν_{jgt} stands for group-specific perception of unobservable endogenous amenities and ι_{jgt} is a

[40] I set R to be sufficiently large, $R = 10,000$

[41] Note that in Equation 21, I impose a simplifying assumption that residents expect the next-period moving cost to be the same as the current-period moving cost. To relax this assumption, one can specify an independent transition process for the moving cost, draw $\widetilde{sc}_{r,t+1}$ alongside $\widetilde{CV}_{r,t+1}$, and average over the additional simulation dimension, replacing sc_t with $\widetilde{sc}_{r,t+1}$ inside the logarithm.

[42] I set $\beta = 0.7$ in practice, given the 7-year time gap between consecutive periods t and the common rule of thumb in the literature that sets $\beta = 0.95$ for the 1-year time gap. Note that $0.95^7 \simeq 0.7$.

normal error. Finally, X_{jgt} is a vector of observable neighborhood characteristics. The endogenous characteristics in X_{jt} are the number of wells within one mile w_{jt}, and the racial composition of the neighborhood r_{jt}. Coefficients on w_{jt} and r_{jt} capture preference for well exposure, and racial homophily. Consistent with the analysis in section 4, I add exogenous controls such as median housing characteristics (number of rooms, and the year the structures were built), violent crime rate, and land use of each neighborhood.

Simple OLS estimation on 23 is likely to produce inconsistent estimate on θ_g for the following reasons. First, the endogenous unobservable ν_{jgt} is likely to be correlated with housing cost p_{jt}. Also, the presence of firm-site sorting in shale gas development creates a simultaneity problem in estimating the coefficient on w_{jt}. Finally, r_{jt} is also an outcome of the residential sorting model and the resulting housing equilibrium, which implies additional simultaneity issues.

Thus, similar to Bayer et al. (2007), and Almagro et al. (2023), I use the following instruments, which is commonly referred to as BLP-style instruments Berry, Levinsohn, and Pakes (1995) in the literature. To be more specific, following Almagro et al. (2023), I start by identifying the neighborhoods that lie within 3–6, 6–10, and 10–15 miles of a given neighborhood j from a given neighborhood j. Then, I construct instruments for p_{jt}, and racial share variables in X_{jt} by taking averages of neighborhood characteristics that are exogenously determined in the model; median number of bedrooms, median year the structures are built, and the number of homeowners.

The relevance condition for these instruments is conceptually straightforward - the neighborhoods are substitutes for one another. Shifts in other neighborhoods' characteristics affect on the equilibrium price of a neighborhood and racial composition. The impact on the racial change becomes more relevant if different racial/ethnic groups have heterogeneous valuations of these neighborhood characteristics. The exclusion restriction is satisfied if changes in unobservable neighborhood amenities are uncorrelated with changes in these observable amenities in the distant neighborhoods, conditional on other excluded instruments, including the fixed effects.[43]

On top of these BLP-style instrumentss, I introduce exogenous variation in well construction costs on w_{jt} leveraging shale depth in each census tract and the average number of days spent on drilling each well. As the geological characteristics are only subject to shale formations more

[43]For more detailed discussion on using BLP-style IV on residential location choice, see (Bayer et al., 2007) and (Almagro et al., 2023)

than 6000 ft below the surface, it is reasonable to argue that the shale depth IV impacts residents' utility only through shale development above. I multiply shale depth by the average number of days spent on drilling to introduce time-series variation in this instrument. The average number of days reflects technological developments in drilling and changes in labor market conditions specific to drilling, which are irrelevant to the neighborhood characteristics and residents' preferences for each neighborhood.

Using this set of instruments, I implement IV-GMM on equation 23, after replacing f_{jgt} with its estimated value $\widehat{f}_{jgt}$, which are recovered from the previous step.

7 Estimation Results

This section presents the estimated model and examines what it implies for household behavior. I report three sets of parameters. The first is the flow utility parameters and moving costs for the six demographic subgroups, which govern how households trade off rent, neighborhood composition, housing stock, and nearby wells within a period. The second is the belief parameters, which govern how households expect choice-specific values for each tracts to evolve. The third translates the flow utility estimates into each subgroup's willingness to pay to avoid an additional well, holding expectations fixed. Two findings organize the discussion that follows. Flow utility estimates alone would suggest that all groups treat nearby wells as a disamenity, with the strongest aversion among non-poor White households. The belief estimates, however, imply that for non-poor Black and Hispanic households well drilling predicts higher future neighborhood values, so the full valuation of well exposure depends on two channels of opposing sign.

Table 2 reports the flow utility parameters, first for the three racial groups and then for the six groups that split each racial group by poverty status.[44] For the three racial groups the estimates line up with he standard picture of neighborhood demand. The coefficient on wells within one mile is negative and significant for White, Black, and Hispanic households alike, the rent coefficient is negative and significant for all three, and preferences over composition display the familiar homophily pattern, with Black and Hispanic households valuing the presence of their own group

[44]Because each group's model is estimated separately, the scale of utility differs across columns, and coefficient magnitudes are comparable within a column but not across columns. Cross-group comparisons are therefore deferred to the willingness to pay measures in Table 4, which express the well disamenity in a common dollar unit (Depro, Timmins, & O'Neil, 2015; Davis et al., 2021).

and White households avoiding both (Bayer et al., 2007; Almagro et al., 2023; Davis et al., 2021; Depro, Timmins, & O'Neil, 2015). All three groups also value owner occupancy in a neighborhood.

Splitting by poverty status shows that the well aversion of each racial group is carried by its non-poor members. The well coefficient remains negative and significant for every non-poor group, while for the three poor groups it is statistically insignificant while being negative. The rent coefficient, the homophily pattern, and the taste for owner occupancy carry over to the split.

The bottom panel reports moving costs, which are not estimated in the GMM step. In the first stage of the estimation the moving cost is the parameter that reconciles the model-implied moving probabilities with the location shares observed in the data: for each group and period it is chosen so that the share of households the model predicts to remain in their neighborhood matches the observed share. Because this condition holds exactly by construction, the moving cost carries no standard error. Moving costs rise for every group between 2000 and 2014.

Table 3 reports the belief parameters from the value transition equation 20. For the three racial groups the coefficient on lagged well exposure is negative for White households and positive for Black and Hispanic households, at -0.074, 0.129, and 0.216 respectively. Splitting by poverty status shows that the positive coefficients are concentrated among the non-poor: the coefficient is 0.137 for non-poor Black and 0.250 for non-poor Hispanic households, while it is negative and statistically significant for poor Black and poor Hispanic households as well as for both White groups.

Conditional on current neighborhood characteristics, non-poor minority households expect neighborhoods with more wells to deliver higher values in the future, whereas every other group expects the opposite. The same two groups are also alone in attaching a positive coefficient to lagged rent, so the asymmetry is not specific to the well variable but reflects a broader difference in how these households extrapolate neighborhood trajectories.[45] I do not attach a causal interpretation to individual transition coefficients, which absorb the correlation between each characteristic and subsequent neighborhood change in the estimation sample; what matters for the welfare analysis

[45]Two channels could plausibly generate this pattern, both operating on next period's outcome rather than on the conditioning variables. Drilling depresses housing costs in exposed neighborhoods (Balthrop & Hawley, 2017), making a neighborhood that is expected to become cheaper more attractive to households for whom housing cost binds on the location decision. Drilling may also shift demographic composition, which the homophily in Table 2 turns into a gain for whichever group's share rises. The transition equation cannot separate the two, but the counterfactual in Section 8 speaks to both, since removing wells re-solves rents and composition jointly.

Table 2: Flow Utility Estimates

	Aggregate			White		Black		Hispanic	
	White	Black	Hispanic	Poor	Non-poor	Poor	Non-poor	Poor	Non-poor
Wells Within 1 mile	-0.0302**	-0.0894**	-0.0352**	-0.0147	-0.0397**	-0.0540	-0.1245***	-0.0209	-0.0627***
	(0.0142)	(0.0354)	(0.0147)	(0.0275)	(0.0154)	(0.0491)	(0.0391)	(0.0517)	(0.0175)
Median Rent ($/Month)	-0.0008**	-0.0030***	-0.0012***	-0.0011**	-0.0007***	-0.0024**	-0.0032***	-0.0026**	-0.0015***
	(0.0004)	(0.0009)	(0.0003)	(0.0006)	(0.0003)	(0.0012)	(0.0009)	(0.0013)	(0.0004)
Hispanic Share	-2.0262***	-1.1677	2.8739***	-0.7802	-2.0985***	1.0636	-1.4674**	5.9519***	2.2544***
	(0.3289)	(0.7305)	(0.3235)	(0.5553)	(0.3343)	(0.9735)	(0.7104)	(0.8490)	(0.3528)
Black Share	-2.4569***	4.6350***	0.6887***	-2.4823***	-2.6145***	6.1388***	4.7290***	1.7884***	0.4478**
	(0.3048)	(0.5217)	(0.1756)	(0.4322)	(0.3401)	(0.6070)	(0.5652)	(0.5648)	(0.1948)
Median # Rooms	-0.0193	0.0825	0.0791*	-0.2396***	-0.0393	-0.3103*	0.1642	-0.0035	0.1061**
	(0.0449)	(0.1127)	(0.0437)	(0.0643)	(0.0355)	(0.1599)	(0.1156)	(0.1548)	(0.0457)
Median Year Built	0.0147***	0.0391***	0.0168***	0.0094*	0.0186***	0.0192*	0.0493***	0.0261**	0.0208***
	(0.0036)	(0.0096)	(0.0034)	(0.0056)	(0.0033)	(0.0114)	(0.0095)	(0.0112)	(0.0038)
Owner-Occupied Units	0.0006***	0.0010***	0.0006***	0.0007***	0.0006***	0.0007***	0.0010***	0.0008***	0.0007***
	(0.0001)	(0.0002)	(0.0001)	(0.0001)	(0.0001)	(0.0002)	(0.0002)	(0.0002)	(0.0001)
Violent Crime Rate	-0.0013***	-0.0015*	0.0003	-0.0009	-0.0012***	-0.0010	-0.0023***	-0.0011	-0.0003
	(0.0003)	(0.0008)	(0.0004)	(0.0007)	(0.0003)	(0.0011)	(0.0009)	(0.0013)	(0.0004)
Commercial Land Share	-0.5511	-0.5406	-0.0584	0.2266	-0.1511	-0.0349	-1.3184*	3.2120***	-0.3822
	(0.4882)	(0.7564)	(0.4060)	(0.7742)	(0.5005)	(1.2035)	(0.7664)	(1.0559)	(0.4372)
Residential Land Share	-0.4602***	-1.3497***	0.0126	-0.2607	-0.3260*	-0.4989	-1.1859***	0.3850	-0.0612
	(0.1704)	(0.3374)	(0.1535)	(0.2726)	(0.1840)	(0.4055)	(0.3496)	(0.3858)	(0.1656)
Moving cost (2000)	4.785	3.623	4.842	4.916	4.815	3.242	3.727	4.321	5.056
Moving cost (2007)	4.900	3.946	4.966	5.028	4.914	3.491	4.098	4.380	5.169
Moving cost (2014)	5.339	4.456	5.467	5.722	5.337	4.623	4.407	6.828	5.466
City FE					Yes				
Year FE					Yes				
N					1,170				

Notes: Iterated GMM estimates of the dynamic model. The first three columns estimate the model on the three aggregate racial groups; the remaining six columns split each group by poverty status. Instruments are the shift-share and mean shale depth instruments together with the first eighteen principal components of the BLP-style distance ring instruments. Standard errors, clustered at the census tract level, are in parentheses. Moving costs are estimated separately for each group and period and are reported in utils. The four endogenous variables are the well count, median rent, and the Hispanic and Black population shares; the weakest first-stage F statistic across the four, computed on the excluded instruments and clustered at the tract level, is 101.7. Significance levels: * $p < 0.10$, ** $p < 0.05$, *** $p < 0.01$.

is that the estimated beliefs imply opposite-signed continuation value responses to drilling across groups.[46]

Table 4 translates the flow utility estimates into each group's monthly willingness to pay to avoid one additional well within one mile, holding expectations, and thus their predictions of choice-specific values of each tracts fixed. Although the utility coefficients cannot be compared across columns, the willingness to pay expresses the well disamenity in a common dollar unit, providing comparability across groups. Taking each racial group as a whole, the figures are $36 for White, $29 for Black, and $30 for Hispanic households.

The poverty split widens the range considerably, from $8 to $57 per month, with the non-poor above the poor within every racial group.[47] The rent coefficient in the denominator is small relative to its sampling variation, which gives the ratio a heavy tailed distribution that a standard error does not summarize well. Appendix Figures 14a and 14b therefore report the bootstrap distribution of each ratio directly, and show that the mass at or below zero is negligible for the non-poor groups but substantial for the poor groups.

For non-poor Black and non-poor Hispanic households the two channels point in opposite directions: their willingness to pay to avoid a well is positive within a period, while their belief parameters imply that drilling raises the continuation value of a neighborhood. The direction of the net welfare effect therefore cannot be read off the parameter estimates and calls for equilibrium counterfactual analyses in Section 8.

Finally, to assess how well the model with the observed characteristics and the parameter estimates capture the demand for each location, I set the unobserved amenity of every neighborhood to zero ($\xi_{jt} = 0$) and predict demand for each neighborhood in future periods while allowing price to adjust so that the market clear with housing supply Equation 12.[48] Starting in 2000, I predict the 2007 population of each demographic group, then roll the exercise forward using the predicted 2007 populations, up to the final period of 2021, so that prediction errors accumulate over subsequent

[46] Appendix B shows that a CCP-based procedure (Hotz & Miller, 1993; Almagro & Domínguez-Iino, 2025; Davis et al., 2021) that does not use this transition equation recovers nearly identical flow utilities, which indicates that equation 20 approximates future choice-specific values well.

[47] These estimates are broadly in line with the prior literature. Expressed as a share of housing cost, a ten percent increase in exposure is worth 0.4 to 2.7 percent across groups, comparable to the 1.4 to 1.8 percent that Bayer et al. (2016) report for a ten percent change in ozone; per well, the estimates for the poor groups fall inside the 1.5 to 3 percent of house value that Balthrop and Hawley (2017) estimate for well presence in this county.

[48] By construction, setting ξ_{jt} equal to the residuals from Equation 23 results in perfect match with observed population with zero error, serving as a benchmark. The method to solve for equilibrium is introduced in Section 8.

Table 3: Belief Parameter Estimates

	Aggregate			White		Black		Hispanic	
	White	Black	Hispanic	Poor	Non-poor	Poor	Non-poor	Poor	Non-poor
Own Value (γ_1)	-0.4878***	0.5640***	0.3800***	0.0076	-0.2441***	0.1231**	0.5676***	-0.1390**	0.1384
	(0.0725)	(0.0504)	(0.0735)	(0.0811)	(0.0546)	(0.0487)	(0.0509)	(0.0662)	(0.0860)
Wells Within 1 mile	-0.0743***	0.1293***	0.2161***	-0.2007***	-0.0630***	-0.2186***	0.1367***	-0.3323***	0.2498***
	(0.0242)	(0.0270)	(0.0256)	(0.0584)	(0.0206)	(0.0687)	(0.0287)	(0.0765)	(0.0325)
Median Rent ($/Month)	-0.0015***	0.0015***	0.0021***	-0.0038***	-0.0013***	-0.0036***	0.0017***	-0.0066***	0.0025***
	(0.0002)	(0.0002)	(0.0003)	(0.0004)	(0.0002)	(0.0004)	(0.0003)	(0.0006)	(0.0003)
Hispanic Share	-4.1503***	1.4789***	3.2853***	-4.2344***	-3.6102***	-1.6369***	1.7348***	-0.5209	4.2898***
	(0.2233)	(0.2725)	(0.3057)	(0.3599)	(0.2155)	(0.4872)	(0.3063)	(0.5351)	(0.3427)
Black Share	-4.8448***	2.0640***	1.6320***	-3.5551***	-4.4206***	3.3581***	2.3493***	0.5999	1.8184***
	(0.3522)	(0.3141)	(0.1598)	(0.3968)	(0.3288)	(0.4850)	(0.3075)	(0.4218)	(0.1691)
Median # Rooms	-0.0534	-0.1482**	-0.0722	-0.1146	-0.0256	-0.2369*	-0.1327**	-0.1116	-0.0842
	(0.0511)	(0.0591)	(0.0575)	(0.1021)	(0.0452)	(0.1300)	(0.0610)	(0.1438)	(0.0668)
Median Year Built	0.0115***	0.0156***	0.0034	-0.0073	0.0160***	0.0150**	0.0181***	-0.0025	0.0068*
	(0.0034)	(0.0045)	(0.0033)	(0.0061)	(0.0035)	(0.0073)	(0.0053)	(0.0085)	(0.0038)
Owner-Occupied Units	0.0008***	0.0001	0.0004***	0.0006***	0.0007***	0.0001	0.0001	0.0007***	0.0005***
	(0.0001)	(0.0001)	(0.0001)	(0.0002)	(0.0001)	(0.0002)	(0.0001)	(0.0003)	(0.0001)
Violent Crime Rate	0.0005***	0.0001	-0.0003*	0.0007**	0.0003**	0.0010**	-0.0000	0.0003	-0.0004*
	(0.0002)	(0.0002)	(0.0002)	(0.0003)	(0.0001)	(0.0004)	(0.0002)	(0.0005)	(0.0002)
Commercial Land Share	-1.4893**	1.7155**	2.5806***	-2.5433**	-0.7855	0.7952	1.1371	-3.2556**	2.5785***
	(0.6291)	(0.7689)	(0.5804)	(0.9977)	(0.5475)	(1.3319)	(0.7881)	(1.3517)	(0.6911)
Residential Land Share	-0.7373***	-0.0147	-0.0282	-0.4820	-0.5435***	0.4837	-0.1457	0.2528	-0.0297
	(0.2306)	(0.2424)	(0.2140)	(0.3823)	(0.2073)	(0.4732)	(0.2481)	(0.5199)	(0.2465)
Constant	-23.8478***	-32.0079***	-8.9269	15.8672	-32.9917***	-30.6730**	-37.2961***	5.7323	-16.7150**
	(6.7638)	(9.1093)	(6.5956)	(12.1823)	(6.9410)	(14.5168)	(10.6334)	(16.8564)	(7.6920)
N					780				
Clusters					390				

Notes: OLS estimates of the value transition equation, in which the choice-specific value of a neighborhood is regressed on its own lag and lagged neighborhood characteristics. The first three columns correspond to the aggregate racial groups and the remaining six to the subgroups divided by poverty status. Standard errors, clustered at the census tract level, are in parentheses. Significance levels: * $p < 0.10$, ** $p < 0.05$, *** $p < 0.01$.

Table 4: Willingness to Pay to Avoid an Additional Well

	All Households			White		Black		Hispanic	
	White	Black	Hispanic	Poor	Non-poor	Poor	Non-poor	Poor	Non-poor
Willingness to pay	35.53	29.41	30.39	12.94	56.69	22.23	38.31	8.05	42.09

Notes: This table reports the monthly willingness to pay, in dollars, to avoid one additional well within one mile, computed as the ratio of the well coefficient to the rent coefficient from Table 2. The calculation holds household expectations about future neighborhood values fixed, so these figures reflect only the contemporaneous trade-off between rent and well exposure. For inference on these measures, Figure 14 in the appendix presents histograms of the willingness to pay from 2000 wild bootstrap trials.

periods.

Figure 15(a) in appendix shows the result for the three racial groups, and Figure 15(b) for the six groups divided by race and poverty status. For the model specification that does not divide race by poverty, observed amenities predict demand well, and the fit survives the finer division by poverty status: the overall correlation exceeds 0.8 for every racial groups in figure 15(a) and every non-poor group in figure 15(b). For the poor groups, unobserved characteristics govern a larger part of utility, making the model predictions weaker than in the other cases.

8 Counterfactual Equilibrium Analysis

8.1 Calculating Counterfactual Equilibrium and Welfare

In this section, I construct counterfactual analyses based on the model estimates for the per-period utility parameters and value transition parameters for each race. Unlike the static models, constructing a counterfactual counterfactual is nontrivial, as the dynamic demand is defined on choice-specific values, not per-period utilities. Typically, this requires solving a value iteration (Rust, 1987) that is defined on individual state space, which is subject to the curse of dimensionality of the state space, making counterfactual analysis often infeasible.

The paper's methodical contribution in this section is to provide an alternative method to calculate counterfactual equilibrium. Note that even a local change in per-period utility triggers a system-wide adjustment in choice specific value to meet the bellman system defined in the following

equation

$$CV_{jt} = f_j(\Omega_t) + \beta E\left[\ln\left(\exp(CV_{jt+1}) + \sum_{l\in\mathcal{J}\setminus\{j\}} \exp(CV_{lt+1} - sc_{t+1})\right) + \gamma \mid \Omega_t\right], \ \forall j, \qquad (25)$$

which is derived from rewriting equation 6, using equation 7. Thus, in constructing a counterfactual, the key is to find a unique fixed point CV_t' that satisfies equation 25, given any change in the mean per-period utilities f_t'. Given the fact that the future expectations are formed from value transition equation (equation 20), which is defined on the choice set, not the state space, I introduce a new value iteration that is defined on choice set. The right-hand side of equation 25, with f_t' in place of f_t and with CV_{t+1} forecast from Equation 20, defines an operator on the vector of inside choice-specific values. Appendix A.2 shows that this operator is a contraction whenever $\beta|\gamma_{1,1}| < 1$, so that CV_t' exists, is unique, and is reached by iterating the operator from any initial guess. Appendix A.1 states the resulting algorithm.

Using the counterfactual choice-specific values CV_t', I compute the counterfactual demand for each location following equation 9. Given these demands, the problem is to solve for the counterfactual equilibrium prices and racial compositions in each census tract j. Because the counterfactual equilibrium reflects adjustments in housing prices, demographic composition, and residents' expectations about the future value of each location, the analysis naturally captures a variety of general equilibrium channels through which welfare and moving decisions are affected in the new environment.

One important identifying assumption of this counterfactual equilibrium is that the resident's belief parameter should remain the same in the counterfactual scenarios.[49] This assumption, reflecting sticky or subjective expectations in counterfactual (An, Hu, & Xiao, 2021; Carroll, Crawley, Slacalek, Tokuoka, & White, 2020), is more reasonable when residents have learned from a historically stable environment, the state space is high-dimensional, and the policy change is relatively small[50].

Given the assumption on the timing of moving and housing stock adjustment, the counterfactual equilibrium in period t is a vector of prices p_t' that satisfies $N_{j,t+1}(p_t', X_t', \xi_t \mid N_{jt}) = S_{j,t+1}(p_{jt}'), \ \forall j,$

[49] Appendix C tests the robustness of counterfactual results against this assumption.

[50] In contrast, if the agents are fully rational and thus are able to fully adjust their belief parameters in equilibrium, the counterfactual may be subject to the Lucas critique (Lucas, 1976).

where $N_{j,t+1}$ and $S_{j,t+1}$ are the housing demand and supply in Equations 11 and 12, and X'_t collects the counterfactual location characteristics, including the new well exposure w'. Note that ξ_t now denotes the estimated unobserved location quality, which is held fixed across the counterfactual and therefore carries no prime. Starting from the initial period, I solve for p'_t by an iterative price-adjustment algorithm and roll the resulting racial composition forward to the next period. Appendix A describes the algorithm, proves that a market-clearing price vector exists in every period, and discusses the uniqueness properties of the computed counterfactual equilibrium.

After calculating counterfactual equilibrium, I measure the welfare of group g as the population-weighted expected value of a group-g resident's location value,

$$\mathcal{W}_g = \frac{1}{N_g} \sum_{j=1}^{J} N_{jg}\, EV_g(j, \Omega), \qquad N_g = \sum_{j=1}^{J} N_{jg}, \tag{26}$$

where $EV_g(j, \Omega)$ is the inclusive value of Equation 7 for a group-g resident currently in census tract j, taken over the choice set of the J inside tracts and the outside option, and N_{jg} is the group-g population in tract j.

Note that the welfare change can be decomposed by margin. Recall that the value of choosing tract j separates into a per-period utility and a continuation value governed by belief on value transition in Equation 20,

$$CV_{jt} = \underbrace{f_j(\Omega_t)}_{\text{per-period utility}} + \underbrace{\beta\, E[EV(j, \Omega_{t+1}) \,|\, \Omega_t]}_{\text{continuation value}}, \tag{27}$$

and both components depend on the state Ω_t. Any change in neighborhood characteristics, such as well exposure from w to w', triggers endogenous adjustment of equilibrium rents from p to p' and of the racial composition of each neighborhood from r to r'.[51]. I denote these elements as $S = (w, p, r)$. Because the two components of (27) can be evaluated at different S, welfare can be written as $\mathcal{W}_g(S^{\text{flow}}, S^{\text{belief}})$ with some abuse of notation, where the per-period utility reads the configuration S^{flow} and the continuation value reads the configuration S^{belief}, with all other elements of Ω common. Moving one configuration while holding the other fixed isolates the corresponding margin: a change in S^{flow} alters what residents experience each period, and a change in S^{belief}

[51] All other elements of Ω, including unobserved amenities, are assumed unchanged.

alters what they expect about values along the future equilibrium path. For the rent element I distinguish two counterfactual paths: p'' clears the market with the composition held at r, while p' clears it after re-sorting to r', so that p' additionally reflects the rent feedback from demographic sorting in a counterfactual experiment.

Walking from the observed state to the full counterfactual one component at a time, flow before belief, gives nine evaluation points,

$$\begin{aligned}
\mathcal{W}_g^{(0)} &= \mathcal{W}_g\big((w,p,r),\,(w,p,r)\big), & \mathcal{W}_g^{(1)} &= \mathcal{W}_g\big((w',p,r),\,(w,p,r)\big),\\
\mathcal{W}_g^{(2)} &= \mathcal{W}_g\big((w',p,r),\,(w',p,r)\big), & \mathcal{W}_g^{(3)} &= \mathcal{W}_g\big((w',p'',r),\,(w',p,r)\big),\\
\mathcal{W}_g^{(4)} &= \mathcal{W}_g\big((w',p'',r),\,(w',p'',r)\big), & \mathcal{W}_g^{(5)} &= \mathcal{W}_g\big((w',p'',r'),\,(w',p'',r)\big),\\
\mathcal{W}_g^{(6)} &= \mathcal{W}_g\big((w',p'',r'),\,(w',p'',r')\big), & \mathcal{W}_g^{(7)} &= \mathcal{W}_g\big((w',p',r'),\,(w',p'',r')\big),\\
\mathcal{W}_g^{(8)} &= \mathcal{W}_g\big((w',p',r'),\,(w',p',r')\big).
\end{aligned}$$

$\mathcal{W}_g^{(0)}$ is the observed state and $\mathcal{W}_g^{(8)}$ is the full counterfactual equilibrium. The eight consecutive differences are the channel contributions, The eight consecutive differences are the channel contributions,[52]

$$\begin{aligned}
\Delta_g^{\text{Wells, flow}} &= \mathcal{W}_g^{(1)} - \mathcal{W}_g^{(0)}, & \Delta_g^{\text{Wells, belief}} &= \mathcal{W}_g^{(2)} - \mathcal{W}_g^{(1)},\\
\Delta_g^{\text{Rent, flow}} &= \mathcal{W}_g^{(3)} - \mathcal{W}_g^{(2)}, & \Delta_g^{\text{Rent, belief}} &= \mathcal{W}_g^{(4)} - \mathcal{W}_g^{(3)},\\
\Delta_g^{\text{Racial Homophily, flow}} &= \mathcal{W}_g^{(5)} - \mathcal{W}_g^{(4)}, & \Delta_g^{\text{Racial Homophily, belief}} &= \mathcal{W}_g^{(6)} - \mathcal{W}_g^{(5)},\\
\Delta_g^{\text{Rent Feedback, flow}} &= \mathcal{W}_g^{(7)} - \mathcal{W}_g^{(6)}, & \Delta_g^{\text{Rent Feedback, belief}} &= \mathcal{W}_g^{(8)} - \mathcal{W}_g^{(7)}.
\end{aligned}$$

Note that these sum up to the total change in welfare,

$$\sum_c \Delta_g^c = \mathcal{W}_g^{(8)} - \mathcal{W}_g^{(0)}. \tag{28}$$

.

[52]Because the channels are activated sequentially and the welfare aggregate is non-separable in them, the decomposition is not order-invariant; the contribution attributed to a given channel may depend on its position in the sequence. The total change in welfare, however, remains unchanged no matter the order of this sequence.

8.2 Removing Wells in Fort Worth, and Its Welfare Implications

In this section I run the counterfactual that removes all wells whose surface locations lie within the city of Fort Worth. The goal is to draw a big picture of the overall welfare implications of urban fracking. I focus on Fort Worth because it is the largest city in Tarrant County and concentrates a substantial share of the county's urban wells, so a city-wide ban is both quantitatively meaningful and administratively coherent as a unit of policy.[53]

To construct the counterfactual, I remove every well whose surface location falls within a Fort Worth census tract, in all periods.[54] Given the counterfactual well exposure, I solve for the new equilibrium period by period, allowing housing prices and racial composition to adjust fully over time. From now on, I call a tract *treated* if its exposure falls under the removal and *untreated* otherwise, and I compare the counterfactual equilibrium to the observed one.

Figure 4 presents the equilibrium rent adjustment under the removal. In the treated census tracts, the equilibrium rent rises, by around $256 per month for the average resident, and the increase is larger in the tracts where more wells are removed. The removal makes these tracts more desirable, and the increased demand raises the market-clearing rent. In the untreated tracts, in contrast, the equilibrium rent falls by around $86 per month for the average resident. As the treated tracts become relatively more attractive, part of the demand for the untreated tracts is reallocated toward them, and the market-clearing rent in the untreated tracts declines. In total, around 64 percent of the county population resides in the tracts where the equilibrium rent falls under the removal.[55]

Figure 5 reports the welfare impact of the removal on the six groups, measured as the change in the expected lifetime value at the 2014 location and converted into a lifetime present value in

[53] City-level restriction of urban drilling is a policy residents have pursued in reality, not a hypothetical construct. In 2014 the neighboring city of Denton passed a voter-initiated ban on hydraulic fracturing, which the Texas legislature preempted the following year through House Bill 40. Grassroots opposition has continued across Tarrant County: Liveable Arlington has contested well permitting in Arlington for over a decade, and within Fort Worth the Environmental Justice Coalition of Fort Worth has campaigned to tighten the city's gas-well ordinance, arguing that drilling disproportionately burdens low-income and minority neighborhoods.

[54] Note that because exposure counts the wells within one mile of a tract centroid, this also lowers exposure for adjacent tracts outside the city boundary.

[55] This sizeable rent adjustment in the untreated census tracts represents a violation of the Stable Unit Treatment Value Assumption (SUTVA), which invalidates the identification of equilibrium effects based on a large class of quasi-experimental research designs, such as difference-in-differences. The outcomes of the untreated tracts are affected by the treatment through the equilibrium price and racial composition, so a comparison between the treated and the untreated tracts would understate the true rent response by the size of the spillover.

dollars per person.[56] For each group, the figure gives the total change in welfare for the entire Tarrant County residents, and the total changes for the residents in the treated and untreated census tracts.

The total welfare change determines the winners and the losers of the removal. Non-poor White residents gain around $23,300 per person in lifetime present value, poor White residents around $19,300, poor Black residents around $14,800, and poor Hispanic residents around $7,900. In contrast, non-poor Hispanic residents lose around $11,700 per person, and the welfare change for non-poor Black residents is close to zero. Note also that the welfare change depends on where the resident lives in 2014. Because of the moving costs, the residents are partially attached to their origin census tracts, so a change in their own neighborhood carries a different welfare implication than a change in a neighborhood elsewhere in the choice set. For instance, non-poor White residents in the treated tracts gain around $29,300 per person, while those in the untreated tracts gain around $20,800. The direction of this gap is not uniform: poor Hispanic residents in the untreated tracts gain around $10,800, nearly twice the gain of those in the treated tracts, for whom the amenity improvement is offset by the rent increase in their own neighborhood.

Figure 16 in appendix presents the eight-channel decomposition, which locates the source of this heterogeneity. Three channels are qualitatively common across all six groups. Every group values the removal in the flow utility, with flow gains ranging from around $3,200 for poor Hispanic residents to over $63,000 for non-poor Black residents, and every group pays for the improvement through the two initial-rent channels, which are negative in both margins. What separates the winners from the losers is the wells term in the choice-specific value transition rule in equation 20. For White residents, poor Black residents, and poor Hispanic residents, the estimated rule implies that lower exposure predicts higher future choice-specific values, so the belief channel reinforces the flow gain, adding between around $12,000 and $24,000 per person. For non-poor Black and non-poor Hispanic residents the same term carries the opposite sign, so removing the wells lowers the future values these residents expect and the belief channel offsets much of the flow gain. Especially for non-poor Hispanic residents the belief loss of around $24,000 outweighs the flow gain of around $26,000 once the rent burden is netted out, leaving the loss reported above.[57] The wells term in

[56] The change in the expected lifetime value is divided by $|\theta_{gp}|$, the per-period utility parameter on monthly rent, and multiplied by the number of months in each period.

[57] These magnitudes are broadly in line with those reported for comparable place-based policies. Dividing the

the transition rule does not predict the future disamenity of the wells alone; it predicts the future trajectory of the future values, which in turn reflects equilibrium rent, demographic composition, and unobserved amenities. For these residents, exposure predicts a favorable trajectory, so removing the wells removes a signal these residents regard as favorable.

The relative magnitudes of the channels reflect three features of the equilibrium adjustment. First, the removal of wells monotonically improves the environmental amenity of every treated tract, so the wells flow channel is positive for all six groups. Second, while the rent rises in the treated tracts, the rent falls in all of the untreated tracts in the choice set, which significantly attenuates the negative welfare impact of the rent channels. Third, the racial homophily channels are small, no larger than around $900 per person in absolute value. The re-sorting changes the racial composition of all the other tracts as well, and these changes partially offset one another in the welfare calculation. In addition, a change in well exposure in a period is reflected in the demographic composition only in the next period, which further mutes this channel.

Finally, I compare these results with the aggregate model that pools the poor and the non-poor residents within each race. The upper panels of table 16 in appendix and Table 5 report the welfare incidence and the decomposition from this three-race model. The aggregate model finds that Black residents lose around $2,200 per person and Hispanic residents around $15,400. The six-group model instead shows that poor Black residents gain around $14,800 per person while non-poor Black residents end close to zero, so neither Black subgroup loses. Similarly, the aggregate Hispanic loss pools a gain of around $7,900 for poor Hispanic residents with the loss for non-poor Hispanic residents. The race-by-poverty specification therefore recovers welfare heterogeneity along the poverty dimension that the three-race specification cannot specify.

8.3 Targeted Removal in Poor-Hispanic Neighborhoods

A central concern in the environmental justice literature is that minority and low-income communities bear disproportionate exposure to polluting facilities (Banzhaf et al., 2019; Zwickl, 2019). A natural policy response is to target remediation at the most vulnerable communities. In this

lifetime present value by $7/(1-\beta) = 23.3$ converts it into a constant annual flow, giving a gain of about $1,000 per person per year for non-poor White residents and a loss of about $500 for non-poor Hispanic residents. Almagro et al. (2023) find that the Chicago public housing demolitions moved general-population welfare between a loss of $429 and a gain of $285 per year.

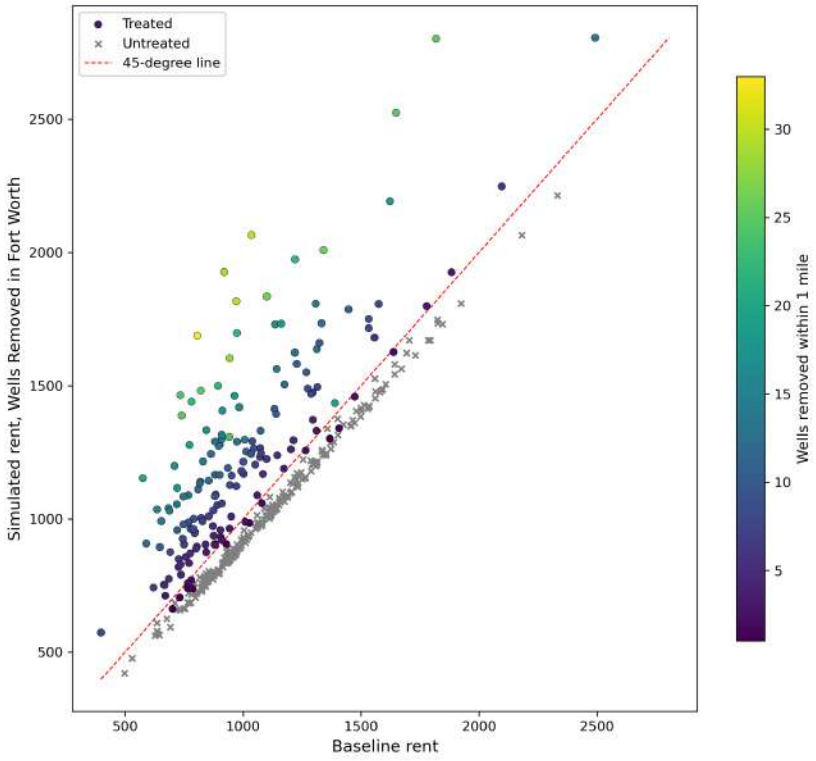
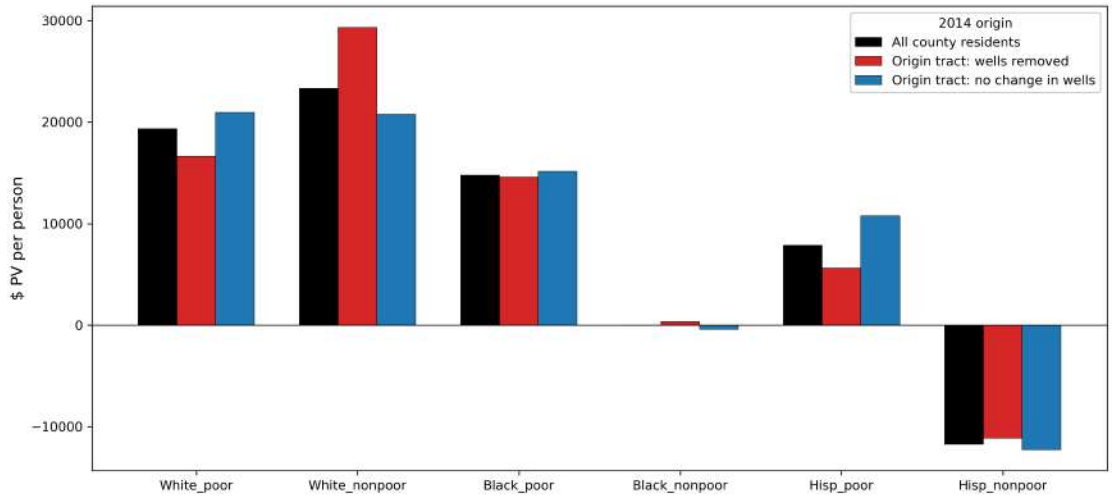
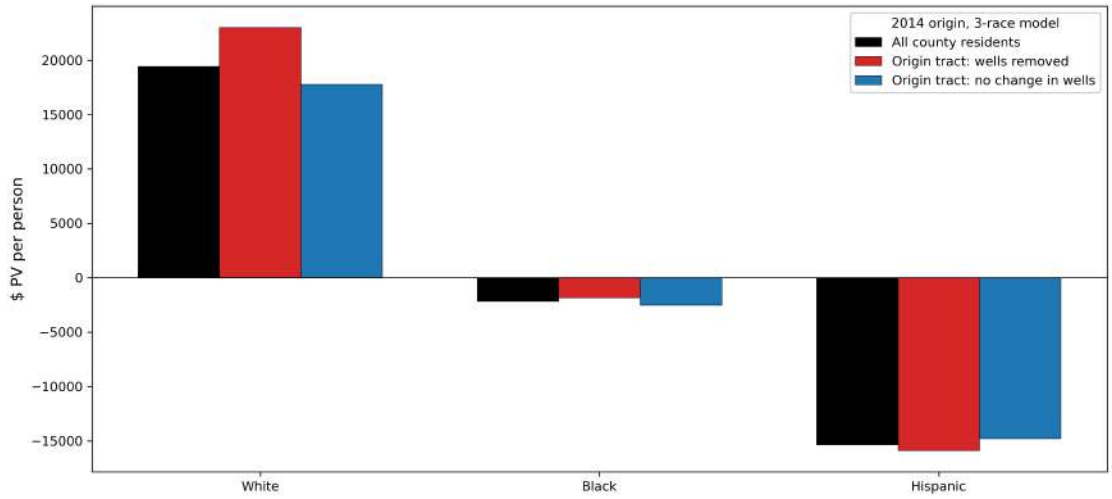


Figure 4: Counterfactual Change in Equilibrium Rent, Fort Worth Removal

Notes: Each point is a census tract in the terminal estimation period. The horizontal axis is the observed equilibrium rent and the vertical axis is the equilibrium rent under the Fort Worth removal, both in logs. Treated census tracts appear as circled dots, colored by the number of wells removed within one mile; untreated census tracts appear as 'x'. The red dashed line is the 45-degree line.



(a) Race-by-poverty model



(b) Aggregate three-race model

Figure 5: Welfare Incidence of the Fort Worth Removal by 2014 Origin

Notes: Lifetime present value in dollars per person, with the population weights fixed at the observed 2014 distribution. Each panel reports the total welfare change and the change for the residents in the treated and untreated census tracts. Panel (b) is from the aggregate model that pools the poor and the non-poor residents within each race.

Table 5: Welfare Decomposition By Channel

	Wells		Rent(Direct)		Racial homophily		Rent(Feedback)		
	Flow	Belief	Flow	Belief	Flow	Belief	Flow	Belief	Total
Aggregate race									
White	9,698	9,803	-1,851	898	461	526	-100	-17	19,418
Black	42,659	-38,590	-5,837	-786	461	-5	-41	-49	-2,188
Hispanic	23,220	-33,688	-2,442	-2,494	-248	443	-102	-50	-15,361
Race by poverty status									
White, poor	3,742	20,684	-4,150	-765	-81	557	-183	-476	19,328
White, non-poor	16,815	12,171	-5,656	-849	852	834	-439	-386	23,342
Black, poor	11,955	24,063	-13,302	-8,181	487	365	-273	-321	14,794
Black, non-poor	63,217	-47,018	-16,288	-241	803	1	-702	189	-39
Hispanic, poor	3,212	20,336	-8,210	-6,378	-492	43	-210	-416	7,886
Hispanic, non-poor	26,049	-24,142	-8,377	-4,630	-534	164	-377	124	-11,723

Notes: Lifetime present value in dollars per person, with the population weights fixed at the observed 2014 distribution. The four channel pairs are the well exposure (Wells), the equilibrium rent on the baseline demographic path (Direct Change in Rent), the racial composition (Racial homophily), and the additional rent adjustment induced by the re-sorting (Rent feedback). Each pair separates the flow-utility margin from the choice-specific value transition margin. The channels form a telescoping sequence and sum to the total by construction. The upper panel is from the aggregate model that pools the poor and the non-poor residents within each race.

section, I evaluate a removal policy of this kind: the scenario removes all wells within one mile of the census tracts in the top decile of the 2000 poor-Hispanic population. From now on, I call these tracts *target tracts*. [58]

To sum up the results, in the counterfactual equilibrium rents rise in most of the treated target tracts, the non-poor population of the treated target tracts rises across all racial groups, and poor Hispanic residents leave the treated target tracts for tracts whose exposure did not change much. The remainder of this section documents these adjustments and their welfare incidence.

Figure 6 shows the change in the 2021 share of each group, with the target tracts outlined and the removed wells marked. The poor Hispanic share falls in nearly every treated tract, with declines exceeding 5 percentage points in the most heavily treated tracts, and rises by small amounts across a wide set of untreated tracts, so poor Hispanic residents leave the treated tracts and disperse across the untreated tracts. The non-poor Hispanic share moves in the opposite direction, rising in the treated tracts and falling in most untreated tracts, and the non-poor Black and non-poor

[58] I distinguish the *target tracts*, the top-decile tracts selected by the targeting rule, from the *treated tracts*, the subset of target tracts within one mile of at least one removed well. Because the targeting rule conditions on the 2000 poor-Hispanic population rather than on well exposure, some target tracts contain no wells within one mile and are therefore untreated.

White shares rise in the treated tracts by smaller amounts.

Figure 17 in appendix and Figure 7 show that rent mediates these flows. Figure 17 in appendix reports the change in residents by group in each target tract together with the change in the 2014 equilibrium monthly rent, with tracts sorted by the size of the poor Hispanic outflow; the tracts with the largest rent increases lose the most poor Hispanic residents and gain the most non-poor residents, while the tracts where rents change little retain or gain poor Hispanic residents. Figure 7 shows that across the target tracts the poor Hispanic outflow rises with both the change in the equilibrium rent and the number of wells removed, so the target tracts where the poor Hispanic population instead rises are the untreated ones (and the ones with minimal treatment), with few or no wells within one mile, where exposure almost did not change and housing becomes relatively cheaper as demand shifts toward the tracts that are treated more intensely. The non-poor Hispanic inflow is the largest of the three non-poor groups because of the racial homophily channel as the treated tracts are heavily Hispanic, and non-poor Hispanic households place a positive value on this composition, so the amenity improvement draws them in more strongly than non-poor White or Black households.

Figure 8 shows the change in the number of residents and the welfare change for the 2014 residents of the treated tracts. The poor Hispanic population of the target tracts falls by around 1,300 persons in total, or around 6 percent of its baseline population, and the outflow reappears in the untreated tracts. The non-poor Hispanic population rises by around 4,600 persons, or around 5 percent, the non-poor Black population by around 11 percent, and the non-poor White population by around 9 percent. The poor Black and poor White populations also fall, so the direction of the population response is determined by poverty status: all three poor groups leave the target tracts and all three non-poor groups move in. The magnitudes differ by race, with Hispanic households dominating both the outflow and the inflow, consistent with the racial homophily channel described above. In the welfare panel, the poor Hispanic residents of the treated tracts lose on average around $1,000 per person in lifetime present value, while every other group gains.

The counterfactual thus reproduces the pattern described in the environmental gentrification literature (Banzhaf et al., 2019). The removal of wells improves environmental amenities, the improvement is capitalized into equilibrium rents, non-poor households move in, and the incumbent poor population relocates to cheaper tracts whose exposure did not change (Ding, Hwang, & Di-

vringi, 2016). The model adds the demographic composition of this adjustment: because of racial homophily, the inflow is led by non-poor Hispanic households rather than non-poor White households, so the treated tracts remain Hispanic while becoming richer, consistent with the evidence that minority household mobility responds to the racial composition of destination neighborhoods (Ferreira, Kenney, & Smith, 2024). The policy would reduce the average exposure of Hispanic residents, but the poor Hispanic residents of the treated tracts bear the welfare loss.

8.4 Removing Under-performing Wells

This subsection explores the welfare consequences of a counterfactual in which under-performing wells were never drilled. Recall that Section 2 documented that more than half of the horizontal wells drilled in the county never recovered their drilling and operating costs.[59] Ex post, these wells not only imposed a direct environmental disamenity on nearby residents but also generated losses for the operators who drilled them. If both operators and residents are better off in the counterfactual state in which these wells were never drilled, that state constitutes a Pareto improvement over the realized outcome and is therefore a natural target for a social planner.

Entry decisions, however, are based on expected rather than realized profits. An increase in the effective cost of entry would therefore deter wells with the lowest expected profitability first. Note that several policies can operate on this margin. For instance, withdrawing the production-tax preference for qualifying high-cost gas wells under Section 201.057 of the Texas Tax Code[60], or imposing an additional per-well charge[61], would raise the expected profitability threshold for entry. For simplicity, I assume that expected and realized profitability are positively correlated, so that increasingly stringent entry barriers would tend to screen out wells that ultimately proved least profitable. The realized-profit ordering used in the counterfactual can therefore be interpreted as an ex post approximation to the sequence of wells deterred by progressively tighter entry policy.[62]

[59] Appendix F.2 describes the construction of well-level profit from production records and lease terms.

[60] Texas normally taxes natural gas production at 7.5 percent of market value, but qualifying high-cost gas received a full production-tax exemption through 2001 and has since remained eligible for a reduced rate that can fall to zero depending on drilling and completion costs. Barnett Shale production falls within the high-cost-gas program. Thomas et al. (2024) discuss how state tax policies affect natural-gas production and extraction incentives.

[61] Pennsylvania provides an example through the impact fee introduced under Act 13. Black et al. (2018) find that the fee significantly reduced acreage leased for shale gas development, providing evidence that such charges can affect upstream investment decisions.

[62] This approach allows me to abstract from explicitly modeling operators' dynamic drilling decisions under uncertainty, as in Herrnstadt et al. (2024).

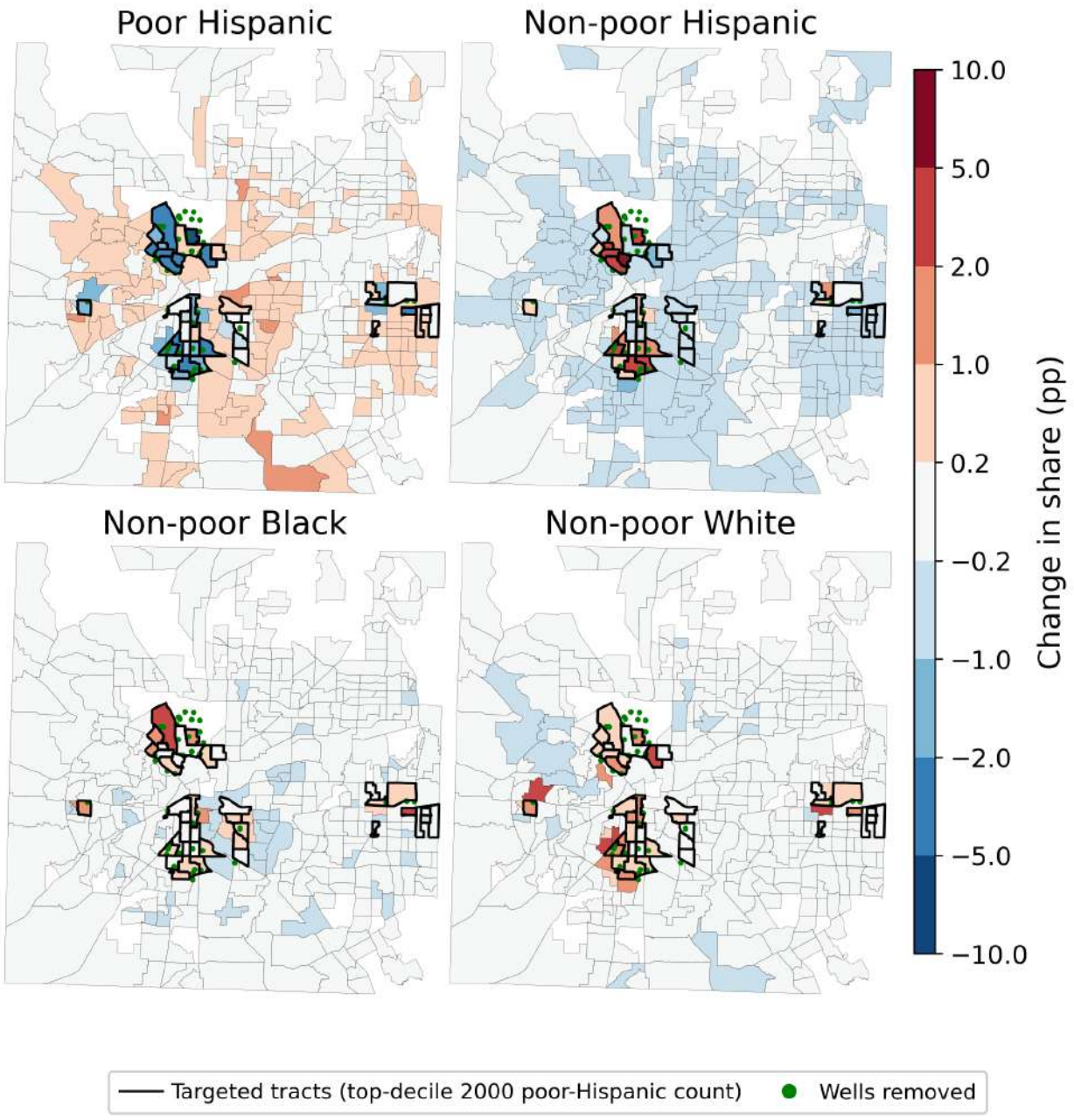


Figure 6: Targeted Removal: Change in Group Shares, 2021

Notes: Each panel shows the change in a group's population share in 2021 between the counterfactual and the observed equilibrium, in percentage points. target tracts are outlined in black and removed wells are marked with green dots. All panels use the same color scale.

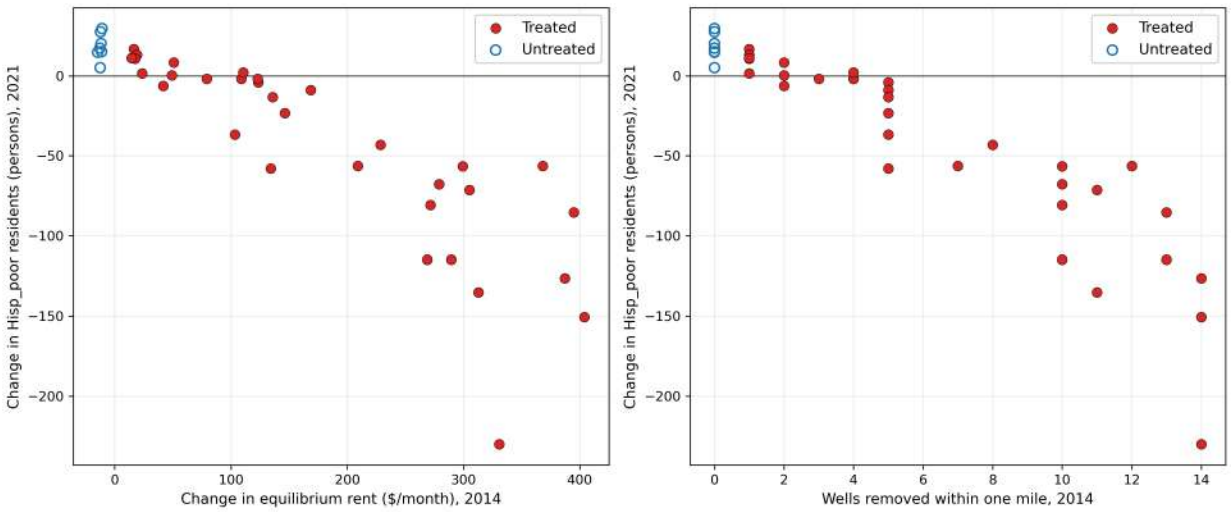


Figure 7: Targeted Removal: Poor Hispanic Outflow, Rent, and Removed Wells

Notes: Each dot is a target tract. The treated tracts appear as red dots and untreated tracts as open blue dots. The left panel plots the change in the poor Hispanic population in 2021 against the change in the 2014 equilibrium monthly rent. The right panel plots the same population change against the number of wells removed within one mile of the tract.

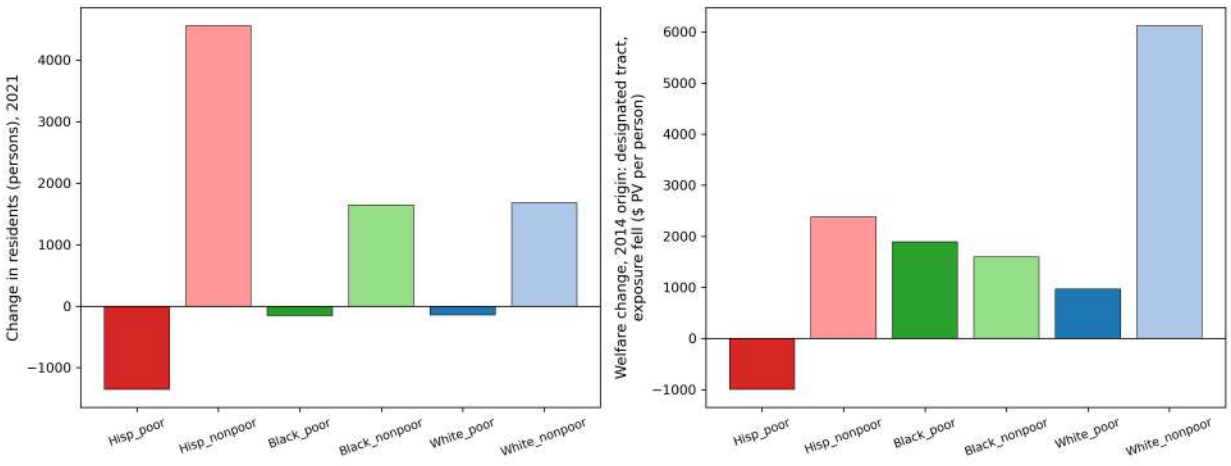


Figure 8: Targeted Removal: Population and Welfare Changes by Group

Notes: The left panel shows the change in the number of residents of the target tracts in 2021, as a total over the target tracts. The right panel shows the welfare change for the 2014 residents of the treated tracts, in lifetime present value per person, as a population-weighted mean over those residents.

Under perfect foresight,[63] the two orderings coincide exactly.

Figure 18 in appendix plots profitable and under-performing wells against tract-level White population shares and shows that under-performing wells are dispersed across the county and located in neighborhoods with widely varying demographic compositions. Conditional on a well being drilled, the relationship between realized profitability and the demographic composition of the surrounding neighborhood is weak: profitable and under-performing wells are often spatially intermingled, and under-performing wells are not concentrated in a specific type of neighborhood.[64] The policy exercise therefore alters drilling exposure across heterogeneous neighborhoods, making the distribution of welfare effects across demographic groups an equilibrium outcome rather than one mechanically determined by targeting a particular demographic group.

I trace the relationship between operator profit and resident welfare by ordering the under-performing wells from lowest to highest realized operator value and progressively expanding the set of wells that are not drilled. Figure 9 plots the resulting operator profit–resident welfare curve for each demographic group. The horizontal axis measures the improvement in operator profit from avoiding these losses, while the vertical axis reports the corresponding change in lifetime welfare per resident, expressed in rent-equivalent present-value dollars. The blue curves are calculated using the dynamic model described above. As a benchmark, I also report the same counterfactual exercise using a separately estimated static residential sorting model. The static model uses the same neighborhood state variables but is estimated under $\beta = 0$; its counterfactual equilibria and welfare changes are then calculated independently from those of the dynamic model.[65]

The static and dynamic models lead to different conclusions about who gains from preventing under-performing wells from being drilled. Under the static model, welfare rises for all six demographic groups at every point along the curve, so avoided operator losses coincide with welfare gains for every group and the counterfactual constitutes a Pareto improvement among all parties considered here. Under the dynamic model, White non-poor residents and all three poor groups still gain, but non-poor Black and Hispanic residents lose, with losses reaching about \$3,700 and

[63] Perfect foresight here includes perfect information about geological productivity, market conditions, and other determinants of future well profitability.

[64] Consistent with this pattern, the average minority population share is approximately 0.42 in tracts containing profitable wells and 0.41 in tracts containing under-performing wells.

[65] Thus, the comparison is between two independently estimated models of residential choice, rather than a decomposition of the dynamic welfare measure.

$64,000 per person, respectively, when none of the under-performing wells are drilled.

Taken together, these results show that a policy that looks unambiguously attractive from a static perspective can have very different distributional consequences once forward-looking behavior and expectations about future neighborhood values are taken into account. Importantly, the static model captures the direct improvement in environmental amenities and the contemporaneous equilibrium adjustments in rents and neighborhood composition, but not how these changes affect households' expectations about future neighborhood values. The comparison therefore shows that incorporating forward-looking behavior can change not only the magnitude of estimated welfare effects, but also who gains and loses from the policy.

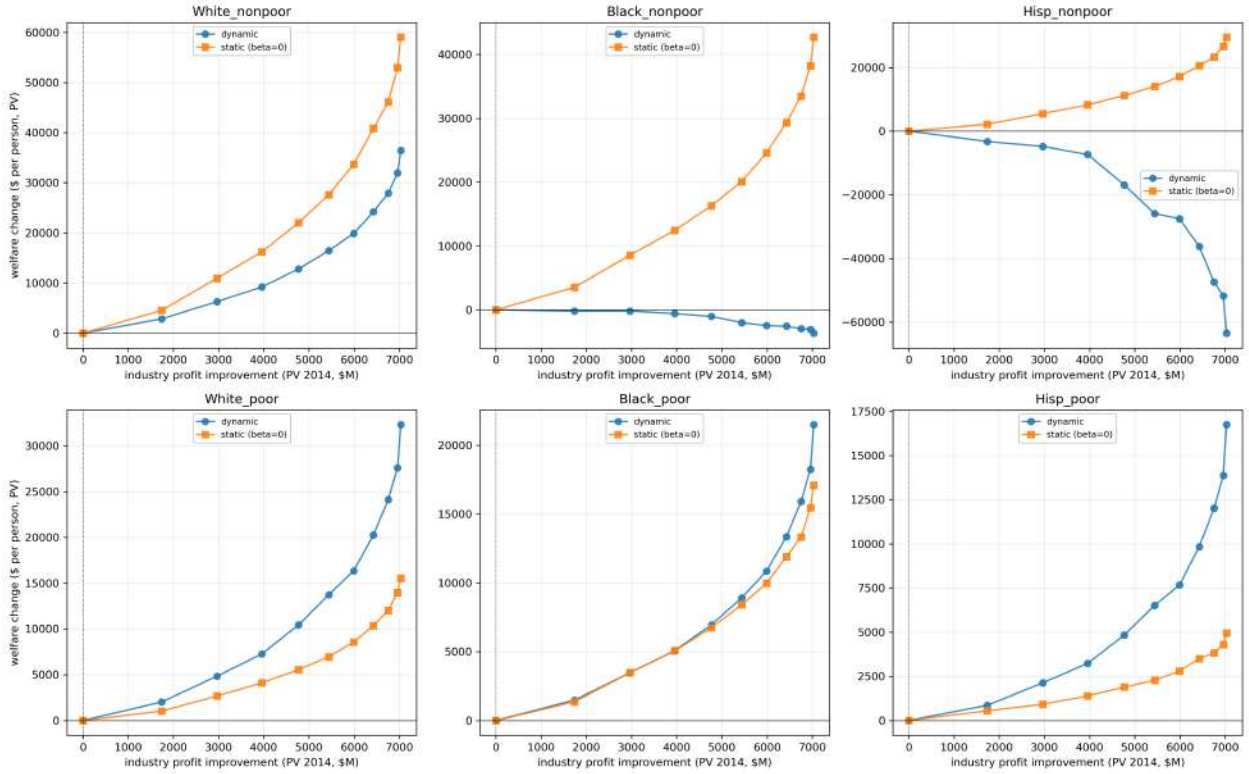


Figure 9: Operator Profit and Resident Welfare from Preventing Under-performing Wells

Notes: Each point corresponds to a progressively larger set of ex post under-performing wells that are assumed not to have been drilled, ordered from lowest to highest realized operator value. The horizontal axis reports the resulting improvement in operator profit in millions of 2014 present-value dollars. The vertical axis reports the change in lifetime welfare per resident in rent-equivalent present-value dollars. The blue curves are calculated from the dynamic model with $\beta = 0.7$. The orange curves are calculated from a separately estimated static residential sorting model with $\beta = 0$. Counterfactual equilibria and welfare are calculated separately for the two models.

9 Conclusion

Urban fracking creates a localized environmental disamenity, but its welfare consequences extend beyond the direct effect of living near a well. Using Tarrant County, Texas, I show that while households perceive nearby well exposure as a direct disamenity, the overall welfare effects of fracking depend on how households sort across neighborhoods, how rents and neighborhood composition adjust in equilibrium, and how residents value these changes over time. The same forces also shape the effects of policies that restrict or remove drilling. Because changes in well exposure alter housing demand and neighborhood trajectories, reducing exposure can redistribute welfare in sharply different ways across demographic groups. As a result, some residents can be made worse off even when stricter regulation reduces their exposure to wells.

The counterfactual exercises show how these equilibrium responses shape the welfare effects of restrictions on drilling. Removing wells in Fort Worth raises rents in directly affected neighborhoods while lowering rents elsewhere, spreading the effects of the policy well beyond the locations where exposure changes. A more targeted removal of wells near neighborhoods with large poor Hispanic populations produces a sharper distributional consequence: improved local amenities attract non-poor households, rents rise, and poor Hispanic residents move toward less affected neighborhoods, leaving poor Hispanic residents in treated neighborhoods worse off. The final counterfactual shows that even removing ex post under-performing wells does not generate gains for all parties, despite simultaneously reducing losses for operators and improving environmental amenities for residents. The full equilibrium dynamics are central to this result. In a static model that does not account for households' expectations about future tract values, the policy appears to be a Pareto improvement, with all resident groups and operators gaining. Once these expectations are incorporated, however, non-poor Black and Hispanic residents suffer welfare losses, and the apparent Pareto improvement disappears.

The paper also shows that dynamic residential sorting can be studied with much less detailed data than is typically required. I develop an estimation approach that recovers choice-specific values and moving costs from aggregate location shares and the aggregate share of non-movers, and then recovers per-period utilities without solving the dynamic model over the full state space. For counterfactual analysis, I reformulate the Bellman recursion in terms of choice-specific values,

which allows the relevant fixed point to be solved over the choice set rather than the full state space. This keeps the computation tractable while allowing expectations about future neighborhood values to adjust with the counterfactual equilibrium. These methods make it possible to study forward-looking residential sorting and equilibrium welfare effects in settings where individual migration histories are unavailable.

The broader lesson extends beyond fracking to any change in neighborhood amenities that induces adjustments in housing markets and residential sorting. The welfare consequences of such changes cannot be understood from their direct effects alone. When households move and housing markets adjust, an amenity change can alter who lives in a neighborhood, what it costs to live there, and how residents value the neighborhood over time. Understanding the welfare consequences therefore requires accounting for how households and housing markets respond after the initial amenity change.

References

Adgate, J. L., Goldstein, B. D., & McKenzie, L. M. (2014). Potential public health hazards, exposures and health effects from unconventional natural gas development. *Environmental Science & Technology*, *48*(15), 8307–8320. Retrieved from https://doi.org/10.1021/es404621d doi: 10.1021/es404621d

Agerton, M. (2020). Learning where to drill: Drilling decisions and geological quality in the haynesville shale. Retrieved from https://ssrn.com/abstract=3583149 (USAEE Working Paper No. 20-439) doi: 10.2139/ssrn.3583149

Aguirregabiria, V., Collard-Wexler, A., & Ryan, S. P. (2021). Chapter 4 - dynamic games in empirical industrial organization. In K. Ho, A. Hortaçsu, & A. Lizzeri (Eds.), *Handbook of industrial organization, volume 4* (Vol. 4, p. 225-343). Elsevier. Retrieved from https://www.sciencedirect.com/science/article/pii/S1573448X21000042 doi: https://doi.org/10.1016/bs.hesind.2021.11.004

Almagro, M., Chyn, E., & Stuart, B. A. (2023, January). *Urban renewal and inequality: Evidence from chicago's public housing demolitions* (Working Paper No. 30838). National Bureau of Economic Research. Retrieved from http://www.nber.org/papers/w30838 doi: 10.3386/w30838

Almagro, M., & Domínguez-Iino, T. (2025). Location sorting and endogenous amenities: Evidence from amsterdam. *Econometrica*, *93*(3), 1031-1071. Retrieved from https://onlinelibrary.wiley.com/doi/abs/10.3982/ECTA21394 doi: https://doi.org/10.3982/ECTA21394

An, Y., Hu, Y., & Xiao, R. (2021). Dynamic decisions under subjective expectations: A structural analysis. *Journal of Econometrics*, *222*(1), 645-675. Retrieved from https://ideas.repec.org/a/eee/econom/v222y2021i1p645-675.html doi: 10.1016/j.jeconom.2020.04.046

Arcidiacono, P., & Miller, R. A. (2011). Conditional choice probability estimation of dynamic discrete choice models with unobserved heterogeneity. *Econometrica*, *79*(6), 1823-1867. Retrieved from https://onlinelibrary.wiley.com/doi/abs/10.3982/ECTA7743 doi: https://doi.org/10.3982/ECTA7743

Balthrop, A. T., & Hawley, Z. (2017). I can hear my neighbors' fracking: The effect of natural gas production on housing values in Tarrant County, TX. *Energy Economics*, *61*(C), 351-362.

Retrieved from https://ideas.repec.org/a/eee/eneeco/v61y2017icp351-362.html doi: 10.1016/j.eneco.2016.11.0

Banzhaf, S., Ma, L., & Timmins, C. (2019, February). Environmental justice: The economics of race, place, and pollution. *Journal of Economic Perspectives*, *33*(1), 185-208. Retrieved from https://www.aeaweb.org/articles?id=10.1257/jep.33.1.185 doi: 10.1257/jep.33.1.185

Bartik, A. W., Currie, J., Greenstone, M., & Knittel, C. R. (2019, October). The local economic and welfare consequences of hydraulic fracturing. *American Economic Journal: Applied Economics*, *11*(4), 105-55. Retrieved from https://www.aeaweb.org/articles?id=10.1257/app.20170487 doi: 10.1257/app.20170487

Baum-Snow, N., & Han, L. (2024). The microgeography of housing supply. *Journal of Political Economy*, *132*(6), 1897-1946. Retrieved from https://doi.org/10.1086/728110 doi: 10.1086/728110

Bayer, P., Ferreira, F., & McMillan, R. (2007). A unified framework for measuring preferences for schools and neighborhoods. *Journal of Political Economy*, *115*(4), 588-638. Retrieved from https://doi.org/10.1086/522381 doi: 10.1086/522381

Bayer, P., McMillan, R., Murphy, A., & Timmins, C. (2016). A dynamic model of demand for houses and neighborhoods. *Econometrica*, *84*(3), 893–942. doi: 10.3982/ECTA10170

Berry, S. (1994). Estimating discrete-choice models of product differentiation. *The RAND Journal of Economics*, *25*(2), 242–262. doi: 10.2307/2555829

Berry, S., Levinsohn, J., & Pakes, A. (1995). Automobile prices in market equilibrium. *Econometrica*, *63*(4), 841–890. doi: 10.2307/2171802

Black, K. J., Boslett, A. J., Hill, E. L., Ma, L., & McCoy, S. J. (2021). Economic, environmental, and health impacts of the fracking boom [Journal Article]. *Annual Review of Resource Economics*, *13*(Volume 13, 2021), 311-334. Retrieved from https://www.annualreviews.org/content/journals/10.1146/annurev-resource-110320-092648 doi: https://doi.org/10.1146/annurev-resource-110320-092648

Black, K. J., McCoy, S. J., & Weber, J. G. (2018). When externalities are taxed: The effects and incidence of pennsylvania's impact fee on shale gas wells. *Journal of the Association of Environmental and Resource Economists*, *5*(1), 107–153. doi: 10.1086/694034

Borsky, S., Fesselmeyer, E., & Vogelsang, L. (2024). Urban heat and within-city residential sorting. *Journal of Environmental Economics and Management*, *127*, 103014. Retrieved from https://www.sciencedirect.com/science/article/pii/S0095069624000883 doi: https://doi.org/10.1016/j.jeem.2024.103014

Cain, L., Hernandez Cortes, D., Timmins, C., & Weber, P. (2024, 02). Recent findings and methodologies in economics research in environmental justice. *Review of Environmental Economics and Policy*, *18*, 000-000. doi: 10.1086/728100

Carroll, C. D., Crawley, E., Slacalek, J., Tokuoka, K., & White, M. N. (2020, July). Sticky expectations and consumption dynamics. *American Economic Journal: Macroeconomics*, *12*(3), 40–76. Retrieved from https://www.aeaweb.org/articles?id=10.1257/mac.20180286 doi: 10.1257/mac.20180286

Christensen, P., & Timmins, C. (2022). Sorting or steering: The effects of housing discrimination on neighborhood choice. *Journal of Political Economy*, *130*(8), 2110-2163. Retrieved from https://doi.org/10.1086/720140 doi: 10.1086/720140

Clough, E. (2018). Environmental justice and fracking: A review. *Current Opinion in Environmental Science Health*, *3*, 14-18. Retrieved from https://www.sciencedirect.com/science/article/pii/S2468584417300478 (Environmental and Health Risks of Hydraulic Fracturing) doi: https://doi.org/10.1016/j.coesh.2018.02.005

Cruz, W. L., Martínez, J. M., & Raydan, M. (2006). Spectral residual method without gradient information for solving large-scale nonlinear systems of equations. *Mathematics of Computation*, *75*(255), 1429–1448. Retrieved 2025-01-07, from http://www.jstor.org/stable/4100282

Davis, M. A., Gregory, J., Hartley, D. A., & Tan, K. T. K. (2021). Neighborhood effects and housing vouchers. *Quantitative Economics*, *12*(4), 1307–1346. Retrieved from https://doi.org/10.3982/QE1664 doi: 10.3982/QE1664

Depro, B., Timmins, C., & O'Neil, M. (2015). White flight and coming to the nuisance: Can residential mobility explain environmental injustice? *Journal of the Association of Environmental and Resource Economists*, *2*(3), 439–468. doi: 10.1086/682718

Depro, B., Timmins, C., & O'Neil, M. (2015). White flight and coming to the nuisance: Can residential mobility explain environmental injustice? *Journal of the Association of Environmental and Resource Economists*, *2*(3), 439-468. Retrieved from https://doi.org/10.1086/682716

doi: 10.1086/682716

Ding, L., Hwang, J., & Divringi, E. (2016). Gentrification and residential mobility in philadelphia. *Regional Science and Urban Economics*, *61*, 38-51. Retrieved from https://www.sciencedirect.com/science/article/pii/S0166046216301223 doi: https://doi.org/10.1016/j.regsciurbeco.2016.09.004

Ferreira, F., Kenney, J., & Smith, B. (2024). Household mobility, networks, and gentrification of minority neighborhoods in the united states. *Journal of Labor Economics*, *42*(S1), S61-S94. Retrieved from https://doi.org/10.1086/728805 doi: 10.1086/728805

Feyrer, J., Mansur, E. T., & Sacerdote, B. (2017, April). Geographic dispersion of economic shocks: Evidence from the fracking revolution. *American Economic Review*, *107*(4), 1313–34. Retrieved from https://www.aeaweb.org/articles?id=10.1257/aer.20151326 doi: 10.1257/aer.20151326

Fry, M. (2013). Urban gas drilling and distance ordinances in the texas barnett shale. *Energy Policy*, *62*, 79–89. Retrieved from https://www.sciencedirect.com/science/article/pii/S0301421513007507

Fry, M., Brannstrom, C., & Sakinejad, M. (2017). Suburbanization and shale gas wells: Patterns, planning perspectives, and reverse setback policies. *Landscape and Urban Planning*, *168*, 9–21. doi: 10.1016/j.landurbplan.2017.08.005

Gülen, G., Browning, J., Ikonnikova, S., & Tinker, S. W. (2013). Well economics across ten tiers in low and high btu (british thermal unit) areas, barnett shale, texas. *Energy*, *60*, 302–315. doi: 10.1016/j.energy.2013.07.041

Hays, J., McCawley, M., & Shonkoff, S. B. (2017). Public health implications of environmental noise associated with unconventional oil and gas development. *Science of The Total Environment*, *580*, 448-456. Retrieved from https://www.sciencedirect.com/science/article/pii/S0048969716325724 doi: https://doi.org/10.1016/j.scitotenv.2016.11.118

Heblich, S., Trew, A., & Zylberberg, Y. (2020, 12). East side story: Historical pollution and persistent neighborhood sorting. *Journal of Political Economy*, *129*. doi: 10.1086/713101

Herrnstadt, E., Kellogg, R., & Lewis, E. (2024). Drilling deadlines and oil and gas development. *Econometrica*, *92*(1), 29-60. Retrieved from https://onlinelibrary.wiley.com/doi/abs/10.3982/ECTA18436 doi: https://doi.org/10.3982/ECTA18436

Hotz, V. J., & Miller, R. A. (1993, 07). Conditional choice probabilities and the estimation of dynamic models. *The Review of Economic Studies*, *60*(3), 497-529. Retrieved from https://doi.org/10.2307/2298122 doi: 10.2307/2298122

Lucas, R. E. (1976). Econometric policy evaluation: A critique. In K. Brunner & A. H. Meltzer (Eds.), *The phillips curve and labor markets* (Vol. 1, pp. 19–46). New York: American Elsevier. (Archived from the original (PDF) on 2021-11-05)

Maniloff, P., & Mastromonaco, R. (2017). The local employment impacts of fracking: A national study. *Resource and Energy Economics*, *49*, 62-85. Retrieved from https://www.sciencedirect.com/science/article/pii/S0928765516300306 doi: https://doi.org/10.1016/j.reseneeco.2017.04.005

McKenzie, L. M., Witter, R. Z., Newman, L. S., & Adgate, J. L. (2012). Human health risk assessment of air emissions from development of unconventional natural gas resources. *Science of The Total Environment*, *424*, 79-87. Retrieved from https://www.sciencedirect.com/science/article/pii/S0048969712001933 doi: https://doi.org/10.1016/j.scitotenv.2012.02.018

Montgomery, S., Jarvie, D., Bowker, K., & Pollastro, R. (2005, 02). Mississippian barnett shale, fort worth basin, north-central texas: Gas-shale play with multi–trillion cubic foot potential. *AAPG Bulletin*, *89*, 155-175. doi: 10.1306/09170404042

Muehlenbachs, L., Spiller, E., & Timmins, C. (2015). The housing market impacts of shale gas development. *American Economic Review*, *105*(12), 3633–3659. doi: 10.1257/aer.20140079

Nevo, A. (2000). A practitioner's guide to estimation of random-coefficients logit models of demand. *Journal of Economics & Management Strategy*, *9*(4), 513-548. Retrieved from https://onlinelibrary.wiley.com/doi/abs/10.1111/j.1430-9134.2000.00513.x doi: https://doi.org/10.1111/j.1430-9134.2000.00513.x

Patzek, T. W., Male, F., & Marder, M. (2013). Gas production in the barnett shale obeys a simple scaling theory. *Proceedings of the National Academy of Sciences*, *110*(49), 19731-19736. Retrieved from https://www.pnas.org/doi/abs/10.1073/pnas.1313380110 doi: 10.1073/pnas.1313380110

Pollastro, R., Jarvie, D., Hill, R., & Adams, C. (2007, 04). Geologic framework of the mississippian barnett shale, barnett-paleozoic total petroleum system, bend arch–fort worth basin, texas.

Aapg Bulletin - AAPG BULL, *91*, 405-436. doi: 10.1306/10300606008

Rust, J. (1987). Optimal replacement of gmc bus engines: An empirical model of harold zurcher. *Econometrica*, *55*(5), 999–1033. Retrieved 2025-01-04, from http://www.jstor.org/stable/1911259

Shcherbakov, O. (2016). Measuring consumer switching costs in the television industry. *The RAND Journal of Economics*, *47*(2), 366–393. Retrieved 2025-08-10, from http://www.jstor.org/stable/43895649

Thomas, P., Collins, A., Etienne, X., & Mugabe, D. (2024). Impacts of state tax and resource ownership policies on extraction: Evidence from U.S. natural gas production. *Energy Economics*, *138*, 107869. doi: 10.1016/j.eneco.2024.107869

Timmins, C., & Vissing, A. (2022). Environmental justice and coasian bargaining: The role of race, ethnicity, and income in lease negotiations for shale gas. *Journal of Environmental Economics and Management*, *114*, 102657. Retrieved from https://www.sciencedirect.com/science/article/pii/S0095069622000353 doi: https://doi.org/10.1016/j.jeem.2022.102657

Yeo, J., & Miller, D. P. (2018). Estimating switching costs with market share data: an application to medicare part d. *International Journal of Industrial Organization*, *61*, 459-501. Retrieved from https://www.sciencedirect.com/science/article/pii/S0167718717303053 doi: https://doi.org/10.1016/j.ijindorg.2018.08.005

Zwickl, K. (2019). The demographics of fracking: A spatial analysis for four u.s. states. *Ecological Economics*, *161*, 202-215. Retrieved from https://www.sciencedirect.com/science/article/pii/S092180091830661X doi: https://doi.org/10.1016/j.ecolecon.2019.02.001

A Counterfactual Equilibrium: Algorithm, Uniqueness, and Numerical Checks

This section describes the computational methods and theoretical discussions behind the counterfactual analysis in Section 8.1. Note that even a local change in per-period utility triggers a system-wide adjustment in choice specific value to meet the bellman system defined in the following equation

$$CV_{jt} = f_j(\Omega_t) + \beta E\left[\ln\left(\exp(CV_{jt+1}) + \sum_{l\in\mathcal{J}\setminus\{j\}} \exp(CV_{lt+1} - sc_{t+1})\right) + \gamma \mid \Omega_t\right], \ \forall j, \qquad (29)$$

which is derived from rewriting equation 6, using equation 7. Thus, in constructing a counterfactual, the key is to find a unique fixed point CV_t' that satisfies equation 29, given any change in the mean per-period utilities f_t'.

Accordingly, calculating the counterfactual equilibrium has two layers. For any candidate current rent vector p_t, the inner layer solves the counterfactual choice-specific values $CV_t'(p_t)$. The outer layer then chooses p_t so that the residential demand in equation 11 equals the housing supply in equation 12 in every inside census tract j. Section A.1 introduces the equilibrium solver. Section A.2 proves that the inner layer has a unique solution. The remaining sections, prove existence of a housing-market equilibrium, prove global uniqueness in the static model, establish local uniqueness of an equilibrium in the dynamic model, and report numerical exercise for the dynamic counterfactual equilibria.

A.1 Equilibrium solver

In this section, I describe the computational process that is used to conduct general equilibrium analysis in counterfactual simulations. The key in the process is to find a unique equilibrium price that equates housing supply, and demand for all the census tracts.[66]

[66] As I allow the resident's belief about the future values to be sticky, I do not impose a restriction on equilibrium belief in counterfactual simulations.

Inner loop: counterfactual choice-specific values

Theorem 1 below implies that one can come up with an iterative algorithm that solves for a unique CV_t' given any initial guess on the new CV_t, once we know all the model parameters. Dropping the group subscript g, the CV_t' can be uniquely calculated by following these steps.

1. Set a small tolerance level ϵ, and come up with any initial guess $CV_t^{(0)}$. Draw a large number ($s = 1, \ldots, S$) of innovations $\omega_{t+1}^{(s)}$ from the empirical distribution of ω. The draws are generated once and held fixed across iterations.

2. For all j, simulate $CV_{j,t+1}^{(s,0)}$ from equation 20, using $\hat{\gamma}$, the current guess $CV_t^{(0)}$, and the draws $\omega_{t+1}^{(s)}$.

3. Using the S simulations, for each j, calculate the expectation in equation 29 by Monte Carlo simulation, setting $sc_{t+1} = sc_t$ as in equation 21:[67]

$$\frac{1}{S}\sum_{s=1}^{S} \ln\left(\exp\left(CV_{j,t+1}^{(s,0)}\right) + \sum_{i\neq j}\exp\left(CV_{i,t+1}^{(s,0)} - sc_t\right)\right) + \gamma$$

4. For all j, update $CV_t^{(0)}$ to $CV_t^{(1)}$, following

$$CV_{j,t}^{(1)} = f_{jt}' + \beta\left[\frac{1}{S}\sum_{s=1}^{S} \ln\left(\exp\left(CV_{j,t+1}^{(s,0)}\right) + \sum_{i\neq j}\exp\left(CV_{i,t+1}^{(s,0)} - sc_t\right)\right) + \gamma\right]$$

5. If $\|CV_t^{(1)} - CV_t^{(0)}\|_\infty < \epsilon$, set $\widehat{CV}_t' = CV_t^{(1)}$. Otherwise, repeat from step 2 with the updated guess $CV_t^{(n)}$ until $\|CV_t^{(n+1)} - CV_t^{(n)}\|_\infty < \epsilon$, and set $\widehat{CV}_t' = CV_t^{(n+1)}$.

Outer loop: market-clearing rents

The equilibrium solver searches for a unique price vector that equates housing supply and demand in every census tract. Given the assumption on the timing of moving and housing stock adjustment, the problem is to find a vector of prices p_t that satisfies $N_{j,t+1}(p_t, X_t', \xi_t \mid N_{jt}) = S_{j,t+1}(p_{jt})$, $\forall j$, where $N_{j,t+1}$ is the housing demand in equation 11, $S_{j,t+1}$ is the calibrated supply function in

[67] This follows the simplifying assumption in Estimation Step 2. Relaxing it, one would draw $\widetilde{sc}_{t+1}^{(s)}$ alongside $CV_{j,t+1}^{(s,0)}$ in step 2 and replace sc_t with $\widetilde{sc}_{t+1}^{(s)}$ inside the logarithm. This does not affect Theorem 1.

equation 12, and X'_t collects the counterfactual location characteristics, including the post-removal well exposure w'. ξ_t denotes the estimated unobserved location quality, which is held fixed across the counterfactual.

Starting from the initial period, the tâtonnement process to search for the counterfactual equilibrium proceeds as follows.

1. Set tolerance level ϵ.
2. With counterfactual characteristics, come up with an initial guess on equilibrium price, p_t^0.
3. (Inner Loop) With counterfactual characteristics and a guess on price, for each group g, iterate on CV_{gt} to find the counterfactual choice-specific values CV'_{gt}, using the value iteration described above.
4. Calculate excess demand for each census tract, defined as

$$ED_{j,t+1}(p_t, X'_t, \xi_t) \equiv N_{j,t+1}(p_t, X'_t, \xi_t | N_{jt}) - S_{j,t+1}(p_{jt}),\ \forall j. \tag{30}$$

5. If $||ED_{t+1}(p_t, X'_t, \xi_t)|| \leq \epsilon$, set the current guess as the counterfactual equilibrium price p'_t, and move on to the next period, updating the next-period racial composition r'_t of each census tract. If $||ED_{t+1}(p_t, X'_t, \xi_t)|| > \epsilon$, move on to the next step.
6. Update the guess on price as

$$p_{jt}^{n+1} = p_{jt}^n + \delta \cdot ED_{j,t+1}(p_t, X'_t, \xi_t)/(ED_{j,t+1}(p_t, X'_t, \xi_t) + S_{j,t+1}(p_{jt})),\ \forall j$$

   where δ stands for an appropriate tuning parameter. Move to step 3, repeat until convergence.

While the theory does not predict the guaranteed convergence, in practice this iterative procedure converged to the same price vector from a large number of random starting guesses. Section A.6 reports this exercise. Figure 10 summarizes the entire process of this equilibrium solver.

A.2 Uniqueness of counterfactual choice-specific values

I suppress the demographic-group subscript g throughout this subsection. The argument is applied separately to every group, with that group's estimated transition parameters. There are J inside

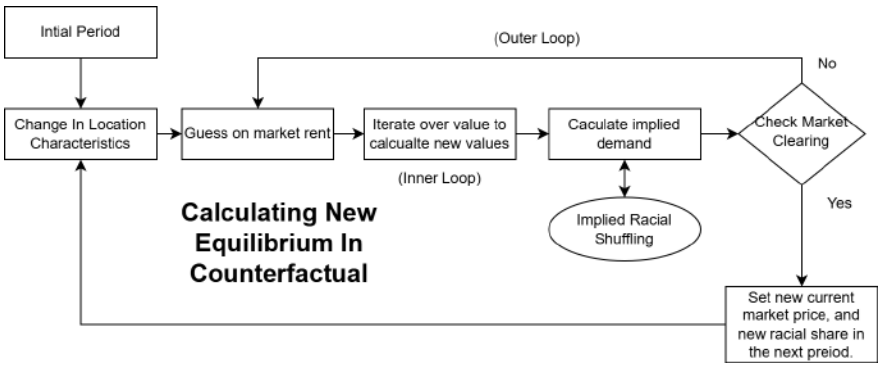


Figure 10: Flow-Chart for Iterative Equilibrium Finder

census tracts and the outside option $J+1$, with choice set $\mathcal{J} \equiv \{1, \ldots, J, J+1\}$. As in section 5, the outside option is terminal for residents, and its choice-specific value is normalized to zero, $CV_{J+1,t} = 0$. Every iteration for choice specific values below therefore practically runs on the J inside values,

$$CV_t \equiv (CV_{1t}, \ldots, CV_{Jt})^\top \in \mathbb{R}^J. \tag{31}$$

Shifting equation 20 one period forward gives, for every inside tract j,

$$CV_{j,t+1} = \gamma_{0,j} + \gamma_{1,1} CV_{jt} + \sum_{l=2}^{L} \gamma_{1,l} CV_{j,t+1-l} + \sum_{l=1}^{L} X_{j,t+1-l}^{\prime\top} \gamma_{2,l} + \gamma_3 (t+1) + \omega_{j,t+1}. \tag{32}$$

Solving for the choice specific values at t, the lagged values $CV_{j,t-1}, \ldots, CV_{j,t+1-L}$ are already known as they are either derived from observed equilibrium or counterfactual values solved in earlier periods. The covariates $X'_{j,t+1-l}$ are the counterfactual characteristics. Every element that enters equation 32 is determined before the location choices are made at t, and in particular the neighborhood composition in X'_{jt} is determined at the beginning of t, and the current rent p_{jt} enters through X'_{jt}. Hence the only object in equation 32 that varies during the inner fixed-point iteration is CV_{jt}. For a candidate vector CV_t and a realization of ω_{t+1}, let $\widetilde{CV}_{t+1}(CV_t, \omega_{t+1})$ denote the J-vector of one-period-ahead forecasts obtained from equation 32 while its dependence on p_t and on the predetermined terms is left implicit.

For an inside origin j, the expected value function in Equation 7, written as an explicit function of the next-period inside values $CV_{t+1} = (CV_{1,t+1}, \ldots, CV_{J,t+1})^\top$ and the next-period moving cost

sc_{t+1}, is

$$EV_j(CV_{t+1}, sc_{t+1}) \equiv \ln \left[\exp(CV_{j,t+1}) + \sum_{\substack{l=1 \\ l \neq j}}^{J} \exp(CV_{l,t+1} - sc_{t+1}) + \exp(-sc_{t+1}) \right] + \gamma, \tag{33}$$

where γ is Euler's constant, so that $EV_j(CV_{t+1}, sc_{t+1}) = EV(j, \Omega_{t+1})$.

For a counterfactual flow utility f'_{jt}, define the operator $T : \mathbb{R}^J \to \mathbb{R}^J$ component by component as

$$T(CV_t)_j = f'_{jt} + \beta E \left[EV_j\left(\widetilde{CV}_{t+1}(CV_t, \omega_{t+1}), sc_{t+1} \right) \mid \Omega_t \right], \qquad j = 1, \ldots, J. \tag{34}$$

The expectation is taken over the value innovation ω_{t+1} and the moving cost sc_{t+1} given Ω_t, with $E[\|\omega_{t+1}\|_\infty \mid \Omega_t] < \infty$ and $E[|sc_{t+1}| \mid \Omega_t] < \infty$. A counterfactual value vector CV'_t is a fixed point of T, that is, a solution of equation 29 with f'_t in place of f_t.

Lemma 1 (The expected value function has a Lipschitz constant of 1)**.** *For every inside origin j, every moving cost sc_{t+1}, and any $CV_{t+1}, CV^\circ_{t+1} \in \mathbb{R}^J$,*

$$\left| EV_j(CV_{t+1}, sc_{t+1}) - EV_j(CV^\circ_{t+1}, sc_{t+1}) \right| \leq \|CV_{t+1} - CV^\circ_{t+1}\|_\infty. \tag{35}$$

Proof. Take a convex combination of the two vectors by $CV_{t+1}(a) = CV^\circ_{t+1} + a(CV_{t+1} - CV^\circ_{t+1})$, $a \in [0, 1]$. For each inside destination m,

$$\frac{\partial EV_j(CV_{t+1}(a), sc_{t+1})}{\partial CV_{m,t+1}} = \frac{\exp(CV_{m,t+1}(a) - sc_{t+1}\mathbb{1}(m \neq j))}{\exp(CV_{j,t+1}(a)) + \sum_{\substack{l=1 \\ l \neq j}}^{J} \exp(CV_{l,t+1}(a) - sc_{t+1}) + \exp(-sc_{t+1})}. \tag{36}$$

These derivatives are nonnegative. Their sum over $m = 1, \ldots, J$ is the probability of choosing an inside location, which is strictly below one because the outside-option term $\exp(-sc_{t+1})$ is strictly positive. By the fundamental theorem of calculus,

$$EV_j(CV_{t+1}, sc_{t+1}) - EV_j(CV^\circ_{t+1}, sc_{t+1}) = \int_0^1 \sum_{m=1}^{J} \frac{\partial EV_j(CV_{t+1}(a), sc_{t+1})}{\partial CV_{m,t+1}} (CV_{m,t+1} - CV^\circ_{m,t+1})\, da, \tag{37}$$

so

$$\begin{aligned}
&\left|EV_j(CV_{t+1}, sc_{t+1}) - EV_j(CV^{\circ}_{t+1}, sc_{t+1})\right| \\
&\quad \leq \|CV_{t+1} - CV^{\circ}_{t+1}\|_{\infty} \int_0^1 \sum_{m=1}^{J} \frac{\partial EV_j(CV_{t+1}(a), sc_{t+1})}{\partial CV_{m,t+1}}\, da \\
&\quad \leq \|CV_{t+1} - CV^{\circ}_{t+1}\|_{\infty}. \qquad (38)
\end{aligned}$$

□

Note that if the outside option were dropped from equation 33, the sum of the derivatives in equation 38 would equal one and the conclusion of this lemma would still hold.

Theorem 1 (Unique counterfactual choice-specific values)**.** *Suppose*

$$\kappa \equiv \beta|\gamma_{1,1}| < 1. \qquad (39)$$

Then T is a contraction on $(\mathbb{R}^J, \|\cdot\|_{\infty})$ with modulus κ. I.e., for any $CV_t, CV_t^{\circ} \in \mathbb{R}^J$,

$$\|T(CV_t) - T(CV_t^{\circ})\|_{\infty} \leq \kappa \|CV_t - CV_t^{\circ}\|_{\infty}. \qquad (40)$$

Consequently, (i) there exists a unique fixed point $CV_t' \in \mathbb{R}^J$; (ii) from any starting vector $CV_t^{(0)} \in \mathbb{R}^J$, the sequence $CV_t^{(n)} = T(CV_t^{(n-1)})$ converges to CV_t'; and (iii) the iteration has the a posteriori error bound

$$\|CV_t^{(n)} - CV_t'\|_{\infty} \leq \frac{\kappa}{1-\kappa} \|CV_t^{(n)} - CV_t^{(n-1)}\|_{\infty}. \qquad (41)$$

Proof. First, I show that T is well defined, that is, the expectation in equation 34 is finite. The argument of the logarithm in equation 33 is a sum of $J+1$ positive terms. Keeping only the first term gives a lower bound, and bounding each of the $J+1$ terms by the largest possible value gives an upper bound:

$$\begin{aligned}
&EV_j(CV_{t+1}, sc_{t+1}) \geq \ln\left[\exp(CV_{j,t+1})\right] + \gamma = CV_{j,t+1} + \gamma \geq -\|CV_{t+1}\|_{\infty} + \gamma, \\
&EV_j(CV_{t+1}, sc_{t+1}) \leq \ln\left[(J+1)\exp(\|CV_{t+1}\|_{\infty} + |sc_{t+1}|)\right] + \gamma = \|CV_{t+1}\|_{\infty} + |sc_{t+1}| + \ln(J+1) + \gamma,
\end{aligned} \qquad (42)$$

where the upper bound uses $CV_{j,t+1} \leq \|CV_{t+1}\|_\infty$, $CV_{l,t+1} - sc_{t+1} \leq \|CV_{t+1}\|_\infty + |sc_{t+1}|$, and $-sc_{t+1} \leq |sc_{t+1}|$. Hence

$$|EV_j(CV_{t+1}, sc_{t+1})| \leq \|CV_{t+1}\|_\infty + |sc_{t+1}| + \ln(J+1) + \gamma. \tag{43}$$

Next, rewrite the one-period ahead forecast in equation 32 as $\widetilde{CV}_{t+1}(CV_t, \omega_{t+1}) = c_t + \omega_{t+1}$, where c_t collects the terms that do not involve ω_{t+1} and is a fixed vector given CV_t and Ω_t. Therefore $\|\widetilde{CV}_{t+1}\|_\infty \leq \|c_t\|_\infty + \|\omega_{t+1}\|_\infty$, and substituting into equation 43 and taking expectations,

$$E\left[\left|EV_j(\widetilde{CV}_{t+1}, sc_{t+1})\right| \mid \Omega_t\right] \leq \|c_t\|_\infty + E[\|\omega_{t+1}\|_\infty \mid \Omega_t] + E[|sc_{t+1}| \mid \Omega_t] + \ln(J+1) + |\gamma| < \infty, \tag{44}$$

by the finite first moments assumed above. The expectation in equation 34 therefore exists and is finite for every $CV_t \in \mathbb{R}^J$.

Now, take two candidate vectors CV_t and CV_t° and fix the same realization of (ω_{t+1}, sc_{t+1}) for both evaluations. Every predetermined term in equation 32 cancels when the two forecasts are subtracted. For every destination m,

$$\widetilde{CV}_{m,t+1}(CV_t, \omega_{t+1}) - \widetilde{CV}_{m,t+1}(CV_t^\circ, \omega_{t+1}) = \gamma_{1,1}(CV_{mt} - CV_{mt}^\circ), \tag{45}$$

so

$$\left\|\widetilde{CV}_{t+1}(CV_t, \omega_{t+1}) - \widetilde{CV}_{t+1}(CV_t^\circ, \omega_{t+1})\right\|_\infty = |\gamma_{1,1}| \, \|CV_t - CV_t^\circ\|_\infty. \tag{46}$$

Applying Lemma 1 to every realization of (ω_{t+1}, sc_{t+1}) gives, for every origin j,

$$\left|EV_j\left(\widetilde{CV}_{t+1}(CV_t, \omega_{t+1}), sc_{t+1}\right) - EV_j\left(\widetilde{CV}_{t+1}(CV_t^\circ, \omega_{t+1}), sc_{t+1}\right)\right| \leq |\gamma_{1,1}| \, \|CV_t - CV_t^\circ\|_\infty. \tag{47}$$

This bound holds for every realization of (ω_{t+1}, sc_{t+1}), and its right side is a constant that does

not depend on the realization. Since f'_{jt} is common to both candidates, equation 34 gives

$$\begin{aligned}|T(CV_t)_j - T(CV_t^\circ)_j| &= \beta \left| E\left[EV_j\Big(\widetilde{CV}_{t+1}(CV_t, \omega_{t+1}), sc_{t+1}\Big) - EV_j\Big(\widetilde{CV}_{t+1}(CV_t^\circ, \omega_{t+1}), sc_{t+1}\Big) \mid \Omega_t \right] \right| \\ &\leq \beta\, E\left[\left| EV_j\Big(\widetilde{CV}_{t+1}(CV_t, \omega_{t+1}), sc_{t+1}\Big) - EV_j\Big(\widetilde{CV}_{t+1}(CV_t^\circ, \omega_{t+1}), sc_{t+1}\Big) \right| \mid \Omega_t \right] \\ &\leq \beta\, E\left[|\gamma_{1,1}|\, \|CV_t - CV_t^\circ\|_\infty \mid \Omega_t \right] = \beta |\gamma_{1,1}|\, \|CV_t - CV_t^\circ\|_\infty, \end{aligned} \tag{48}$$

where the first inequality follows from $|E[Y \mid \Omega_t]| \leq E[|Y| \mid \Omega_t]$ and the second inequality follows from equation 47. The last line does not depend on j, so taking the maximum over $j = 1, \ldots, J$ on the left side proves equation 40. Since $(\mathbb{R}^J, \|\cdot\|_\infty)$ is complete and $\kappa < 1$, the Banach fixed-point theorem implies (i) and (ii).

For (iii), repeated application of equation 40 gives $\|CV_t^{(n+r)} - CV_t^{(n+r-1)}\|_\infty \leq \kappa^r \|CV_t^{(n)} - CV_t^{(n-1)}\|_\infty$. Hence, for $m > n$,

$$\|CV_t^{(m)} - CV_t^{(n)}\|_\infty \leq \sum_{r=1}^{m-n} \kappa^r \, \|CV_t^{(n)} - CV_t^{(n-1)}\|_\infty \leq \frac{\kappa}{1-\kappa} \|CV_t^{(n)} - CV_t^{(n-1)}\|_\infty. \tag{49}$$

Letting $m \to \infty$ yields equation 41. □

Remark 1. In practice, I use $L = 1$, and do not include linear trend in equation 32. Note that only the first lag $\gamma_{1,1}$ enters the contraction modulus, because every value lag beyond the first is predetermined at the period-t solve, and the sign of $\gamma_{1,1}$ is irrelevant as the condition is on its absolute value. The lag length L changes nothing else in this appendix as lagged values and lagged covariates, including lagged rents, are absorbed into the predetermined part of equation 32, which no later argument uses.

The inner loop in Section A.1 replaces the expectation in equation 34 by an average of Monte Carlo simulations. The next result shows that the implementation inherits Theorem 1 if the draws are held fixed across iterations.

Corollary 1 (Monte Carlo value iteration)**.** *Fix S draws $\{(\omega_{t+1}^{(s)}, sc_{t+1}^{(s)})\}_{s=1}^S$ once, before the iteration starts, and define*

$$T^S(CV_t)_j = f'_{jt} + \frac{\beta}{S} \sum_{s=1}^{S} EV_j\Big(\widetilde{CV}_{t+1}(CV_t, \omega_{t+1}^{(s)}), sc_{t+1}^{(s)}\Big). \tag{50}$$

Under equation 39, T^S is a contraction on $(\mathbb{R}^J, \|\cdot\|_\infty)$ with the same modulus κ. It has a unique fixed point $CV_t'^{,S}$, the iteration $CV_t^{(n)} = T^S(CV_t^{(n-1)})$ converges to it from any starting vector, the bound in equation 41 applies with $CV_t'^{,S}$ in place of CV_t', and

$$\|CV_t'^{,S} - CV_t'\|_\infty \leq \frac{1}{1-\kappa}\|T^S(CV_t') - T(CV_t')\|_\infty. \tag{51}$$

Proof. Equation 47 holds for each draw s separately. Averaging over the fixed draws gives Equation 48 with T^S in place of T, so Equation 40 holds for T^S and the Banach fixed-point theorem applies as before. For equation 51, use the two fixed-point conditions $CV_t'^{,S} = T^S(CV_t'^{,S})$ and $CV_t' = T(CV_t')$, add and subtract $T^S(CV_t')$, and apply the triangle inequality:

$$\begin{aligned}
\|CV_t'^{,S} - CV_t'\|_\infty &= \|T^S(CV_t'^{,S}) - T(CV_t')\|_\infty \\
&\leq \|T^S(CV_t'^{,S}) - T^S(CV_t')\|_\infty + \|T^S(CV_t') - T(CV_t')\|_\infty \\
&\leq \kappa\,\|CV_t'^{,S} - CV_t'\|_\infty + \|T^S(CV_t') - T(CV_t')\|_\infty,
\end{aligned} \tag{52}$$

where the last step uses that T^S is a contraction with modulus κ. Rearranging the terms in $\|CV_t'^{,S} - CV_t'\|_\infty$ on the left and dividing the both sides by $1-\kappa > 0$ gives equation 51. □

Remark 2. If instead the S draws were refreshed at every iteration, the sequence $CV_t^{(n)}$ would be a stochastic process, the stopping rule $\|CV_t^{(n+1)} - CV_t^{(n)}\|_\infty < \epsilon$ could be triggered by simulation noise, and neither (ii) nor (iii) of Theorem 1 would apply.

Note that the term on the right hand side of equation 51 is the Monte Carlo error of T^S at the exact fixed point CV_t'. Due to the construction of the Monte Carlo simulations, it can be shown that as $S \to \infty$, the error converges to zero almost surely.

Lemma 2 (Consistency of the Monte Carlo operator T^S)**.** *Suppose the draws $\{(\omega_{t+1}^{(s)}, sc_{t+1}^{(s)})\}_{s=1}^S$ are independent and identically distributed according to the conditional distribution of (ω_{t+1}, sc_{t+1}) given Ω_t, and that $E[\|\omega_{t+1}\|_\infty \mid \Omega_t] < \infty$ and $E[|sc_{t+1}| \mid \Omega_t] < \infty$. Then*

$$\|T^S(CV_t') - T(CV_t')\|_\infty \to 0 \qquad \text{almost surely as } S \to \infty, \tag{53}$$

and consequently $\|CV_t'^{,S} - CV_t'\|_\infty \to 0$ almost surely. If in addition $E[\|\omega_{t+1}\|_\infty^2 \mid \Omega_t] < \infty$ and

$E[sc_{t+1}^2 \mid \Omega_t] < \infty$, *then* $\|T^S(CV_t') - T(CV_t')\|_\infty = O_p(S^{-1/2})$.

Proof. Take any inside j and define

$$Z_j^{(s)} \equiv EV_j\Big(\widetilde{CV}_{t+1}(CV_t', \omega_{t+1}^{(s)}), sc_{t+1}^{(s)}\Big), \qquad s = 1, \ldots, S. \tag{54}$$

Because CV_t' is a fixed vector given Ω_t, each $Z_j^{(s)}$ is a function of the sth draw alone, so the $Z_j^{(s)}$ are independent and identically distributed with mean $E[Z_j^{(1)} \mid \Omega_t] = E[EV_j(\widetilde{CV}_{t+1}(CV_t', \omega_{t+1}), sc_{t+1}) \mid \Omega_t]$. The flow utility f_{jt}' is common to T^S and T, so equations 34 and 50 give

$$T^S(CV_t')_j - T(CV_t')_j = \beta \left[\frac{1}{S}\sum_{s=1}^{S} Z_j^{(s)} - E[Z_j^{(1)} \mid \Omega_t]\right]. \tag{55}$$

Equation 43 and the finite first moments give $E[|Z_j^{(1)}| \mid \Omega_t] < \infty$, so the strong law of large numbers implies that the right side of equation 55 converges to zero almost surely. Since j ranges over a finite set, the maximum over j also converges to zero almost surely, which is equation 53. The convergence of $CV_t'^{,S}$ then follows from equation 51. Under finite second moments, equation 43 gives $\mathrm{Var}(Z_j^{(1)} \mid \Omega_t) < \infty$, and the central limit theorem applied to equation 55 gives the rate of convergence as $S^{-1/2}$. □

A.3 Housing-market equilibrium and its rent derivative

I now restore the demographic-group subscript g. For each candidate p_t in the inner iteration, Theorem 1 gives one counterfactual value vector $CV_{gt}'(p_t)$. Substituting it into equation 9 gives, for destination $j \in \mathcal{J}$ and origin $k \in \mathcal{J}$,

$$P_{jkgt}(p_t) = \frac{\exp\Big(CV_{jgt}'(p_t) - CV_{kgt}'(p_t) - sc_{gt}\mathbb{1}(j \neq k)\Big)}{\sum_{l=1}^{J+1}\exp\Big(CV_{lgt}'(p_t) - CV_{kgt}'(p_t) - sc_{gt}\mathbb{1}(l \neq k)\Big)}, \tag{56}$$

with $CV_{J+1,gt}' = 0$. Therefore Equation 11 becomes

$$N_{j,t+1}(p_t) = \sum_{g\in\mathcal{G}}\sum_{k\in\mathcal{J}} N_{kgt}P_{jkgt}(p_t), \qquad j = 1, \ldots, J, \tag{57}$$

where, as in section 5, $N_{J+1,g,t}$ is the number of potential in-migrants from outside the market. Recall that housing supply is equation 12,

$$S_{j,t+1}(p_{jt}) = \lambda_{jt} p_{jt}^{\varphi}. \tag{58}$$

Holding the current population N_{kgt}, counterfactual characteristics X_t', and unobserved location amenities ξ_t fixed, define

$$ED_{j,t+1}(p_t) \equiv N_{j,t+1}(p_t) - S_{j,t+1}(p_{jt}), \qquad j = 1, \ldots, J. \tag{59}$$

similar to the excess-demand object in equation 30, with the fixed arguments X_t', ξ_t, and N_{jt} suppressed for notational simplicity.

Derivative of counterfactual choice-specific values

Take any group g. Suppressing g for parameters in equation 32, let $\gamma_{2p,1}$ denote the element of $\gamma_{2,1}$ multiplying rent in equation 32.[68] Equation 23 gives

$$\frac{\partial f'_{jgt}}{\partial p_{mt}} = \theta_{gp} \mathbb{1}(j = m). \tag{60}$$

From equation 32,

$$\frac{\partial CV_{lg,t+1}}{\partial CV'_{mgt}} = \gamma_{1,1} \mathbb{1}(l = m), \qquad \left.\frac{\partial CV_{lg,t+1}}{\partial p_{mt}}\right|_{CV'_{gt} \text{ fixed}} = \gamma_{2p,1} \mathbb{1}(l = m). \tag{61}$$

Next differentiate the expected value function. Equation 36 is the next-period logit probability of choosing inside destination l when the resident begins the next period in inside origin j. Therefore

$$\frac{\partial EV_j}{\partial CV_{lg,t+1}} = P_{ljg,t+1}. \tag{62}$$

Define

$$A_{g,jl,t}(p_t) \equiv E\left[P_{ljg,t+1} \mid \Omega_{gt}\right], \qquad j, l = 1, \ldots, J, \tag{63}$$

[68] With $L > 1$, the rent coefficients in the $l \geq 2$ terms multiply predetermined rents and never enter a derivative with respect to p_t.

and let $A_{gt}(p_t)$ denote the $J \times J$ matrix with elements $A_{g,jl,t}(p_t)$. Each row j of $A_{gt}(p_t)$ is the expected distribution of next-period destinations for a group-g resident who begins the next period in tract j, so $A_{gt}(p_t)$ is the expected next-period transition matrix over inside tracts. Because choosing the outside option has positive probability, each row sum is strictly below one while the missing mass is the expected probability of choosing the outside option.

Assuming differentiability[69], let

$$D_{g,jm,t}(p_t) \equiv \frac{\partial CV'_{jgt}(p_t)}{\partial p_{mt}}. \tag{64}$$

Differentiating the fixed-point condition $CV'_{gt} = T(CV'_{gt})$ in equation 34 with respect to p_{mt} and applying equations 60–62 gives

$$D_{g,jm,t} = \theta_{gp}\mathbb{1}(j = m) + \beta \sum_{l=1}^{J} A_{g,jl,t} \left[\gamma_{1,1} D_{g,lm,t} + \gamma_{2p,1}\mathbb{1}(l = m)\right]. \tag{65}$$

Stacking first over j and then over m,

$$D_{gt} = \theta_{gp} I_J + \beta\gamma_{1,1} A_{gt} D_{gt} + \beta\gamma_{2p,1} A_{gt}, \tag{66}$$

where $D_{gt} \equiv \partial CV'_{gt}/\partial p_t^\top$. Since $\|\cdot\|_\infty$ applied to a matrix is the maximum absolute row sum, $\|A_{gt}\|_\infty < 1$, and therefore

$$\|\beta\gamma_{1,1} A_{gt}\|_\infty = \beta|\gamma_{1,1}| \, \|A_{gt}\|_\infty \beta|\gamma_{1,1}| < 1, \tag{67}$$

where the last inequality comes from the condition of Theorem 1. Note that for any $J \times J$ matrix B with $\|B\|_\infty < 1$, the geometric series of matrices $\sum_{k=0}^{\infty} B^k$ converges and equals $(I_J - B)^{-1}$, so $I_J - \beta\gamma_{1,1} A_{gt}$ is nonsingular with[70]

$$(I_J - \beta\gamma_{1,1} A_{gt})^{-1} = \sum_{k=0}^{\infty} (\beta\gamma_{1,1} A_{gt})^k. \tag{68}$$

[69] I prove that counterfactual choice-specific values are continuously differentiable in p_t later.

[70] The series has a direct interpretation. A change in current rents shifts next-period values, which feeds back into current values through the belief coefficient $\gamma_{1,1}$ and the transition matrix A_{gt}, and each round of feedback is attenuated by $\beta|\gamma_{1,1}|$ times the probability of remaining inside the market.

Rearranging Equation 66,

$$\frac{\partial CV'_{gt}}{\partial p_t^\top} = \left(I_J - \beta\gamma_{1,1}A_{gt}\right)^{-1}\left(\theta_{gp}I_J + \beta\gamma_{2p,1}A_{gt}\right). \tag{69}$$

This can be calculated separately for every group using that group's estimated transition parameters.

It remains to verify the differentiability assumed above.

Lemma 3 (Differentiability of the counterfactual choice-specific values)**.** *Suppose* $\beta|\gamma_{1,1}| < 1$*. Then the fixed point* $CV'_{gt}(p_t)$ *of Theorem 1 is continuously differentiable in* p_t *on* $\mathbb{R}^J_{++}$*.*

Proof. Fix group g and write the fixed-point condition as $\Psi(CV_{gt}, p_t) \equiv CV_{gt} - T(CV_{gt}; p_t) = 0$, where $T(\cdot\,; p_t)$ is the operator in equation 34.

The rent vector enters T in two places: in f'_{jgt} through the term $\theta_{gp}p_{jt}$ in equation 23, and in $\widetilde{CV}_{g,t+1}$ through the element of X'_{jt} in equation 32. Both are linear in p_{jt}. Hence the integrand $EV_j(\widetilde{CV}_{g,t+1}(CV_{gt}, \omega_{t+1}; p_t), sc_{g,t+1})$ inside the expectation in equation 34 is continuously differentiable in (CV_{gt}, p_t) for every realization ω_{t+1}, and by equations 61 and 62 its derivatives are choice probabilities times $\gamma_{1,1}$ or $\gamma_{2p,1}$, hence bounded.

Differentiation under the expectation is therefore allowed, and Ψ is continuously differentiable with $\partial\Psi/\partial CV_{gt}^\top = I_J - \beta\gamma_{1,1}A_{gt}$, which is nonsingular as shown after equation 66. The implicit function theorem gives a continuously differentiable solution of $\Psi = 0$ near every p_t, and by the uniqueness in Theorem 1 that solution is $CV'_{gt}(\cdot)$. □

Derivative of housing demand and excess demand

Canceling the common term $-CV'_{kgt}$ in equation 56 yields

$$P_{jkgt}(p_t) = \frac{\exp\Big(CV'_{jgt}(p_t) - sc_{gt}\mathbb{1}(j \neq k)\Big)}{\sum_{r=1}^{J+1}\exp\big(CV'_{rgt}(p_t) - sc_{gt}\mathbb{1}(r \neq k)\big)}. \tag{70}$$

For inside destinations $j, l \leq J$, direct differentiation gives

$$\begin{aligned}\frac{\partial P_{jkgt}}{\partial CV'_{lgt}} &= P_{jkgt}\mathbb{1}(j=l) - P_{jkgt}P_{lkgt} \\ &= P_{jkgt}\left[\mathbb{1}(j=l) - P_{lkgt}\right]. \end{aligned} \tag{71}$$

Hence, differentiating equation 57 with respect to p_{mt},

$$\begin{aligned}\frac{\partial N_{j,t+1}}{\partial p_{mt}} &= \sum_{g\in\mathcal{G}}\sum_{k\in\mathcal{J}} N_{kgt}\sum_{l=1}^{J}\frac{\partial P_{jkgt}}{\partial CV'_{lgt}}\frac{\partial CV'_{lgt}}{\partial p_{mt}} \\ &= \sum_{g\in\mathcal{G}}\sum_{l=1}^{J}\left[\sum_{k\in\mathcal{J}} N_{kgt}P_{jkgt}\left(\mathbb{1}(j=l) - P_{lkgt}\right)\right] D_{g,lm,t}. \end{aligned} \tag{72}$$

Define

$$M_{g,jl,t}(p_t) \equiv \sum_{k\in\mathcal{J}} N_{kgt}P_{jkgt}\left[\mathbb{1}(j=l) - P_{lkgt}\right], \tag{73}$$

and let $M_{gt}(p_t)$ be the corresponding $J \times J$ matrix, where its (j,l) element is the change in group-g demand for tract j when the value of tract l rises by one unit, holding rents fixed, so $M_{gt}(p_t)$ is the migration response of demand to values. Then

$$\frac{\partial N_{t+1}(p_t)}{\partial p_t^\top} = \sum_{g\in\mathcal{G}} M_{gt}(p_t)D_{gt}(p_t). \tag{74}$$

From Equation 12,

$$\frac{\partial S_{j,t+1}(p_{jt})}{\partial p_{mt}} = \varphi\lambda_{jt}p_{jt}^{\varphi-1}\mathbb{1}(j=m). \tag{75}$$

Let $\Phi_t(p_t)$ denote the diagonal matrix of supply slopes,

$$\Phi_t(p_t) \equiv \operatorname{diag}\left(\varphi\lambda_{1t}p_{1t}^{\varphi-1}, \ldots, \varphi\lambda_{Jt}p_{Jt}^{\varphi-1}\right). \tag{76}$$

Then, the Jacobian of the excess demand is

$$\nabla ED_{t+1}(p_t) \equiv \frac{\partial ED_{t+1}(p_t)}{\partial p_t^\top} = \sum_{g\in\mathcal{G}} M_{gt}(p_t)D_{gt}(p_t) - \Phi_t(p_t). \tag{77}$$

A.4 Existence of a housing-market equilibrium

In this section, I prove the existence of housing market equilibrium in section 5, and section 8.1.

Theorem 2 (Existence)**.** *Take the state at the beginning of period t as given. Let $\lambda_{jt} > 0, \forall j \in (1, ..., J)$, $\varphi > 0$, and the total market size $\sum_{g\in\mathcal{G}} \sum_{k\in\mathcal{J}} N_{kgt}$ is finite and positive, and the conditions of Theorem 1 hold for every group. Then there exists at least one $p_t^* \in \mathbb{R}^J_{++}$ satisfying*

$$N_{j,t+1}(p_t^*) = S_{j,t+1}(p_{jt}^*), \qquad j = 1, \ldots, J. \tag{78}$$

Proof. Let

$$\overline{N}_t \equiv \sum_{g\in\mathcal{G}} \sum_{k\in\mathcal{J}} N_{kgt}. \tag{79}$$

For every finite p_t, equation 56 gives strictly positive logit probabilities, so

$$0 < N_{j,t+1}(p_t) < \overline{N}_t \qquad \forall j. \tag{80}$$

Since supply is unbounded in p_{jt}, one can find $\overline{p}_t > 0$ large enough that

$$\lambda_{jt}\overline{p}_t^{\varphi} > \overline{N}_t \qquad \forall j. \tag{81}$$

By Lemma 3, $CV'_{gt}(p_t)$, the probabilities in equation 56, and $N_{j,t+1}(p_t)$ are continuous in p_t. Because $N_{j,t+1}(\cdot)$ is continuous on the compact set $[0, \overline{p}_t]^J$, the extreme value theorem gives that

$$\underline{N}_{jt} \equiv \min_{p_t\in[0,\overline{p}_t]^J} N_{j,t+1}(p_t) \tag{82}$$

exists, and equation 80 then gives $\underline{N}_{jt} > 0$. Since $\lambda_{jt} > 0$ and $\varphi > 0$, $\lambda_{jt}p^{\varphi} \to 0$ as $p \to 0$, so any

$$0 < \underline{p}_t < \min_j \left(\frac{\underline{N}_{jt}}{\lambda_{jt}}\right)^{1/\varphi} \tag{83}$$

satisfies $\lambda_{jt}\underline{p}_t^{\varphi} < \underline{N}_{jt}$ for every j. Such $\underline{p}_t$ lies below $\overline{p}_t$, because

$$\lambda_{jt}\underline{p}_t^{\varphi} < \underline{N}_{jt} \leq \overline{N}_t < \lambda_{jt}\overline{p}_t^{\varphi}. \tag{84}$$

Let $Q_t \equiv [\underline{p}_t, \overline{p}_t]^J$. Equation 84 pins down the sign of excess demand at the boundary of Q_t. For any $p_t \in Q_t$ with $p_{jt} = \underline{p}_t$, supply in tract j is $\lambda_{jt}\underline{p}_t^{\varphi}$ while demand is at least $\underline{N}_{jt}$, so $ED_{j,t+1}(p_t) > 0$. For any $p_t \in Q_t$ with $p_{jt} = \overline{p}_t$, supply is $\lambda_{jt}\overline{p}_t^{\varphi}$ while demand is below $\overline{N}_t$, so $ED_{j,t+1}(p_t) < 0$.

Let Λ_{Q_t} denote the coordinate-wise projection onto Q_t, which truncates each p_{jt} to $[\underline{p}_t, \overline{p}_t]$. For any $\delta > 0$, consider the map $Q_t \to Q_t$ defined by

$$p_t \;\mapsto\; \Lambda_{Q_t}(p_t + \delta\, ED_{t+1}(p_t))\,. \tag{85}$$

Q_t is nonempty, compact, and convex, and the map is continuous and sends Q_t into itself, so Brouwer's fixed-point theorem gives a fixed point $p_t^* \in Q_t$.

It remains to show that p_t^* is interior to Q_t, since in the interior the projection Λ_{Q_t} does not bind and the fixed-point condition reduces to $ED_{t+1}(p_t^*) = 0$. Fix any j and suppose $p_{jt}^* = \underline{p}_t$. Then $ED_{j,t+1}(p_t^*) > 0$, so $p_{jt}^* + \delta ED_{j,t+1}(p_t^*) > \underline{p}_t$ and its projection onto $[\underline{p}_t, \overline{p}_t]$ is strictly above $\underline{p}_t = p_{jt}^*$. The map therefore moves the jth coordinate, contradicting that p_t^* is a fixed point. If instead $p_{jt}^* = \overline{p}_t$, then $ED_{j,t+1}(p_t^*) < 0$, the projection of $p_{jt}^* + \delta ED_{j,t+1}(p_t^*)$ is strictly below $\overline{p}_t = p_{jt}^*$, and the same contradiction follows. Hence $\underline{p}_t < p_{jt}^* < \overline{p}_t$ for every j, so $ED_{t+1}(p_t^*) = 0$, and p_t^* is strictly positive since $\underline{p}_t > 0$. □

A.5 Global uniqueness in the static model

In this section, I show that one can prove a global uniqueness of an equilibrium price vector when $\beta = 0$.

Theorem 3 (Global uniqueness in the static model)**.** *Set $\beta = 0$ and suppose $\theta_{gp} < 0$ for every group with positive population. Under equation 12, with $\lambda_{jt} > 0$ and $\varphi > 0$, the static model has exactly one strictly positive market-clearing rent vector.*

Proof. When $\beta = 0$, equation 69 reduces to

$$D_{gt}(p_t) = \frac{\partial CV'_{gt}}{\partial p_t^{\top}} = \theta_{gp} I_J. \tag{86}$$

For origin $k \in \mathcal{J}$, let $P_{kgt} \equiv (P_{1kgt}, \ldots, P_{Jkgt})^{\top}$ denote the vector of inside-destination probabilities

in equation 56. Then equation 73 can be written as

$$M_{gt} = \sum_{k \in \mathcal{J}} N_{kgt} \left[\operatorname{diag}(P_{kgt}) - P_{kgt} P_{kgt}^{\top} \right]. \tag{87}$$

For any $d \in \mathbb{R}^J$,

$$d^{\top} \left[\operatorname{diag}(P_{\cdot kgt}) - P_{\cdot kgt} P_{\cdot kgt}^{\top} \right] d = \sum_{j=1}^{J} P_{jkgt} d_j^2 - \left(\sum_{j=1}^{J} P_{jkgt} d_j \right)^2 \geq 0. \tag{88}$$

The inequality follows because the right-hand side is the variance of a random variable that equals d_j when inside destination j is chosen and zero when the outside option is chosen. Thus $d^{\top} M_{gt} d \geq 0$.

Substituting equation 86 into equation 77, for every $d \neq 0$,

$$d^{\top} \nabla E D_{t+1}(p_t)\, d = \sum_{g \in \mathcal{G}} \theta_{gp}\, d^{\top} M_{gt} d - \sum_{j=1}^{J} \varphi \lambda_{jt} p_{jt}^{\varphi - 1} d_j^2 < 0. \tag{89}$$

The first term is weakly negative because $\theta_{gp} < 0$ and M_{gt} is positive semidefinite. The supply term is strictly negative for every nonzero d because $\varphi > 0$, $\lambda_{jt} > 0$, and $p_{jt} > 0$.

Now suppose, toward a contradiction, that two distinct vectors p_t and q_t both clear the market. Let $d = p_t - q_t \neq 0$. Since $\mathbb{R}^J_{++}$ is convex, $q_t + ad \in \mathbb{R}^J_{++}$ for every $a \in [0, 1]$. The fundamental theorem of calculus gives

$$\begin{aligned} 0 &= d^{\top} \left[E D_{t+1}(p_t) - E D_{t+1}(q_t) \right] \\ &= \int_0^1 d^{\top} \nabla E D_{t+1}(q_t + ad)\, d\, da < 0, \end{aligned} \tag{90}$$

which is a contradiction. Hence there is at most one static equilibrium. Theorem 2 establishes existence, so the equilibrium is globally unique when $\beta = 0$. □

A.6 Local uniqueness in the dynamic model

When $\beta > 0$, D_{gt} in equation 69 is no longer a scalar multiple of I_J, and the quadratic-form argument of Theorem 3 does not extend. Providing an analytical proof on global uniqueness of the dynamic equilibrium is difficult. Instead, I establish local uniqueness of a dynamic equilibrium,

and conduct numerical tests.

Theorem 4 (Local uniqueness of a regular dynamic equilibrium)**.** *Let $p_t^* \in \mathbb{R}^J_{++}$ satisfy $ED_{t+1}(p_t^*) = 0$, and call p_t^* regular if $\nabla ED_{t+1}(p_t^*)$ is nonsingular. A regular equilibrium is locally unique. I.e., there is a neighborhood of p_t^* containing no other market-clearing rent vector.*

Proof. By Lemma 3, ED_{t+1} is continuously differentiable. If its Jacobian at p_t^* is nonsingular, the inverse function theorem implies that ED_{t+1} is one-to-one on an open neighborhood of p_t^*, so that neighborhood contains no second zero. □

Theorem 4 is an analytical statement about an exact market-clearing rent vector. I supplement it with two numerical exercises, carried out at every equilibrium on the observed baseline path and at every counterfactual equilibrium used in the paper, for both the three-group aggregate specification and the six-group race-by-poverty specification.

The first exercise verifies the hypothesis of Theorem 4 at every observed and counterfactual equilibrium. I evaluate the exact Jacobian in equation 77 at market-clearing price vector and compute the largest eigenvalue of its symmetric part, $\left[\nabla ED_{t+1}(p_t') + \nabla ED_{t+1}(p_t')^\top\right]/2$. A negative value means that $d^\top \nabla ED_{t+1}(p_t')\, d < 0$ for every $d \neq 0$, which rules out a null vector and hence implies that $\nabla ED_{t+1}(p_t')$ is nonsingular. For all equilibria, it is strictly negative at every equilibrium, so every reported equilibrium in this paper is locally unique, following Theorem 4.[71]

The second exercise addresses dependence on the initial rent vector in the equilibrium solver. Holding the inherited state for each period fixed, I draw 1,000 initial guesses on the rent vector, independently across tracts, from

$$p_{jt}^0 \sim U\left[\frac{p_{jt}'}{2.5},\, 2.5\, p_{jt}'\right], \qquad j = 1, \ldots, J, \tag{91}$$

and re-solve the same period-specific market-clearing problem from each starting vector. Every run converges to the reported rent vector, on the baseline path and in every counterfactual environment, and no distinct market-clearing rent vector is found. This provides numerical evidence that the counterfactual results are not driven by the particular initial rent vector used by the solver.

[71] In practice, I computed the smallest eigenvalue of the negative symmetric part, which is the same quantity with the sign reversed.

Local uniqueness, period by period, extends to the full-period counterfactual path. Recall from Section A.1 that the state inherited by period $t+1$, namely the populations $N_{jg,t+1} = \sum_k N_{kgt} P_{jkgt}$, the racial composition r'_{t+1}, and the lagged values entering equation 32, is a deterministic function of the inherited state at period t and the equilibrium rent vector at t.

Corollary 2 (Local uniqueness of the counterfactual path)**.** *Let $\{p'_t\}_{t=1}^T$ be the reported counterfactual path, and suppose p'_t is regular for every t. Then there exist neighborhoods U_t of p'_t such that $\{p'_t\}_{t=1}^T$ is the only counterfactual equilibrium path $\{q_t\}_{t=1}^T$ with $q_t \in U_t$ for every t.*

Proof. The proof is by induction on t. In period 1 the inherited state is the observed pre-policy state. By Theorem 4, there is a neighborhood U_1 of p'_1 in which p'_1 is the only market-clearing rent vector, so $q_1 \in U_1$ forces $q_1 = p'_1$. Suppose $q_s = p'_s$ for all $s < t$. Then both paths inherit the same state at period t and face the same market-clearing problem, and Theorem 4 applied to p'_t gives a neighborhood U_t in which $q_t \in U_t$ forces $q_t = p'_t$. □

A.7 Summary and conclusion

To summarize, the inner counterfactual value problem has a unique solution for each group under $\beta|\gamma_{1,1}| < 1$, and a housing-market equilibrium exists in every period. In the static model, the market-clearing rent vector is globally unique. In the dynamic model, any regular equilibrium is locally unique, and, conditional on regularity in every period, the corresponding counterfactual equilibrium path is locally unique. Numerically, the Jacobian evaluated at every reported equilibrium satisfies the sufficient regularity condition described above. In addition, across all counterfactual context-year combinations, re-solving the equilibrium from 1,000 independently drawn starting rent vectors in each case yields the reported equilibrium in all trials and reveals no distinct market-clearing solution. These numerical exercises provide evidence against economically relevant multiplicity and sensitivity to initialization.

B Alternative Estimation Method

In this appendix, I evaluate the three-step estimation procedure introduced in Section 6 by comparing its flow-utility and preference estimates with those obtained from an alternative procedure based

on conditional choice probabilities (CCP). This alternative draws on conditional-choice-probability methods building on the Hotz and Miller (1993) inversion, including the approach in Davis et al. (2021) and Almagro and Domínguez-Iino (2025)'s Euler Equation in Conditional Choice Probabilities (ECCP) estimator. Rather than specifying a transition process for choice-specific values, the CCP-based procedure uses renewal actions to difference out continuation values and identify differences in flow utilities.[72] The three-step approach instead specifies a transition process for choice-specific values and integrates over their predicted future distribution. The comparison therefore provides a methodological benchmark for the three-step approach using an alternative way of recovering flow utilities and preference parameters from the model.

The alternative CCP-based procedure proceeds as follows. First, I use the inversion in Step 1 of Section 6.1 to construct conditional choice probabilities from the aggregate data. Second, I use these probabilities and a renewal action to recover tract-level flow utilities up to a year-specific constant. Third, I estimate the preference parameters using the same IV-GMM specification as in the three-step approach.

The first step uses the objects recovered from the BLP inversion to construct the CCPs. As described in Section 6.1, the first step of the three-step approach recovers the choice-specific values $\widehat{CV}_{jt}$ and moving cost $\widehat{sc}_t$ from aggregate tract shares and the aggregate share of non-movers. Given these objects, Equation 9 implies the probability that a resident currently in tract k chooses tract j. Suppressing the demographic-group subscript g,

$$\widehat{P}_{jkt} = \frac{\exp\left(\widehat{CV}_{jt} - \widehat{CV}_{kt} - \widehat{sc}_t \mathbb{1}(j \neq k)\right)}{\sum_{l=1}^{J+1} \exp\left(\widehat{CV}_{lt} - \widehat{CV}_{kt} - \widehat{sc}_t \mathbb{1}(l \neq k)\right)}. \tag{92}$$

Thus, although individual origin-destination choices are not observed, the aggregate inversion provides the full matrix of model-implied CCPs needed for the alternative procedure.

In the second step, I use the recovered CCPs and the outside option, $J+1$, as a renewal action

[72] A key advantage of this class of CCP-based methods is that they can avoid specifying agents' beliefs over future equilibrium paths and, with suitable renewal actions, much of the transition process for the underlying state variables. This is particularly useful in settings with a large state space, where specifying and solving the full dynamic equilibrium can be difficult. Constructing counterfactuals, however, generally requires the researcher to solve the dynamic problem under the counterfactual policy and reintroduce assumptions about the evolution of the state variables and agents' beliefs over future equilibrium paths. This re-introduces the curse of dimensionality.

to identify differences in per period utilities. For two distinct interior tracts j and k, define

$$Y_{jkt} = \log\left(\frac{\widehat{P}_{jkt}}{\widehat{P}_{kkt}}\right) + \widehat{sc}_t + \beta\left[\log \widehat{P}_{J+1,j,t+1} - \log \widehat{P}_{J+1,k,t+1}\right]. \tag{93}$$

Conditional on choosing to leave the area and exit the market $(J+1)$ in the following period, the continuation-value difference between the two residential paths is eliminated, so Y_{jkt} identifies the difference in their current flow utilities up to an expectational error.[73] Averaging these pairwise differences over interior reference tracts k recovers tract-level per-period utility up to a year-specific constant.

For the first two census waves (2000 and 2007), the future CCPs entering Equation 93 are constructed from the choice-specific values and moving costs recovered at the subsequent wave. For 2014, since 2021 is the terminal census wave, I instead rely on the future choice-specific values implied by the transition process in Equation 20 to derive the future CCPs defined in Equation 92.

Finally, I estimate the preference parameters by IV-GMM using the per-period utilities recovered in the second step as the dependent variable in Equation 23. I maintain the same controls, endogenous variables, instruments, fixed effects, and inference procedure as in the three-step approach.

Tables 6 and 7 show that the preference estimates from the CCP-based procedure are remarkably close to those from the three-step approach. Across the four endogenous neighborhood characteristics and nine demographic specifications, 31 of the 36 estimated coefficients on the observed endogenous state variables differ from their three-step counterparts by less than one-half of a standard error, and 35 differ by less than one standard error. The qualitative implications are unchanged across the two procedures. For example, the estimated well coefficient changes from -0.0302 to -0.0313 for White residents and from -0.0894 to -0.0870 for Black residents. The largest difference occurs for non-poor Hispanic residents, for whom the well coefficient changes from -0.0627 to -0.0443. The estimates on rent and neighborhood demographic composition are similarly close across most specifications. Overall, the two procedures yield highly consistent preference estimates despite relying on different assumptions about future state transitions and equilibrium

[73] The outside option, $J+1$, is a valid renewal action because choosing it corresponds to leaving the area and exiting the market represented in the model. The continuation value following market exit is normalized to zero, so $EV(J+1, \Omega_{t+2}) = 0$ by construction. Once both residential paths choose $J+1$ at $t+1$, their subsequent continuation values are therefore both zero and their difference is exactly zero.

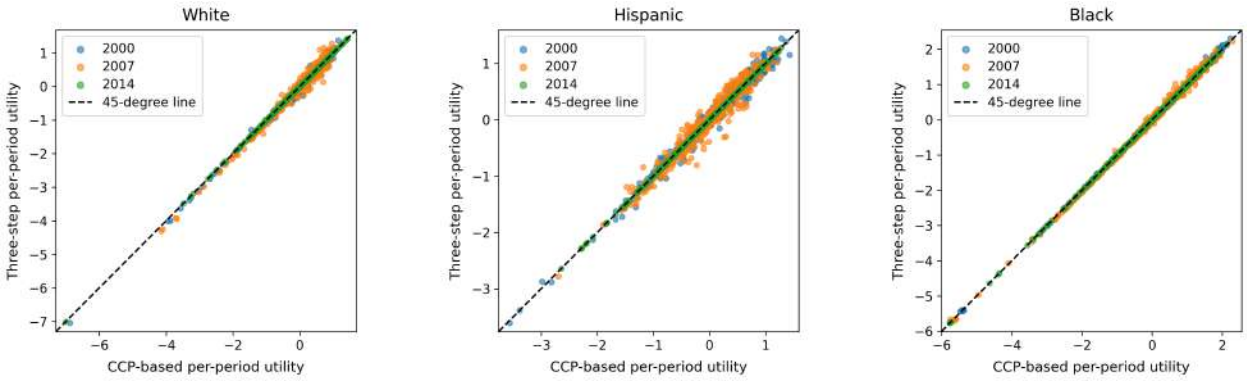
beliefs.

Figure 11 compares the per-period utilities recovered by the two procedures. Because these utilities are identified up to a year-specific constant, I remove their year-specific means before making the comparison. The 2014 observations lie on the 45-degree line to numerical precision, which is expected because the CCP-based procedure uses the transition process from the three-step approach to construct the required future CCPs in that period. The comparisons for the first two census waves are more informative: the CCP-based procedure instead uses objects recovered from the subsequent observed wave, yet the resulting utilities remain closely aligned with those from the three-step approach across most tracts and demographic groups. For these first two waves, the CCP-based procedure remains agnostic about the transition process governing future choice-specific values and agents' beliefs over future equilibrium paths. The close alignment between the recovered utilities therefore indicates that the transition process in Equation 20 closely approximates future choice-specific values, allowing the three-step approach to recover nearly the same current per-period utilities.

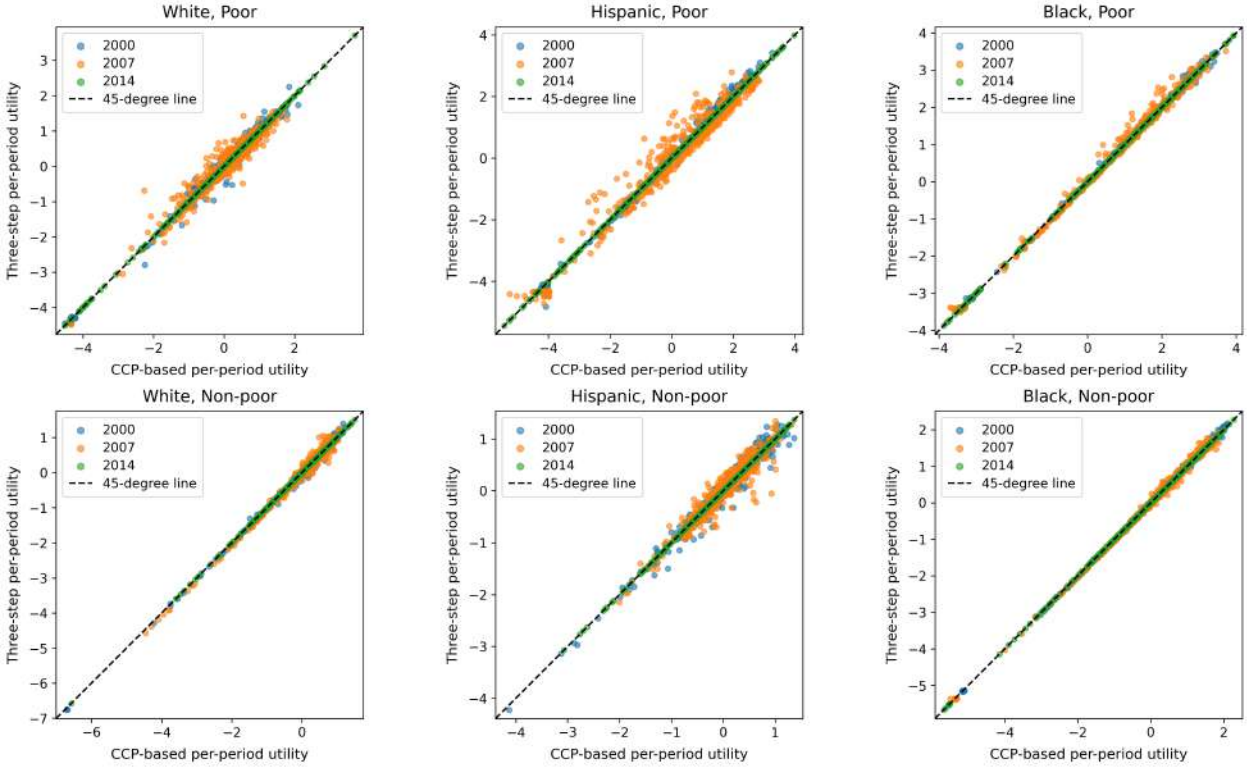
Table 6: Preference Estimates across Different Estimation Procedures: By Race

	White			Hispanic			Black		
	Static	Three-step	CCP	Static	Three-step	CCP	Static	Three-step	CCP
Wells Within 1 mile	-0.0370	-0.0302	-0.0313	-0.0101	-0.0352	-0.0251	-0.0818	-0.0894	-0.0870
	(0.0126)	(0.0142)	(0.0134)	(0.0146)	(0.0148)	(0.0141)	(0.0360)	(0.0354)	(0.0349)
Median Rent	-0.0010	-0.0008	-0.0010	-0.0009	-0.0012	-0.0009	-0.0029	-0.0030	-0.0029
	(0.0003)	(0.0004)	(0.0003)	(0.0003)	(0.0003)	(0.0003)	(0.0009)	(0.0009)	(0.0008)
Hispanic Share	-2.3642	-2.0262	-2.1561	3.3952	2.8739	2.8858	-1.0764	-1.1677	-1.0793
	(0.3002)	(0.3289)	(0.2936)	(0.3184)	(0.3235)	(0.2968)	(0.7369)	(0.7305)	(0.7208)
Black Share	-2.8384	-2.4569	-2.4165	0.8206	0.6887	0.6617	4.9037	4.6350	4.5520
	(0.2813)	(0.3048)	(0.2811)	(0.1779)	(0.1756)	(0.1623)	(0.5287)	(0.5217)	(0.5129)

Notes: The table compares preference estimates across the static model, the three-step approach used in the main analysis, and the alternative CCP-based procedure described in Appendix B. "Static" sets the discount factor to zero. For the first two census waves, the CCP-based procedure constructs future CCPs using the choice-specific values and moving costs recovered at the subsequent wave. For 2014, the required future CCPs are constructed using the transition process in Equation 20. All of the specifications use the same controls, instruments, fixed effects, discount factor, and IV-GMM procedure. Standard errors clustered at the census-tract-level are reported in parentheses.



(a) Race



(b) Race and poverty status

Figure 11: Recovered Per-Period Utility: Three-Step and CCP-Based Procedures

Notes: Each point represents a census tract. The horizontal axis reports per-period utility recovered using the CCP-based procedure, and the vertical axis reports per-period utility recovered using the three-step approach. Utilities are demeaned separately by year because they are identified up to a year-specific constant. For the first two census waves, the CCP-based procedure constructs future CCPs using the choice-specific values and moving costs recovered at the subsequent wave. For 2014, the required future CCPs are constructed using the transition process in Equation 20. The dashed line is the 45-degree line.

Table 7: Preference Estimates across Different Estimation Procedures: By Race and Poverty Status

Panel A. White Residents

	Poor			Non-poor		
	Static	Three-step	CCP	Static	Three-step	CCP
Wells Within 1 mile	-0.0341	-0.0147	-0.0213	-0.0455	-0.0397	-0.0405
	(0.0274)	(0.0275)	(0.0269)	(0.0141)	(0.0154)	(0.0146)
Median Rent	-0.0016	-0.0011	-0.0014	-0.0009	-0.0007	-0.0008
	(0.0005)	(0.0006)	(0.0005)	(0.0002)	(0.0003)	(0.0003)
Hispanic Share	-1.2406	-0.7803	-0.9692	-2.3882	-2.0985	-2.1777
	(0.5523)	(0.5553)	(0.5168)	(0.3120)	(0.3343)	(0.3059)
Black Share	-2.8676	-2.4823	-2.5868	-3.0257	-2.6145	-2.5576
	(0.4315)	(0.4322)	(0.4029)	(0.3203)	(0.3401)	(0.3200)

Panel B. Black Residents

	Poor			Non-poor		
	Static	Three-step	CCP	Static	Three-step	CCP
Wells Within 1 mile	-0.0575	-0.0540	-0.0508	-0.1173	-0.1245	-0.1219
	(0.0490)	(0.0491)	(0.0484)	(0.0398)	(0.0391)	(0.0387)
Median Rent	-0.0026	-0.0024	-0.0023	-0.0032	-0.0033	-0.0032
	(0.0012)	(0.0012)	(0.0012)	(0.0009)	(0.0009)	(0.0009)
Hispanic Share	0.9897	1.0636	1.0351	-1.4047	-1.4674	-1.4014
	(0.9733)	(0.9735)	(0.9496)	(0.7176)	(0.7104)	(0.7032)
Black Share	6.3349	6.1388	6.1059	5.0070	4.7291	4.6576
	(0.5999)	(0.6070)	(0.5854)	(0.5751)	(0.5652)	(0.5606)

Panel C. Hispanic Residents

	Poor			Non-poor		
	Static	Three-step	CCP	Static	Three-step	CCP
Wells Within 1 mile	-0.0418	-0.0209	-0.0100	-0.0350	-0.0627	-0.0443
	(0.0509)	(0.0517)	(0.0495)	(0.0170)	(0.0175)	(0.0155)
Median Rent	-0.0031	-0.0026	-0.0025	-0.0012	-0.0015	-0.0013
	(0.0013)	(0.0013)	(0.0013)	(0.0003)	(0.0004)	(0.0003)
Hispanic Share	5.8493	5.9519	5.3335	2.8429	2.2544	2.2876
	(0.8404)	(0.8490)	(0.7935)	(0.3392)	(0.3528)	(0.3149)
Black Share	1.8456	1.7884	1.7094	0.5532	0.4478	0.4097
	(0.5575)	(0.5648)	(0.5222)	(0.1930)	(0.1948)	(0.1743)

Notes: The table compares preference estimates by race and poverty status across the static model, the three-step approach used in the main analysis, and the alternative CCP-based procedure described in Appendix B. "Static" sets the discount factor to zero. For the first two census waves, the CCP-based procedure constructs future CCPs using the choice-specific values and moving costs recovered at the subsequent wave. For 2014, the required future CCPs are constructed using the transition process in Equation 20. All of the specifications use the same controls, instruments, fixed effects, discount factor, and IV-GMM procedure. Standard errors clustered at the census-tract-level are reported in parentheses.

C Robustness of Counterfactual Value Transition Parameters

The counterfactual exercises, and thus the welfare calculations, rely on the assumption that the parameters governing the choice-specific value transition in Equation 20 remain unchanged when the neighborhood environment changes. This appendix examines how much this restriction matters for the results. I focus primarily on the progressive reduction of under-performing wells in Section 8.4, because it provides a stream of counterfactual environments of increasing magnitude in change and therefore shows where the assumption begins to be less likely to hold.[74] I re-estimate the value transition parameters using the choice-specific values and neighborhood characteristics generated along each counterfactual path and compare the resulting welfare calculations with the original counterfactual results. The welfare estimates are nearly identical to Baseline for small removals, and the differences grow with the size of the counterfactual, but the qualitative welfare implications remain largely unchanged.

I compare four calculations while holding the estimated per-period utility parameters $\widehat{\theta}_g$ fixed throughout. *Baseline* is the counterfactual calculation used in the main analysis: $\beta = 0.7$, the original estimated value transition parameters $\widehat{\gamma}_g$, and a counterfactual equilibrium in which housing prices and racial composition adjust as described in Section 8.1. For *Belief Adjusted*, I re-estimate Equation 20 using the Baseline counterfactual path, denote the resulting parameters by $\widehat{\gamma}_g^{CF}$, and recalculate choice-specific values and welfare while holding the counterfactual equilibrium housing prices and racial composition at their Baseline values. For *Belief and Equilibrium Adjusted*, I use the same $\widehat{\gamma}_g^{CF}$ but solve the housing-market equilibrium again, allowing housing prices, racial composition, choice-specific values, and residential demand to adjust to the updated value transition parameters.[75] In both cases, $\widehat{\gamma}_g^{CF}$ is estimated once from the Baseline counterfactual path. Finally, I include *Myopic* for reference, where I keep the same $\widehat{\theta}_g$ but set $\beta = 0$ and solve the counterfactual

[74] Blocking the entry of all the wells that turned out to be under-performing removes 63 percent of the total wells in Tarrant County.

[75] *Belief and Equilibrium Adjusted* is the more demanding of the two checks. *Belief Adjusted* changes only the continuation values entering residential choices, holding counterfactual housing prices and racial composition at their *Baseline* values, whereas *Belief and Equilibrium Adjusted* lets that change propagate through residential demand into market-clearing prices and neighborhood composition, which in turn feed back into choice-specific values. I do not iterate between re-estimating the parameters and solving the equilibrium. Doing so would require searching for a fixed point at which the value transition parameters reproduce the path they themselves generate, a stronger requirement than the model imposes and one whose existence is beyond the scope of this paper. In the observed equilibrium, however, this condition holds by construction.

equilibrium again, so that continuation values no longer enter residential choices.[76]

Figure 12 shows that re-estimating the value transition parameters leaves the qualitative welfare implications largely unchanged. When only a small number of under-performing wells are prevented from being drilled, the Belief Adjusted results are nearly identical to the Baseline results. The differences become larger as progressively more under-performing wells are not drilled, and larger still when the counterfactual equilibrium is solved again using the re-estimated value transition parameters. Even then, the main welfare pattern remains, as White residents and the poor groups continue to gain, while non-poor Hispanic residents continue to lose. The exception is non-poor Black residents, whose Baseline welfare effect is the closest to zero and changes sign under some of the alternative counterfactuals that adjust both belief coefficients and equilibrium outcomes.

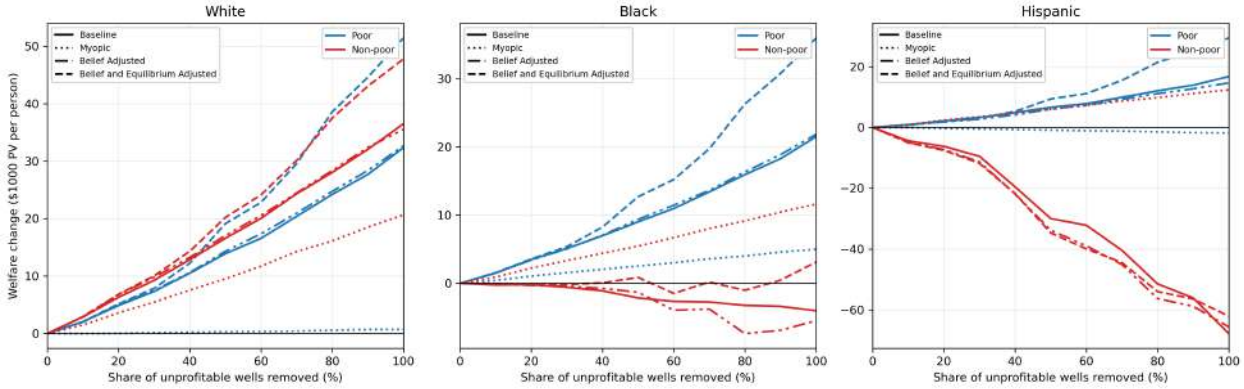


Figure 12: Welfare Effects of Blocking Under-performing Wells under Alternative Belief and Equilibrium

Notes: Each panel reports the welfare change for poor and non-poor residents of the racial or ethnic group named in the panel title as progressively more under-performing wells are prevented from being drilled, following the realized-profit ordering in Section 8.4. Myopic keeps the Baseline per-period utility parameters but sets $\beta = 0$ and solves a new counterfactual equilibrium. Belief Adjusted uses the value transition parameters $\widehat{\gamma}_g^{CF}$ re-estimated from the Baseline counterfactual path while holding the Baseline counterfactual housing prices and racial composition fixed. Belief and Equilibrium Adjusted uses the same $\widehat{\gamma}_g^{CF}$ and solves the counterfactual equilibrium again. Line color distinguishes poverty status and line style distinguishes the four calculations. Blocking all of the under-performing wells results in a counterfactual without 63 percent of the total wells in Tarrant County.

To assess how far the invariance assumption departs from the counterfactual estimates, Table 8 compares the original value transition parameters with those re-estimated along each counterfactual path. I focus on the four key variables of interest, which are well exposure, median rent, the Hispanic share, and the Black share. For each counterfactual estimate, the number in parentheses reports its

[76]This calculation differs from the separately estimated static residential sorting model reported in Section 8.4. The Myopic calculation in this appendix keeps the per-period utility parameters from the dynamic model fixed and changes only β, whereas the static model in Section 8.4 re-estimates the preference parameters under $\beta = 0$.

deviation from the original estimate in units of the original standard error, $(\widehat{\gamma}_{kg}^{CF} - \widehat{\gamma}_{kg})/SE(\widehat{\gamma}_{kg})$. For the smallest change in the number of wells the re-estimated parameters stay close to their original values, with about 96 percent of the coefficients lying within one standard error of the original estimate. The deviations grow as progressively more wells are removed, but no transition coefficient changes sign for any demographic group along any of the ten counterfactual paths. The invariance assumption therefore appears reasonable for counterfactuals close to the observed environment, and at least qualitatively so for the more distant ones.

Table 9 repeats the exercise for the fracking ban in Fort Worth in Section 8.2 and the targeted ban in Section 8.3, with comparable implications. The three forward-looking calculations agree on the sign of the welfare effect for every demographic group, and re-estimating the value transition parameters moves welfare by at most \$438 per person under the targeted ban against \$5,723 under the Fort Worth ban, which eliminates about 48 rather than 10 percent of well exposure. When myopia is assumed instead, the welfare effect reverses sign for three of the six groups under the Fort Worth ban and for poor Hispanic residents under the targeted ban, which is to be expected because setting $\beta = 0$ removes the continuation values through which the value transition parameters operate.

Table 8: Value Transition Parameters Re-estimated along the Progressive Blocking of Unprofitable Wells

		Share of unprofitable wells removed (percent)									
	Original	10	20	30	40	50	60	70	80	90	100
Panel A. Wells Within 1 Mile											
White, poor	−0.2007	−0.1918	−0.2090	−0.2087	−0.2062	−0.2171	−0.2307	−0.2227	−0.2253	−0.2305	−0.2252
	(0.0493)	(0.18)	(−0.17)	(−0.16)	(−0.11)	(−0.33)	(−0.61)	(−0.45)	(−0.50)	(−0.60)	(−0.50)
White, non-poor	−0.0630	−0.0632	−0.0698	−0.0682	−0.0641	−0.0631	−0.0621	−0.0581	−0.0583	−0.0571	−0.0503
	(0.0226)	(−0.01)	(−0.30)	(−0.23)	(−0.05)	(−0.01)	(0.04)	(0.22)	(0.21)	(0.26)	(0.56)
Black, poor	−0.2186	−0.2065	−0.2072	−0.2047	−0.2092	−0.2242	−0.2272	−0.2066	−0.2111	−0.2141	−0.2000
	(0.0626)	(0.19)	(0.18)	(0.22)	(0.15)	(−0.09)	(−0.14)	(0.19)	(0.12)	(0.07)	(0.30)
Black, non-poor	0.1367	0.1328	0.1370	0.1301	0.1282	0.1259	0.1365	0.1347	0.1445	0.1403	0.1324
	(0.0411)	(−0.09)	(0.01)	(−0.16)	(−0.21)	(−0.26)	(−0.00)	(−0.05)	(0.19)	(0.09)	(−0.11)
Hispanic, poor	−0.3323	−0.2855	−0.2761	−0.2639	−0.2585	−0.2778	−0.2919	−0.2887	−0.2817	−0.2790	−0.2536
	(0.0785)	(0.60)	(0.72)	(0.87)	(0.94)	(0.69)	(0.52)	(0.56)	(0.65)	(0.68)	(1.00)
Hispanic, non-poor	0.2498	0.2362	0.2419	0.2425	0.2341	0.2262	0.2356	0.2273	0.2211	0.2116	0.1987
	(0.0368)	(−0.37)	(−0.21)	(−0.20)	(−0.43)	(−0.64)	(−0.39)	(−0.61)	(−0.78)	(−1.04)	(−1.39)
Panel B. Median Rent											
White, poor	−0.0038	−0.0037	−0.0037	−0.0036	−0.0036	−0.0035	−0.0035	−0.0034	−0.0034	−0.0033	−0.0032
	(0.0003)	(0.06)	(0.29)	(0.42)	(0.58)	(0.78)	(0.93)	(1.08)	(1.27)	(1.44)	(1.66)
White, non-poor	−0.0013	−0.0013	−0.0013	−0.0012	−0.0012	−0.0012	−0.0012	−0.0012	−0.0012	−0.0012	−0.0011
	(0.0002)	(0.08)	(0.29)	(0.39)	(0.46)	(0.59)	(0.73)	(0.83)	(0.92)	(1.00)	(1.10)
Black, poor	−0.0036	−0.0037	−0.0036	−0.0035	−0.0035	−0.0034	−0.0033	−0.0033	−0.0032	−0.0031	−0.0030
	(0.0004)	(−0.18)	(−0.00)	(0.15)	(0.31)	(0.52)	(0.65)	(0.78)	(0.98)	(1.15)	(1.39)
Black, non-poor	0.0017	0.0017	0.0016	0.0016	0.0016	0.0016	0.0015	0.0015	0.0015	0.0014	0.0014
	(0.0003)	(−0.29)	(−0.37)	(−0.41)	(−0.50)	(−0.65)	(−0.84)	(−0.87)	(−1.02)	(−1.06)	(−1.17)
Hispanic, poor	−0.0066	−0.0066	−0.0065	−0.0064	−0.0064	−0.0063	−0.0062	−0.0061	−0.0061	−0.0060	−0.0059
	(0.0005)	(0.00)	(0.16)	(0.26)	(0.40)	(0.60)	(0.71)	(0.86)	(1.04)	(1.21)	(1.40)
Hispanic, non-poor	0.0025	0.0023	0.0023	0.0022	0.0020	0.0018	0.0018	0.0017	0.0015	0.0014	0.0013
	(0.0002)	(−0.94)	(−1.10)	(−1.34)	(−2.07)	(−2.83)	(−2.96)	(−3.52)	(−4.26)	(−4.53)	(−5.32)

Notes: Each panel reports the coefficient on one lagged neighborhood characteristic from the value transition equation 20, estimated separately for each demographic group. The Original column reports the estimate from the observed data used throughout the paper, with its standard error in parentheses. The remaining columns report $\widehat{\gamma}_{kg}^{CF}$ re-estimated on the Baseline counterfactual path, with the column heading giving the share of the ex post unprofitable well pool prevented from being drilled along the progressive removal in Section 8.4. The number in parentheses below each counterfactual estimate is $(\widehat{\gamma}_{kg}^{CF} - \widehat{\gamma}_{kg})/SE(\widehat{\gamma}_{kg})$, the difference from the original estimate in units of its standard error. These are descriptive magnitudes, not test statistics for equality between the original and counterfactual estimates. Panels C and D continue in the next table.

Table 8: Value Transition Parameters Re-estimated along the Progressive Blocking of Unprofitable Wells(continued)

		Share of unprofitable wells removed (percent)									
	Original	10	20	30	40	50	60	70	80	90	100
Panel C. Hispanic Share											
White, poor	−4.2344	−4.1788	−4.1888	−4.1768	−4.1401	−4.0982	−4.0860	−4.0347	−3.9956	−3.9668	−3.9109
	(0.3807)	(0.15)	(0.12)	(0.15)	(0.25)	(0.36)	(0.39)	(0.52)	(0.63)	(0.70)	(0.85)
White, non-poor	−3.6102	−3.6455	−3.6192	−3.5955	−3.5639	−3.5347	−3.5138	−3.4791	−3.4402	−3.4002	−3.3656
	(0.1724)	(−0.20)	(−0.05)	(0.09)	(0.27)	(0.44)	(0.56)	(0.76)	(0.99)	(1.22)	(1.42)
Black, poor	−1.6369	−1.5208	−1.5231	−1.5027	−1.4540	−1.4053	−1.3721	−1.3128	−1.2547	−1.2124	−1.1405
	(0.4792)	(0.24)	(0.24)	(0.28)	(0.38)	(0.48)	(0.55)	(0.68)	(0.80)	(0.89)	(1.04)
Black, non-poor	1.7348	1.7939	1.8007	1.7954	1.7866	1.7515	1.7282	1.7333	1.7241	1.7359	1.7116
	(0.3136)	(0.19)	(0.21)	(0.19)	(0.17)	(0.05)	(−0.02)	(−0.00)	(−0.03)	(0.00)	(−0.07)
Hispanic, poor	−0.5209	−0.7040	−0.7118	−0.7000	−0.6503	−0.5907	−0.5534	−0.4747	−0.4280	−0.3934	−0.3222
	(0.6586)	(−0.28)	(−0.29)	(−0.27)	(−0.20)	(−0.11)	(−0.05)	(0.07)	(0.14)	(0.19)	(0.30)
Hispanic, non-poor	4.2898	3.9418	4.0511	4.0437	3.8815	3.7312	3.8741	3.7336	3.5563	3.5056	3.3032
	(0.3332)	(−1.04)	(−0.72)	(−0.74)	(−1.23)	(−1.68)	(−1.25)	(−1.67)	(−2.20)	(−2.35)	(−2.96)
Panel D. Black Share											
White, poor	−3.5551	−3.5383	−3.5597	−3.5582	−3.5444	−3.5194	−3.5235	−3.5040	−3.4961	−3.4899	−3.4618
	(0.4095)	(0.04)	(−0.01)	(−0.01)	(0.03)	(0.09)	(0.08)	(0.12)	(0.14)	(0.16)	(0.23)
White, non-poor	−4.4206	−4.4082	−4.3837	−4.3498	−4.3097	−4.2727	−4.2422	−4.1972	−4.1483	−4.1044	−4.0436
	(0.2007)	(0.06)	(0.18)	(0.35)	(0.55)	(0.74)	(0.89)	(1.11)	(1.36)	(1.58)	(1.88)
Black, poor	3.3581	3.3185	3.3351	3.3405	3.3437	3.3610	3.3820	3.4010	3.3986	3.4044	3.4237
	(0.5679)	(−0.07)	(−0.04)	(−0.03)	(−0.03)	(0.01)	(0.04)	(0.08)	(0.07)	(0.08)	(0.12)
Black, non-poor	2.3493	2.2969	2.2989	2.3044	2.3019	2.2929	2.2824	2.2826	2.2893	2.2999	2.3042
	(0.3758)	(−0.14)	(−0.13)	(−0.12)	(−0.13)	(−0.15)	(−0.18)	(−0.18)	(−0.16)	(−0.13)	(−0.12)
Hispanic, poor	0.5999	0.4711	0.4839	0.4888	0.5054	0.5437	0.5632	0.5887	0.5890	0.6059	0.6369
	(0.6165)	(−0.21)	(−0.19)	(−0.18)	(−0.15)	(−0.09)	(−0.06)	(−0.02)	(−0.02)	(0.01)	(0.06)
Hispanic, non-poor	1.8184	1.7307	1.7571	1.7468	1.6733	1.5916	1.6257	1.5679	1.4961	1.4763	1.3828
	(0.2834)	(−0.31)	(−0.22)	(−0.25)	(−0.51)	(−0.80)	(−0.68)	(−0.88)	(−1.14)	(−1.21)	(−1.54)

Notes: Table 8 continued.

Table 9: Welfare Effects of the Fort Worth and Targeted Removals under Alternative Belief Parameters and Equilibrium

	Baseline	Myopic	Belief adjusted	Belief and equilibrium adjusted
Panel A. Removing all wells in Fort Worth				
White, poor	19,328	893	21,186	19,660
White, non-poor	23,342	14,758	28,584	27,797
Black, poor	14,794	3,574	12,673	11,214
Black, non-poor	−39	9,300	−1,904	−2,812
Hispanic, poor	7,886	−3,091	9,659	7,365
Hispanic, non-poor	−11,723	10,608	−6,120	−6,000
Panel B. Targeted removal in poor-Hispanic neighborhoods				
White, poor	3,177	347	3,036	3,118
White, non-poor	3,011	2,031	3,130	3,167
Black, poor	2,182	936	2,199	2,282
Black, non-poor	1,199	1,675	1,244	1,295
Hispanic, poor	1,390	−1,001	952	1,070
Hispanic, non-poor	423	2,879	185	289

Notes: Welfare change in lifetime present value, measured in rent-equivalent dollars per person, with population weights fixed at the observed 2014 distribution. Panel A reports the removal of all wells located in Fort Worth from Section 8.2 and Panel B the targeted removal around census tracts with the highest concentrations of poor Hispanic residents from Section 8.3.

D Robustness to the Size of the Outside Option

Section 6.1 sets the total population of group g, including the outside option, equal to its largest observed Tarrant County population plus 10,000. I examine alternative values of this total population. In addition to adding 5,000 or 20,000 to the largest observed population, I choose N_{gt} so that the outside option accounts for 3, 5, 10, or 20 percent of the total population when the observed Tarrant County population reaches its sample maximum. In every specification,

$$N_{J+1,gt} = N_{gt} - \sum_{j=1}^{J} N_{jgt},$$

and the outside option continues to represent leaving the market, a terminal option that is normalized to $CV_{J+1,gt} = 0$. I repeat the full estimation procedure and the Fort Worth counterfactual under each specification.

Table 10 shows that the flow utility estimates are highly stable. Across the four endogenous neighborhood characteristics and nine demographic specifications, none of the 36 coefficients changes sign, and all remain within one baseline standard error of the estimates reported in Table 2. In particular, the coefficient on wells within one mile remains negative for every group and retains the same significance pattern across poor and non-poor residents.

The value transition parameters vary more in magnitude, but the relationships that matter for the welfare results remain intact. As shown in Table 11, the coefficients on lagged well exposure and rent retain their signs for every group. In particular, well exposure continues to predict higher future neighborhood values for non-poor Black and Hispanic residents and lower future values for the other race-by-poverty groups, as in Table 3. The only sign change among the four reported transition variables is the Hispanic-share coefficient for poor Hispanic residents, which is statistically insignificant in the baseline specification.

Finally, Table 12 shows that the main welfare pattern from the Fort Worth removal in Section 8.2 is unchanged. Poor White, poor Black, poor Hispanic, and non-poor White residents gain under every specification, while non-poor Hispanic residents lose under every specification. The exception is non-poor Black residents, whose baseline welfare loss is only $39 per person and whose estimated effect changes sign across specifications. Thus, as in Table 16, the model delivers little net welfare change for this group rather than a robust gain or loss.

E Institutional Details on Urban Shale Development

This appendix provides additional institutional details supporting the interpretation of urban shale development used in Section 2. I first describe how horizontal drilling made large-scale extraction possible in densely developed areas and why the associated environmental effects are spatially localized. I then provide additional evidence on mineral ownership and employment, the two main channels through which drilling could otherwise create residential demand for proximity to wells. Finally, I describe the state and municipal rules governing well placement and residential development around existing wells.

Table 10: Flow Utility Estimates under Alternative Sizes of the Outside Option

	Added population			Outside option share			
	5,000	Baseline	20,000	3%	5%	10%	20%
Panel A. Wells Within 1 mile							
Aggregate race							
White	-0.0308	-0.0302	-0.0296	-0.0294	-0.0292	-0.0295	-0.0300
	(0.0144)	(0.0142)	(0.0140)	(0.0140)	(0.0138)	(0.0136)	(0.0134)
Black	-0.0927	-0.0894	-0.0856	-0.0896	-0.0867	-0.0829	-0.0795
	(0.0355)	(0.0354)	(0.0352)	(0.0354)	(0.0353)	(0.0351)	(0.0350)
Hispanic	-0.0336	-0.0352	-0.0363	-0.0362	-0.0364	-0.0358	-0.0360
	(0.0148)	(0.0148)	(0.0147)	(0.0147)	(0.0146)	(0.0145)	(0.0146)
Race by poverty status							
White, poor	-0.0171	-0.0147	-0.0122	-0.0222	-0.0189	-0.0157	-0.0131
	(0.0280)	(0.0275)	(0.0275)	(0.0290)	(0.0284)	(0.0277)	(0.0274)
White, non-poor	-0.0398	-0.0397	-0.0396	-0.0396	-0.0397	-0.0401	-0.0408
	(0.0155)	(0.0154)	(0.0153)	(0.0153)	(0.0152)	(0.0150)	(0.0149)
Black, poor	-0.0554	-0.0540	-0.0510	-0.0566	-0.0560	-0.0549	-0.0523
	(0.0493)	(0.0491)	(0.0490)	(0.0495)	(0.0494)	(0.0492)	(0.0490)
Black, non-poor	-0.1271	-0.1245	-0.1211	-0.1254	-0.1230	-0.1192	-0.1151
	(0.0393)	(0.0391)	(0.0390)	(0.0392)	(0.0390)	(0.0389)	(0.0387)
Hispanic, poor	-0.0258	-0.0209	-0.0128	-0.0279	-0.0246	-0.0189	-0.0040
	(0.0522)	(0.0517)	(0.0521)	(0.0525)	(0.0520)	(0.0517)	(0.0534)
Hispanic, non-poor	-0.0603	-0.0627	-0.0650	-0.0641	-0.0656	-0.0671	-0.0689
	(0.0175)	(0.0175)	(0.0175)	(0.0175)	(0.0175)	(0.0174)	(0.0175)
Panel B. Median Rent ($/Month)							
Aggregate race							
White	-0.0009	-0.0008	-0.0008	-0.0008	-0.0008	-0.0008	-0.0008
	(0.0004)	(0.0004)	(0.0004)	(0.0004)	(0.0003)	(0.0003)	(0.0003)
Black	-0.0031	-0.0030	-0.0030	-0.0030	-0.0030	-0.0030	-0.0029
	(0.0009)	(0.0009)	(0.0009)	(0.0009)	(0.0009)	(0.0009)	(0.0009)
Hispanic	-0.0012	-0.0012	-0.0011	-0.0011	-0.0011	-0.0011	-0.0010
	(0.0003)	(0.0003)	(0.0003)	(0.0003)	(0.0003)	(0.0003)	(0.0003)
Race by poverty status							
White, poor	-0.0012	-0.0011	-0.0011	-0.0013	-0.0012	-0.0012	-0.0011
	(0.0006)	(0.0006)	(0.0006)	(0.0006)	(0.0006)	(0.0006)	(0.0006)
White, non-poor	-0.0007	-0.0007	-0.0007	-0.0007	-0.0007	-0.0006	-0.0006
	(0.0003)	(0.0003)	(0.0003)	(0.0003)	(0.0003)	(0.0003)	(0.0002)
Black, poor	-0.0025	-0.0024	-0.0024	-0.0025	-0.0025	-0.0024	-0.0024
	(0.0012)	(0.0012)	(0.0012)	(0.0013)	(0.0012)	(0.0012)	(0.0012)
Black, non-poor	-0.0033	-0.0032	-0.0032	-0.0033	-0.0032	-0.0032	-0.0032
	(0.0009)	(0.0009)	(0.0009)	(0.0009)	(0.0009)	(0.0009)	(0.0009)
Hispanic, poor	-0.0027	-0.0026	-0.0025	-0.0028	-0.0027	-0.0026	-0.0023
	(0.0013)	(0.0013)	(0.0012)	(0.0013)	(0.0013)	(0.0013)	(0.0012)
Hispanic, non-poor	-0.0015	-0.0015	-0.0015	-0.0015	-0.0015	-0.0015	-0.0014
	(0.0004)	(0.0004)	(0.0004)	(0.0004)	(0.0004)	(0.0004)	(0.0004)

Table 10: Flow Utility Estimates under Alternative Sizes of the Outside Option (continued)

	5,000	Baseline	20,000	3%	5%	10%	20%
Panel C. Hispanic Share							
Aggregate race							
White	-2.0361	-2.0262	-2.0123	-2.0065	-1.9905	-1.9523	-1.8542
	(0.3318)	(0.3289)	(0.3248)	(0.3231)	(0.3191)	(0.3135)	(0.3086)
Black	-1.1793	-1.1677	-1.1548	-1.1683	-1.1584	-1.1456	-1.1376
	(0.7326)	(0.7305)	(0.7283)	(0.7306)	(0.7289)	(0.7264)	(0.7223)
Hispanic	2.9167	2.8739	2.8262	2.8346	2.7946	2.7250	2.5913
	(0.3244)	(0.3235)	(0.3218)	(0.3222)	(0.3204)	(0.3180)	(0.3165)
Race by poverty status							
White, poor	-0.8385	-0.7803	-0.6857	-0.9329	-0.8723	-0.8068	-0.7193
	(0.5682)	(0.5553)	(0.5488)	(0.5895)	(0.5766)	(0.5604)	(0.5497)
White, non-poor	-2.1058	-2.0985	-2.0853	-2.0811	-2.0621	-2.0150	-1.9058
	(0.3354)	(0.3343)	(0.3323)	(0.3318)	(0.3296)	(0.3260)	(0.3220)
Black, poor	1.0661	1.0636	1.0554	1.0573	1.0638	1.0658	1.0586
	(0.9776)	(0.9735)	(0.9673)	(0.9819)	(0.9796)	(0.9758)	(0.9699)
Black, non-poor	-1.4680	-1.4674	-1.4672	-1.4675	-1.4672	-1.4674	-1.4712
	(0.7135)	(0.7104)	(0.7073)	(0.7114)	(0.7090)	(0.7057)	(0.7012)
Hispanic, poor	5.9819	5.9519	5.9171	5.9889	5.9762	5.9384	5.9322
	(0.8553)	(0.8490)	(0.8514)	(0.8591)	(0.8534)	(0.8481)	(0.8667)
Hispanic, non-poor	2.3180	2.2544	2.1860	2.2148	2.1601	2.0696	1.9144
	(0.3528)	(0.3528)	(0.3521)	(0.3526)	(0.3516)	(0.3488)	(0.3465)
Panel D. Black Share							
Aggregate race							
White	-2.4662	-2.4569	-2.4428	-2.4366	-2.4190	-2.3782	-2.2862
	(0.3071)	(0.3048)	(0.3016)	(0.3003)	(0.2972)	(0.2929)	(0.2883)
Black	4.6894	4.6350	4.5776	4.6378	4.5944	4.5243	4.4010
	(0.5231)	(0.5217)	(0.5206)	(0.5218)	(0.5209)	(0.5196)	(0.5162)
Hispanic	0.7085	0.6887	0.6682	0.6715	0.6564	0.6362	0.6061
	(0.1757)	(0.1756)	(0.1756)	(0.1756)	(0.1757)	(0.1758)	(0.1767)
Race by poverty status							
White, poor	-2.5635	-2.4823	-2.3575	-2.6866	-2.6086	-2.5196	-2.4003
	(0.4389)	(0.4322)	(0.4282)	(0.4507)	(0.4433)	(0.4349)	(0.4289)
White, non-poor	-2.6207	-2.6145	-2.6029	-2.5990	-2.5816	-2.5376	-2.4383
	(0.3411)	(0.3401)	(0.3384)	(0.3379)	(0.3360)	(0.3327)	(0.3282)
Black, poor	6.2025	6.1388	6.0182	6.2479	6.2262	6.1766	6.0696
	(0.6105)	(0.6070)	(0.6018)	(0.6144)	(0.6123)	(0.6089)	(0.6040)
Black, non-poor	4.7876	4.7291	4.6616	4.7485	4.6999	4.6198	4.4869
	(0.5666)	(0.5652)	(0.5639)	(0.5656)	(0.5646)	(0.5631)	(0.5598)
Hispanic, poor	1.8045	1.7884	1.7701	1.8095	1.8011	1.7815	1.7807
	(0.5692)	(0.5648)	(0.5659)	(0.5718)	(0.5679)	(0.5641)	(0.5748)
Hispanic, non-poor	0.4618	0.4478	0.4323	0.4388	0.4265	0.4076	0.3785
	(0.1952)	(0.1948)	(0.1944)	(0.1946)	(0.1942)	(0.1934)	(0.1933)

Notes: Each panel reports IV-GMM estimates of the flow utility parameter on the neighborhood characteristic named in the panel; standard errors clustered at the census-tract level are in parentheses. Columns correspond to the alternative definitions of N_{gt} described in Appendix D, where the Baseline is adding 10,000.

Table 11: Belief Parameter Estimates under Alternative Sizes of the Outside Option

	Added population			Outside option share			
	5,000	Baseline	20,000	3%	5%	10%	20%
Panel A. Wells Within 1 mile							
Aggregate race							
White	-0.0740	-0.0743	-0.0729	-0.0717	-0.0674	-0.0577	-0.0461
	(0.0250)	(0.0242)	(0.0228)	(0.0222)	(0.0206)	(0.0184)	(0.0167)
Black	0.1702	0.1293	0.0944	0.1312	0.1035	0.0725	0.0512
	(0.0303)	(0.0270)	(0.0248)	(0.0271)	(0.0253)	(0.0239)	(0.0235)
Hispanic	0.2594	0.2161	0.1768	0.1830	0.1560	0.1258	0.1060
	(0.0313)	(0.0256)	(0.0207)	(0.0215)	(0.0183)	(0.0152)	(0.0138)
Race by poverty status							
White, poor	-0.2158	-0.2007	-0.1851	-0.2048	-0.2167	-0.2088	-0.1882
	(0.0614)	(0.0584)	(0.0575)	(0.0649)	(0.0630)	(0.0596)	(0.0574)
White, non-poor	-0.0640	-0.0630	-0.0609	-0.0602	-0.0569	-0.0496	-0.0401
	(0.0210)	(0.0206)	(0.0200)	(0.0198)	(0.0191)	(0.0179)	(0.0170)
Black, poor	-0.2474	-0.2186	-0.1914	-0.2742	-0.2616	-0.2339	-0.2001
	(0.0700)	(0.0687)	(0.0684)	(0.0729)	(0.0712)	(0.0693)	(0.0684)
Black, non-poor	0.1803	0.1367	0.0986	0.1500	0.1187	0.0814	0.0526
	(0.0324)	(0.0287)	(0.0262)	(0.0298)	(0.0274)	(0.0254)	(0.0245)
Hispanic, poor	-0.3391	-0.3323	-0.3215	-0.3362	-0.3387	-0.3280	-0.3265
	(0.0773)	(0.0765)	(0.0781)	(0.0779)	(0.0770)	(0.0766)	(0.0822)
Hispanic, non-poor	0.2969	0.2498	0.2061	0.2236	0.1917	0.1534	0.1239
	(0.0384)	(0.0325)	(0.0272)	(0.0293)	(0.0255)	(0.0213)	(0.0187)
Panel B. Median Rent ($/Month)							
Aggregate race							
White	-0.0014	-0.0014	-0.0014	-0.0014	-0.0014	-0.0012	-0.0011
	(0.0002)	(0.0002)	(0.0002)	(0.0002)	(0.0002)	(0.0001)	(0.0001)
Black	0.0020	0.0015	0.0010	0.0015	0.0011	0.0007	0.0004
	(0.0003)	(0.0002)	(0.0002)	(0.0002)	(0.0002)	(0.0002)	(0.0002)
Hispanic	0.0027	0.0021	0.0015	0.0016	0.0012	0.0008	0.0005
	(0.0003)	(0.0003)	(0.0002)	(0.0002)	(0.0002)	(0.0001)	(0.0001)
Race by poverty status							
White, poor	-0.0043	-0.0037	-0.0034	-0.0047	-0.0045	-0.0040	-0.0035
	(0.0004)	(0.0004)	(0.0004)	(0.0005)	(0.0004)	(0.0004)	(0.0004)
White, non-poor	-0.0013	-0.0013	-0.0013	-0.0013	-0.0013	-0.0012	-0.0011
	(0.0002)	(0.0002)	(0.0002)	(0.0002)	(0.0002)	(0.0001)	(0.0001)
Black, poor	-0.0041	-0.0036	-0.0031	-0.0047	-0.0044	-0.0039	-0.0033
	(0.0005)	(0.0004)	(0.0004)	(0.0005)	(0.0005)	(0.0004)	(0.0004)
Black, non-poor	0.0023	0.0017	0.0012	0.0019	0.0015	0.0010	0.0006
	(0.0003)	(0.0003)	(0.0003)	(0.0003)	(0.0003)	(0.0003)	(0.0002)
Hispanic, poor	-0.0070	-0.0066	-0.0062	-0.0072	-0.0069	-0.0064	-0.0062
	(0.0006)	(0.0006)	(0.0006)	(0.0006)	(0.0006)	(0.0006)	(0.0006)
Hispanic, non-poor	0.0031	0.0025	0.0019	0.0022	0.0017	0.0012	0.0008
	(0.0004)	(0.0003)	(0.0003)	(0.0003)	(0.0002)	(0.0002)	(0.0002)

Table 11: Belief Parameter Estimates under Alternative Sizes of the Outside Option (continued)

	5,000	Baseline	20,000	3%	5%	10%	20%
Panel C. Hispanic Share							
Aggregate race							
White	-4.3200	-4.1503	-3.8725	-3.7493	-3.4362	-2.9655	-2.5578
	(0.2399)	(0.2233)	(0.2007)	(0.1920)	(0.1729)	(0.1520)	(0.1419)
Black	1.9151	1.4789	1.1063	1.4994	1.2039	0.8706	0.6344
	(0.2879)	(0.2725)	(0.2628)	(0.2731)	(0.2650)	(0.2584)	(0.2555)
Hispanic	3.6803	3.2853	2.9428	2.9961	2.7665	2.5092	2.3349
	(0.3613)	(0.3057)	(0.2570)	(0.2646)	(0.2322)	(0.1970)	(0.1733)
Race by poverty status							
White, poor	-4.8691	-4.2344	-3.8249	-5.6258	-5.2137	-4.4998	-3.9046
	(0.3827)	(0.3599)	(0.3503)	(0.4279)	(0.3988)	(0.3687)	(0.3512)
White, non-poor	-3.6969	-3.6102	-3.4625	-3.4179	-3.2405	-2.9382	-2.6357
	(0.2231)	(0.2155)	(0.2037)	(0.2003)	(0.1880)	(0.1707)	(0.1587)
Black, poor	-1.8999	-1.6369	-1.3631	-2.0819	-2.0115	-1.7813	-1.4528
	(0.5163)	(0.4872)	(0.4692)	(0.5708)	(0.5385)	(0.5009)	(0.4742)
Black, non-poor	2.1831	1.7348	1.3414	1.8714	1.5489	1.1634	0.8613
	(0.3271)	(0.3063)	(0.2912)	(0.3123)	(0.2988)	(0.2855)	(0.2776)
Hispanic, poor	0.0970	-0.5209	-0.9266	0.5217	-0.0918	-0.6692	-1.1924
	(0.5720)	(0.5351)	(0.5131)	(0.5891)	(0.5625)	(0.5244)	(0.5250)
Hispanic, non-poor	4.8726	4.2898	3.7612	3.9705	3.5904	3.1440	2.8085
	(0.4002)	(0.3427)	(0.2903)	(0.3111)	(0.2734)	(0.2294)	(0.1972)
Panel D. Black Share							
Aggregate race							
White	-5.1011	-4.8448	-4.4452	-4.2745	-3.8553	-3.2603	-2.7796
	(0.3594)	(0.3522)	(0.3431)	(0.3398)	(0.3333)	(0.3287)	(0.3291)
Black	2.0688	2.0640	2.0592	2.0642	2.0609	2.0509	2.0278
	(0.3358)	(0.3141)	(0.2987)	(0.3150)	(0.3024)	(0.2906)	(0.2828)
Hispanic	1.8528	1.6320	1.4368	1.4674	1.3355	1.1899	1.1012
	(0.1908)	(0.1598)	(0.1342)	(0.1380)	(0.1223)	(0.1086)	(0.1041)
Race by poverty status							
White, poor	-4.3025	-3.5551	-3.1540	-5.5127	-4.7899	-3.8477	-3.2277
	(0.4244)	(0.3968)	(0.3831)	(0.4824)	(0.4446)	(0.4074)	(0.3853)
White, non-poor	-4.5641	-4.4206	-4.1828	-4.1125	-3.8395	-3.3975	-2.9881
	(0.3329)	(0.3288)	(0.3228)	(0.3212)	(0.3157)	(0.3093)	(0.3063)
Black, poor	3.8135	3.3581	3.1159	4.8105	4.2031	3.5631	3.1823
	(0.5103)	(0.4850)	(0.4660)	(0.5476)	(0.5266)	(0.4975)	(0.4717)
Black, non-poor	2.4340	2.3493	2.2773	2.3747	2.3152	2.2440	2.1827
	(0.3293)	(0.3075)	(0.2919)	(0.3137)	(0.2997)	(0.2859)	(0.2766)
Hispanic, poor	0.9078	0.5999	0.4412	1.1272	0.8114	0.5336	0.3762
	(0.4544)	(0.4218)	(0.4062)	(0.4733)	(0.4451)	(0.4137)	(0.4167)
Hispanic, non-poor	2.0960	1.8184	1.5632	1.6646	1.4801	1.2619	1.1009
	(0.1975)	(0.1691)	(0.1449)	(0.1542)	(0.1377)	(0.1215)	(0.1144)

Notes: Each panel reports OLS estimates of the coefficient on the lagged neighborhood characteristic named in the panel from Equation 20; standard errors clustered at the census-tract level are in parentheses. Columns correspond to the alternative definitions of N_{gt} described in Appendix D, where the baseline is adding 10,000.

Table 12: Welfare Effects of the Fort Worth Removal under Alternative Sizes of the Outside Option

	Added population			Outside option share			
	5,000	Baseline	20,000	3%	5%	10%	20%
Aggregate race							
White	18,903	19,420	20,239	20,993	21,824	22,125	21,103
Black	-3,832	-2,187	854	-2,244	118	3,427	5,285
Hispanic	-13,324	-15,361	-18,044	-17,344	-19,222	-19,702	-17,702
Race by poverty status							
White, poor	18,772	19,328	18,786	14,197	17,063	19,309	17,990
White, non-poor	24,540	23,342	23,577	25,118	25,259	25,581	25,386
Black, poor	16,060	14,794	13,634	15,489	15,806	15,217	13,332
Black, non-poor	-1,263	-39	2,580	-502	1,170	3,973	6,009
Hispanic, poor	5,946	7,886	8,505	7,199	8,489	9,326	8,632
Hispanic, non-poor	-13,703	-11,723	-11,365	-11,332	-11,209	-10,766	-8,754

Notes: Welfare change in lifetime present value, measured in rent-equivalent dollars per person, with population weights fixed at the observed 2014 distribution. Each column re-estimates the model and solves the Fort Worth fracking ban counterfactual under the corresponding definition of N_{gt} described in Appendix D, where the baseline is adding 10,000.

E.1 Urban Shale Gas Extraction and Local Environmental Effects

Horizontal drilling and hydraulic fracturing sharply reduced the surface footprint required for natural gas extraction. A single well pad can reach hydrocarbons across a wide subsurface area, so that gas beneath densely built neighborhoods can be produced without the dense grid of surface wells required by conventional vertical drilling. This technological change made large-scale extraction feasible in an urban county such as Tarrant, bringing wells into close proximity with homes, schools, parks, and other developed land.

The environmental and quality-of-life effects associated with shale gas development are concentrated near well sites. Previous studies document exposure to air pollutants, noise, risks to groundwater, and induced seismicity associated with shale development (Adgate et al., 2014; Hays et al., 2017; Black et al., 2021). These effects are particularly salient in an urban setting because a single well site can be located near a large number of residents. Nearly one million Tarrant County residents lived within half a mile of oil and gas activity during the shale boom. The expansion of extraction into Tarrant County therefore combined a highly localized source of environmental exposure with a large and demographically heterogeneous urban population (Zwickl, 2019).

Local opposition to urban drilling provides additional evidence that these effects were salient to residents. In 2014, voters in the neighboring city of Denton approved a ban on hydraulic fracturing, which the Texas legislature preempted the following year through House Bill 40. Opposition has also continued within Tarrant County. Liveable Arlington has challenged well permitting in Arlington, while the Environmental Justice Coalition of Fort Worth has sought tighter restrictions on gas development in Fort Worth, including stronger protections for neighborhoods located near existing and proposed well sites. These efforts do not establish the magnitude of residents' willingness to pay to avoid drilling, which is estimated in the model, but they show that proximity to urban drilling was an active local amenity concern during and after the Barnett boom.

E.2 Mineral Rights and Local Economic Benefits

The direct financial benefit of drilling to a nearby resident would primarily arise through ownership of the mineral estate. When an operator seeks to develop an area, it approaches mineral owners and offers to lease their rights, typically in exchange for an up-front bonus per acre and a royalty, a share of the value of production retained by the mineral owner over the life of the lease. Where a resident owns the relevant minerals, this income could in principle offset some of the disamenity associated with nearby drilling.

The financial benefit, however, is not tied closely to residential proximity to a surface well. A mineral lease generates payments only for owners of minerals included in the producing unit, and the mineral owner need not be the resident living above or near the well. Mineral ownership can be severed from surface ownership, transferred independently, or held by owners living elsewhere. Renters, roughly 41 percent of Tarrant County households, hold no mineral interest through their tenancy, and 14 percent of royalty owners recorded in the appraisal roll reside outside Tarrant County. Moreover, horizontal wells extend laterally beneath many parcels, so the location of the surface well does not determine which nearby residents receive royalty payments.

The benefit is also small for most mineral owners in Tarrant County. A residential lot in an urban area represents a small share of a producing unit, and the corresponding mineral interest is typically highly fractionalized. Table 13 reports the appraised value of mineral interests in the 2019 Tarrant Appraisal District mineral roll. Among positive-value royalty interests, the median appraised value is $60 and 94.2 percent of all royalty interests are valued at no more than $500.

The median fractional ownership share is only 0.015 percent. These magnitudes are also consistent with the signing bonuses below $400 reported by Timmins and Vissing (2022) for the average leased property in the Barnett.

Table 13: Tarrant County mineral interests by type: 2019 appraised market value

	Including $0			Excluding $0		
Interest type	*N*	Median	Mean	*N*	Median	Mean
Royalty (RI)	1,073,416	$30	$372	742,813	$60	$537
Override (OR)	24,500	$40	$1,160	16,355	$200	$1,738
Working interest (WI)	8,169	$18,160	$79,616	6,749	$28,280	$96,368

Source: Author's calculations from the Tarrant Appraisal District 2019 Mineral Appraisal Roll. The unit of observation is a mineral interest held by one owner in one lease or unit; values are the interest's appraised market value.
Notes: A royalty interest (RI) is a share of production free of drilling and operating costs, the form of interest most relevant for a residential mineral owner. An overriding royalty (OR) is a cost-free share carved out of the working interest, usually held by brokers or landmen. A working interest (WI) bears the costs of drilling and operation and therefore represents an operating and investment stake rather than a passive landowner claim. Values are the maximum across overlapping taxing jurisdictions. Interests appraised at $0 are non-producing but remain valid mineral accounts; the "Including $0" columns retain them, while the "Excluding $0" columns condition on positive value. Residential parcels with no mineral account are outside the roll, so the reported royalty-interest medians are upper bounds on what a typical resident holds.

The contrast with a traditional producing region helps put these amounts in perspective. Table 14 compares royalty interests in Tarrant County with those in Midland County, located at the center of the Permian Basin in West Texas. The median Midland royalty owner holds $3,050 in appraised royalty value, compared with $110 in Tarrant County, and the gap becomes substantially larger in the upper tail. Midland's mineral wealth is also concentrated among far fewer owners: 17,596 owners appear in the Midland roll, compared with 223,330 in Tarrant. The comparison is not intended as a controlled estimate, since the two counties differ in resource type, year, and development history. It illustrates, however, how differently mineral ownership operates in a traditional producing region and in the highly fractionalized urban Barnett.

A second potential economic benefit is employment. A body of research documents substantial labor-market effects from shale development, particularly in less populated producing regions, where drilling can raise local wages and employment enough to induce migration.[77] These effects operate at a different geographic margin from residential proximity to an individual well. Employment is

[77]Bartik et al. (2019) estimate a net local welfare gain from allowing hydraulic fracturing of about $2,500 per household per year, although the amenity component is negative. Feyrer et al. (2017) find income and employment effects concentrated near producing regions. Both analyses operate at the county or broader regional level.

Table 14: Royalty-interest value: Tarrant (Barnett) vs. Midland (Permian)

	Midland 2021 (Permian, oil & gas)	Tarrant 2019 (Barnett, gas)
Panel A. Per interest (value > 0)		
N interests	168,568	742,813
Median	\$460	\$60
Mean	\$17,303	\$537
p90	\$16,340	\$400
p99	\$242,369	\$8,260
Share at \$0[a]	0.0%	30.8%
Share $\leq$ \$500[a]	51.3%	94.2%
Panel B. Per owner[b]		
Owners	17,596	223,330
Interests/owner, median	2	3
Interests/owner, mean	9.6	4.8
Interests/owner, p90	21	10
Value/owner, median	\$3,050	\$110
Value/owner, mean	\$165,756	\$1,787
Value/owner, p90	\$110,215	\$1,000
Value/owner, p99	\$2,249,376	\$15,780

Source: Author's calculations from the Tarrant Appraisal District 2019 and Midland Central Appraisal District 2021 mineral rolls. The unit of observation in Panel A is a royalty interest.

Notes: Midland County sits at the center of the Permian Basin and is shown as a traditional producing-region contrast to the urban Barnett gas field in Tarrant County. The two rolls differ in year and underlying resource, so the comparison is illustrative rather than controlled. Per-owner figures aggregate all royalty interests associated with the same appraisal-roll owner identifier; owners recorded under more than one identifier are counted separately.

[a] Value statistics are conditional on positive appraised value. The two share rows use the full set of royalty interests, including those appraised at zero.

[b] Aggregated by appraisal-roll owner identifier.

concentrated in the labor-intensive drilling and completion phase, which lasts on the order of weeks per well. A producing well can remain active for decades while requiring relatively little continuing labor, and lease operators typically service multiple wells along a route rather than remaining at one site.

This distinction is particularly important in Tarrant County. The county forms a major part of the Dallas–Fort Worth metropolitan labor market, which is large and diversified. In the 2021 American Community Survey, agriculture, forestry, fishing, hunting, and mining together employed 5,793 of Tarrant County's 1,061,812 civilian workers, or about 0.5 percent. Because the ACS category also includes activities outside mining, this figure is an upper bound on the share attributable to oil and gas extraction. The employment effects of the Barnett boom could therefore be meaningful at the metropolitan or county level without creating a persistent incentive for residents to locate near individual wells within Tarrant County.

E.3 Drilling Regulation and Residential Development

Drilling regulation in Tarrant County operated at both the state and municipal levels. At the state level, the Railroad Commission of Texas issued drilling permits subject to acreage, spacing, and density requirements.[78] The Railroad Commission did not regulate local noise, traffic, or similar land-use effects around wells (Timmins & Vissing, 2022). Those issues were primarily addressed through municipal drilling ordinances.

Cities in the Barnett Shale regulated drilling through local ordinances that imposed setbacks, permitting requirements, and restrictions on activities such as noise and working hours (Fry, 2013; Timmins & Vissing, 2022). These ordinances constrained how drilling occurred but did not generally prevent wells from being developed inside urban areas. Denton went further in 2014 when voters approved a ban on hydraulic fracturing. The Texas legislature responded in 2015 with House Bill 40, which limited municipal authority to enact rules that effectively prohibited oil and gas operations. The legislation postdates most drilling in the sample, but the episode illustrates the division between state authority over mineral development and local efforts to regulate its surface effects.

Within this regulatory structure, an individual resident had limited ability to prevent nearby

[78] Texas Administrative Code, Chapter 3, Rules 3.37 and 3.38. Once permitted, an operator typically had two years to begin drilling.

mineral development. Under Texas law, the mineral estate is dominant over the surface estate. A mineral lessee therefore has the right to make reasonable use of the surface necessary to develop the minerals even without the surface owner's consent. Surface owners receive written notice of a drilling permit only after the permit has been issued.[79]

An individual mineral owner also cannot necessarily prevent development by refusing to lease. Rule 37 allows spacing exceptions under specified circumstances, and the Texas Mineral Interest Pooling Act permits the Railroad Commission to pool unleased mineral interests after a good-faith leasing offer.[80] In practice, an individual resident's bargaining margin is therefore more closely related to the terms of the mineral lease than to whether surrounding mineral development occurs.

Regulation of new housing near existing wells was generally less restrictive than regulation of new wells near existing housing. In Fort Worth, a new well had to be at least 600 feet from a protected use, while a new habitable structure could be built 200 feet from an existing wellbore and, on lots platted before 2009, as close as 125 feet from a permitted multi-well pad site.[81] Arlington similarly required a 600-foot setback for a new well but only 300 feet for new residential development near an existing well.

These reverse setbacks allowed residential construction to continue around established production sites. Fry et al. (2017) document substantial residential development around existing wells throughout the Dallas–Fort Worth area through 2015. They also imply that the housing stock near a well need not be fixed at the date the well is drilled. New development can occur around an existing pad, while operators can later add additional wells to that pad. The resulting exposure is therefore shaped jointly by the sequence of drilling and residential development rather than by a rule that permanently removes land surrounding a well from residential use.

[79] Warren Petroleum Corp. v. Martin, 271 S.W.2d 410 (Tex. 1954); Texas Natural Resources Code §91.703. The accommodation doctrine, established in cases including Tarrant County Water Control & Improvement Dist. No. 1 v. Haupt, Inc., 854 S.W.2d 909 (Tex. 1993), can require an operator to accommodate an existing surface use when established industry alternatives are available.

[80] Texas Natural Resources Code, Chapter 102. For an application in the urban Barnett, see Railroad Commission Docket No. 09-0252375, involving a 96-acre Tarrant County unit containing numerous unleased residential lots.

[81] City of Fort Worth Fire Code §5706.3.1.3.3. The gas-well ordinance also requires plats near a well to disclose the applicable distance limitation, and the city council may grant variances in some cases.

F Data Appendix

F.1 Geological Variables

This subsection describes how geological variables are acquired and processed. The geological variables are digitized from three published maps in Pollastro et al. (2007): a map of the depth of the formation (structure contours on the underlying Ellenburger Group; their Figure 5), a map of its thickness (isopach; their Figure 6), and a map of its thermal maturity, which determines whether the rock yields dry gas (vitrinite isoreflectance; their Figure 12); Montgomery et al. (2005) publish earlier versions of the same maps. Appendix Figure 13 shows the source maps. I geo-reference each figure in QGIS, manually digitize the contour lines, interpolate between contours with multilevel B-splines to obtain a continuous surface, and average each surface within 2020 census tract boundaries.

These maps are well suited for identification for two reasons. First, they describe properties of the rock itself, measured from the logs that drillers record about the layers a well passes through; they do not reflect how much gas any well produced. Second, they were compiled from well data assembled by 2003–2004, when Barnett drilling was still concentrated in the rural counties north of Tarrant, as the data locations plotted on the maps show. The wells in my sample were drilled almost entirely after this, so the geological variation used for identification predates the drilling it instruments.

Depth is the variable used in the analysis; thickness and thermal maturity are digitized for completeness but vary little in the county. Thickness matters little for horizontal wells, whose production depends on the length of wellbore in contact with the rock rather than on its vertical extent, and even the thinnest part of the county exceeds the threshold Pollastro et al. (2007) associate with commercial production. Thermal maturity is nearly uniform because the entire county produces dry gas. Depth, by contrast, ranges from 6,149 to 8,317 feet, and deeper rock is more expensive to reach: a 2016 EIA study puts the cost of additional drilling distance at $143 to $245 per foot, so the depth range implies cost differences of roughly $310,000 to $530,000 per well across the county.[82]

[82] See `http://www.eia.gov/petroleum/drilling/`. Well pads in the area typically host multiple wells, so per-location differences are larger.

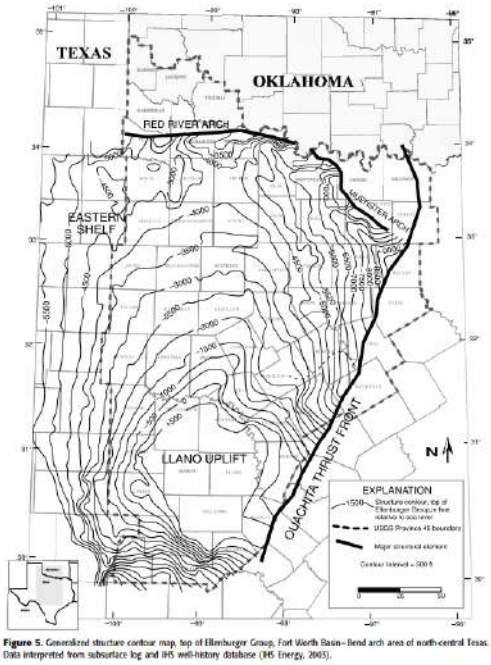


Figure 5. Generalized structure contour map, top of Ellenburger Group, Fort Worth Basin–Bend arch area of north-central Texas. Data interpreted from subsurface log and IHS well-history database (IHS Energy, 2003).

(a) Depth: structure contours on top of the Ellenburger Group (feet relative to sea level, 500-foot interval).

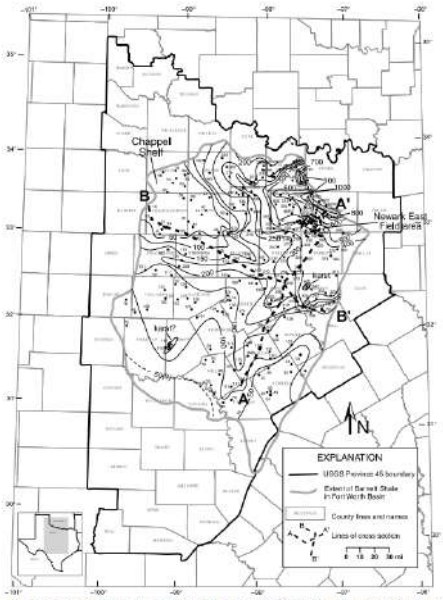


Figure 6. Map showing regional extent of Barnett Shale, thickness of Barnett Shale in selected wells, generalized regional isopachs of Barnett Shale, and lines of well-log cross sections AA' of Figure 9 and BB' of Figure 10. Contour intervals are 50 ft (15 m) for thicknesses from 0 to 300 ft (0 to 91 m) and 100 ft (30 m) for thicknesses from 300 to 1000 ft (91 to 305 m). Modified from Pollastro (2003).

(b) Thickness: isopach map with well data locations (50-foot interval below 300 feet, 100-foot above).

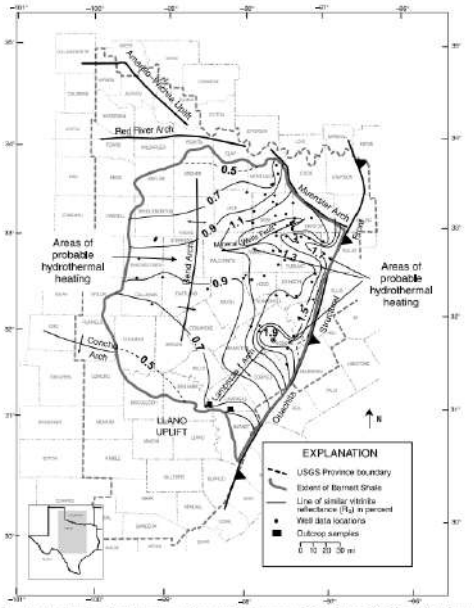


Figure 12. Map shows lines of equal thermal maturity as determined from mean vitrinite reflectance (R_o) of Barnett Shale. Based on data from Humble Geochemical Services, Humble, Texas. Areas of probable high hydrothermal heating and anomalously high R_o are also indicated (arrows).

(c) Thermal maturity: mean vitrinite reflectance (R_o) with well data locations.

Figure 13: Source maps for the geological variables. Reproduced from Figures 5, 6, and 12 of Pollastro et al. (2007). Contour lines are digitized by hand after georeferencing.

F.2 Operator Value Construction

This subsection describes the construction of the operator value of each well. The valuation follows the discounted cash flow approach of Gülen et al. (2013) from the petroleum engineering literature on shale well economics. Each well ℓ is valued as the discounted sum of the cash flows it generates over the sample window; the three inputs to that calculation are the path of monthly production, the prices and costs applied to it, and the royalty rate.

Production. Production comes from RRC lease-level records, which report cumulative gas output per lease. In Texas gas reporting a lease corresponds to a single wellbore for the wells in this sample, so lease-level production maps one to one to wells.[83]

Although the records provide only cumulative production, the production cycle of a shale well follows a predictable and consistent physical pattern, which makes it possible to infer the monthly flow: I recover the monthly path $q_{\ell t}$ from the decline curve of Patzek, Male, and Marder (2013), under which output falls with the square root of well age, scaled so that its cumulative sum matches the observed total. A well produces until its gas rate falls below 0.05 MMcf per day, its monthly cash flow turns negative, or the production records end, whichever comes first; no production is projected beyond the records. The paper values each well over the sample window, summing its discounted cash flows through 2021.[84]

Cash flows. The monthly net cash flow of well ℓ in month t is

$$CF_{\ell t} \;=\; \underbrace{(p_t - b)\,\gamma\, q_{\ell t}}_{\text{revenue}}\,(1 - r_\ell - \tau_t) \;-\; \underbrace{\big(c_t\, q_{\ell t} + f_t\big)}_{\text{operating cost}}, \tag{94}$$

where p_t is the Henry Hub spot price, b is a regional basis adjustment, γ converts gas volume to heat content, r_ℓ is the royalty rate owed to mineral owners, τ_t is the severance tax rate (7.5 percent, with the high-cost gas exemption approximated as a five-year waiver, following Gülen et al. (2013)), and c_t and f_t are variable and fixed operating costs, escalated to month t with a producer price

[83] I verify this in the data, and wells without a production match or a valid spud date are retained for the exposure measure but not valued

[84] Seventy-three percent of valued wells are still producing in 2021, so their values are lower bounds on lifetime value.

index. The well's value is

$$\Pi_\ell \;=\; \sum_{t=t_\ell^0}^{T_\ell} \frac{CF_{\ell t}}{(1+\rho)^{(t-t_\ell^0)/12}} \;-\; DC_\ell, \tag{95}$$

where t_ℓ^0 is the spud date, T_ℓ is the earlier of the end of production and the 2021 sample end, $\rho = 0.10$ is the annual discount rate, the value used by Herrnstadt et al. (2024), and DC_ℓ is the drilling and completion cost. Wells that stop producing within the window also incur an abandonment cost.

All parameter values are the Barnett-specific estimates of Gülen et al. (2013). Their dollar figures are stated in 2011 dollars, while the wells in my sample are drilled across two decades over which drilling and service costs moved substantially, so I convert each cost to the prices of the relevant date using producer price indexes from the Bureau of Labor Statistics. These indexes track the average prices charged by firms in a given industry, so multiplying a 2011 cost by the ratio of the index at another date to its 2011 level restates the cost at that date's prices. I use the index for the oil and gas well drilling industry to restate the drilling cost DC_ℓ at each well's spud date, and the index for oil field support activities to restate the operating costs c_t and f_t in each month of production.[85] Finally, I deflate the resulting Π_ℓ to 2014 dollars using CPI from FRED.

Royalty rates. The royalty rate r_ℓ is measured for each well rather than assumed. Because a horizontal well drains the minerals along its underground path rather than at its surface location, I trace each wellbore from its surface location to its endpoint, split it across the census tracts it passes through in proportion to length, and set r_ℓ to the length-weighted average of the tract-level royalty rates recovered from the lease corpus described in Appendix F.3.[86] The resulting median rate is 24.5 percent, above the 20 percent assumed in Gülen et al. (2013).

Table 15 reports the distribution of well values.

F.3 Lease Extraction

This subsection describes the extraction of royalty rates from the lease corpus. The corpus consists of 84,250 documents recorded with the Tarrant County clerk, digitized by the *New York Times* in the course of its reporting on the Barnett Shale and hosted on DocumentCloud; each document is

[85] FRED series PCU213111213111 and PCU213112213112.

[86] The median underground path is roughly one kilometer long and 97 percent cross a tract boundary, so assigning rates by surface location would misstate where royalty obligations accrue. Tracts without a lease-based rate receive the county median.

Table 15: Operator Value of Wells

Valued wells	4,014
Cumulative gas production (Bcf), median	1.68
Realized royalty rate, median	0.245
Still producing in 2021 (share)	0.73
Operator value Π_ℓ *(million 2014 USD)*	
Mean	−0.23
10th percentile	−3.05
25th percentile	−2.06
Median	−0.79
75th percentile	0.88
90th percentile	3.16
Share negative	0.63
Total (billion 2014 USD)	−0.93

Notes: Cash flows valued through 2021, the end of the sample window; no production is projected beyond it. Values for wells still producing in 2021 are lower bounds on lifetime value.

the recorded memorandum of a mineral lease. Timmins and Vissing (2022) use these documents to study how lease terms vary with neighborhood demographics in Tarrant County, showing that negotiated protections differ across communities. I do not use their extracted data; I process the raw documents myself with a similar approach, since my use requires fields and coverage tailored to the royalty calculation.

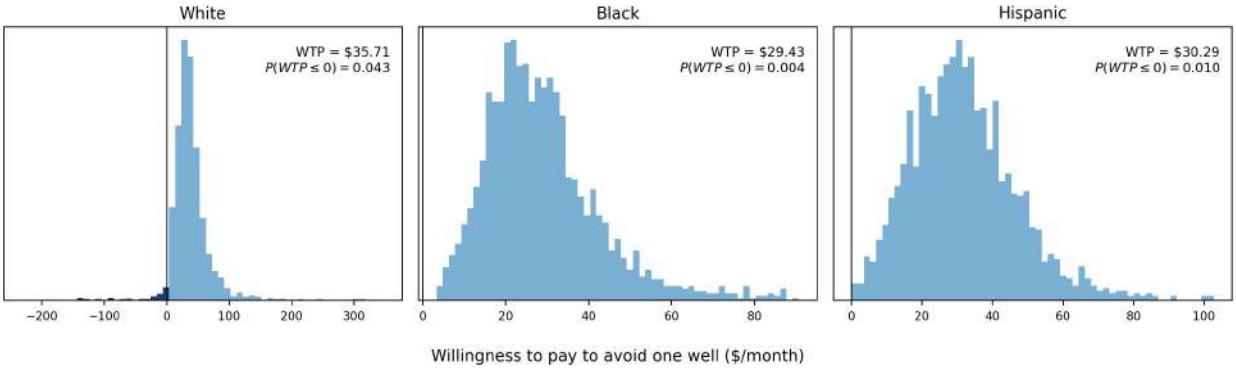
Extraction proceeds in three steps. First, I run Optical Character Recognition (OCR) on every document to convert the scanned images to text. Second, I parse the recognized text with rule-based patterns that locate each field where lease forms conventionally state it: the royalty fraction, the primary term, the acreage, and the subdivision in which the parcel lies. This recovers the royalty rate for 83 percent of documents, the lease term for 81 percent, the acreage for 75 percent, and the subdivision name for 91 percent; the contracting parties are taken from the document catalog rather than the scanned text.

Third, leases are assigned to census tracts through the subdivision named in the document. I standardize extracted subdivision names by removing platting suffixes and punctuation, match them to the subdivision boundaries maintained by the Tarrant Appraisal District, first exactly and then by fuzzy string matching, which tolerates the spelling variation and recognition errors that survive the first two steps, and assign each matched lease the census tract containing its

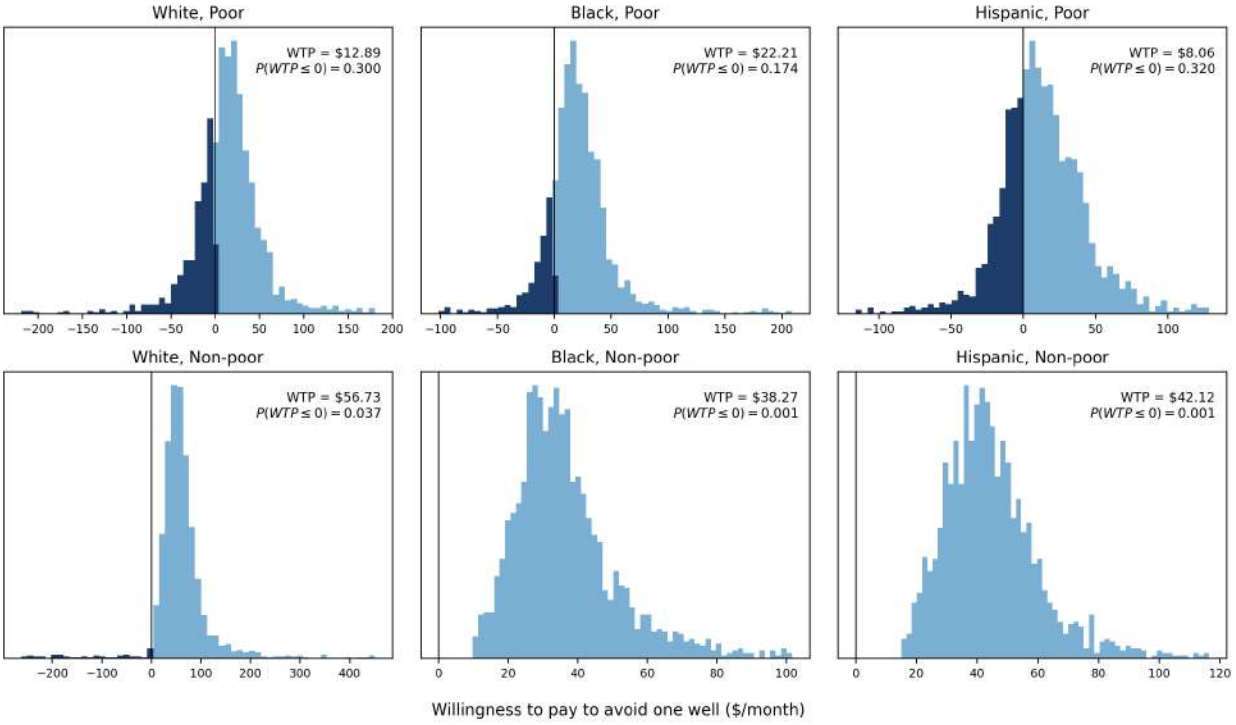
subdivision's centroid; 77 percent of leases naming a subdivision are matched. Averaging matched leases within tracts yields a tract-level mean royalty rate covering 419 tracts, with a county median of 24.6 percent; this is the rate schedule used in the operator value construction of Appendix F.2. Lease documents record royalty terms but not signing bonuses, which by convention are negotiated outside the recorded memorandum. [87]

G Additional Tables And Figures

[87] Timmins and Vissing (2022) observe bonus amounts for under one percent of their leases from voluntary reporting.



(a) WTP Distribution By Race



(b) WTP Distribution By Race and Poverty Status

Figure 14: Bootstrap Distributions of the Willingness to Pay

Notes: Each panel shows the distribution of the willingness to pay to avoid one additional well within one mile across 2,000 wild cluster bootstrap replications, computed as the ratio of the well coefficient to the rent coefficient on each replication. The annotation reports the point estimate from Table 4 and the share of replications at or below zero, shown in dark blue. The distributions are long tailed because the rent coefficient in the denominator is small relative to its sampling variation. Thus, the bootstrap distribution is shown directly rather than being summarized by a standard error.

Table 16: Welfare Impact of the Fort Worth Removal by 2014 Origin

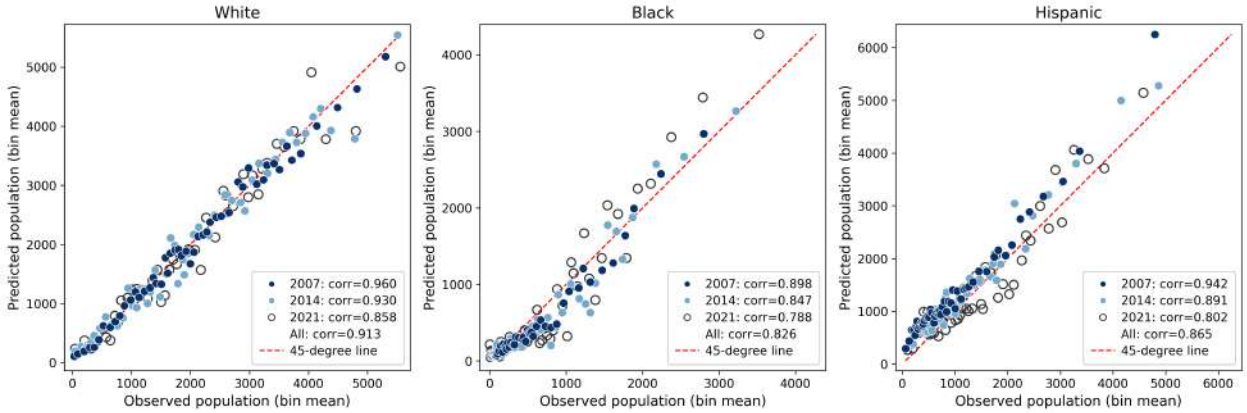
	Total	Treated	Untreated
Aggregate race			
White	19,418	23,027	17,791
Black	-2,188	-1,842	-2,535
Hispanic	-15,361	-15,911	-14,810
Race by poverty status			
White, poor	19,328	16,632	20,955
White, non-poor	23,342	29,340	20,797
Black, poor	14,794	14,559	15,152
Black, non-poor	-39	382	-405
Hispanic, poor	7,886	5,625	10,764
Hispanic, non-poor	-11,723	-11,138	-12,258

Notes: Lifetime present value in dollars per person. A census tract is treated if its well exposure falls under the removal. The population weights are fixed at the observed 2014 distribution. The upper panel is from the aggregate model that pools the poor and the non-poor residents within each race.

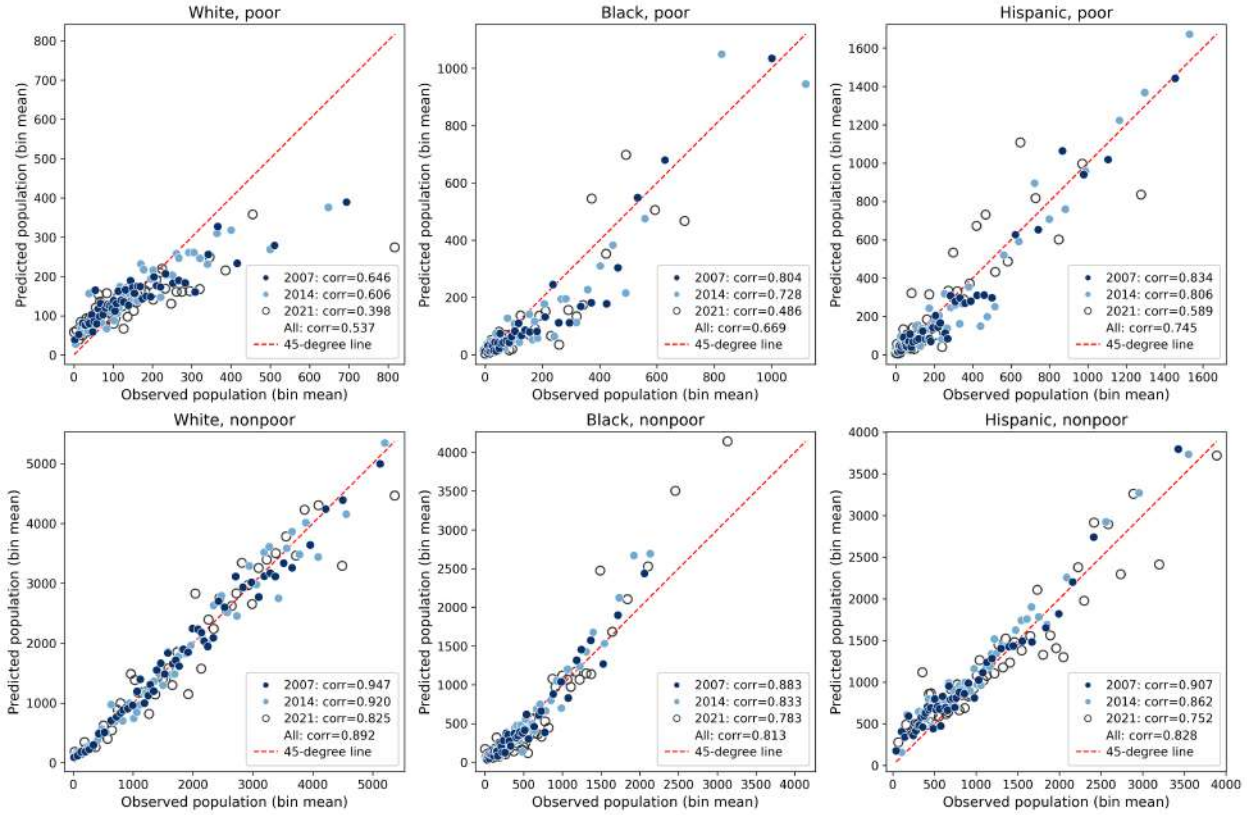
Table 17: Targeted Removal: Population Changes in the Target Tracts, 2021

Group	Baseline	Counterfactual	Change	Change (%)	Change, untreated
Poor White	4,657	4,514	−143	−3.06	+516
Non-poor White	19,487	21,170	+1,683	+8.64	−729
Poor Black	6,784	6,629	−155	−2.29	+768
Non-poor Black	15,175	16,820	+1,645	+10.84	−1,283
Poor Hispanic	21,809	20,458	−1,351	−6.19	+2,628
Non-poor Hispanic	89,770	94,332	+4,562	+5.08	−4,525

Notes: The first four columns report the population of the target tracts in 2021 in the observed and the counterfactual equilibrium, the change in persons, and the change as a percent of the baseline population. The last column reports the change in the group's population in the untreated tracts.



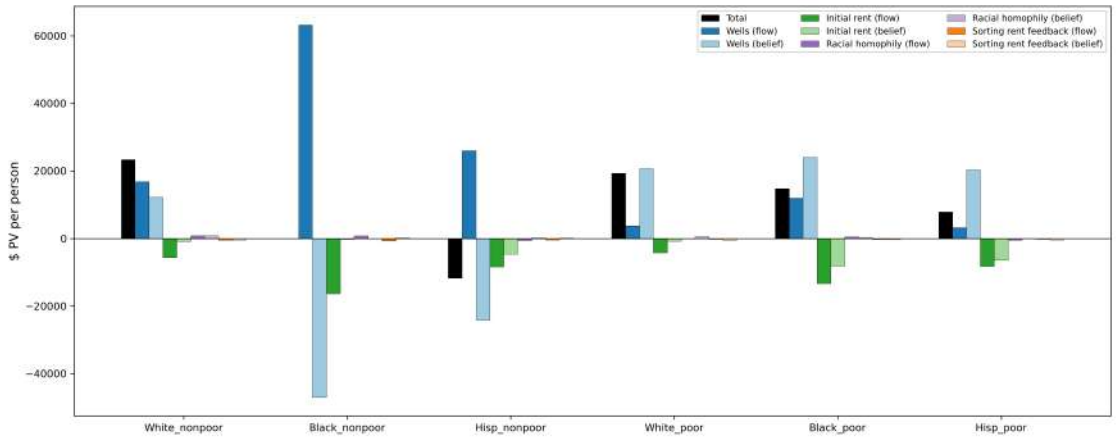
(a) Aggregate



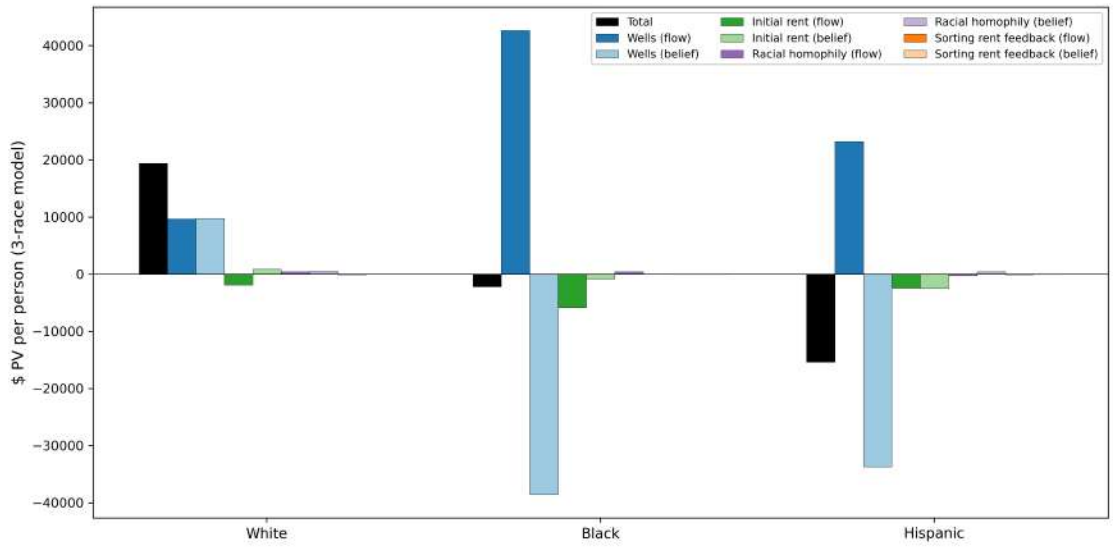
(b) Divided By Poverty Status

Figure 15: Predicted Population By Observed Neighborhood Characteristics

Notes: Each panel plots the model-predicted population (setting $\xi_{jt} = 0$) against the observed population by census tract. Observations are grouped into 50 equal-count bins based on observed population, and each marker shows the within-bin means of the observed and predicted values. The legend reports the correlation between predicted and observed populations by period and pooled across periods, calculated on the underlying tract-level data, not the binned means. The dashed line is the 45-degree line, which serves as a benchmark for a perfect fit. Panel (b) splits each racial group by poverty status.



(a) Race-by-poverty model



(b) Aggregate three-race model

Figure 16: Eight-Channel Welfare Decomposition, Fort Worth Removal

Notes: Lifetime present value in dollars per person, with the population weights fixed at the observed 2014 distribution. Panel (b) is from the aggregate model that pools the poor and the non-poor residents within each race.

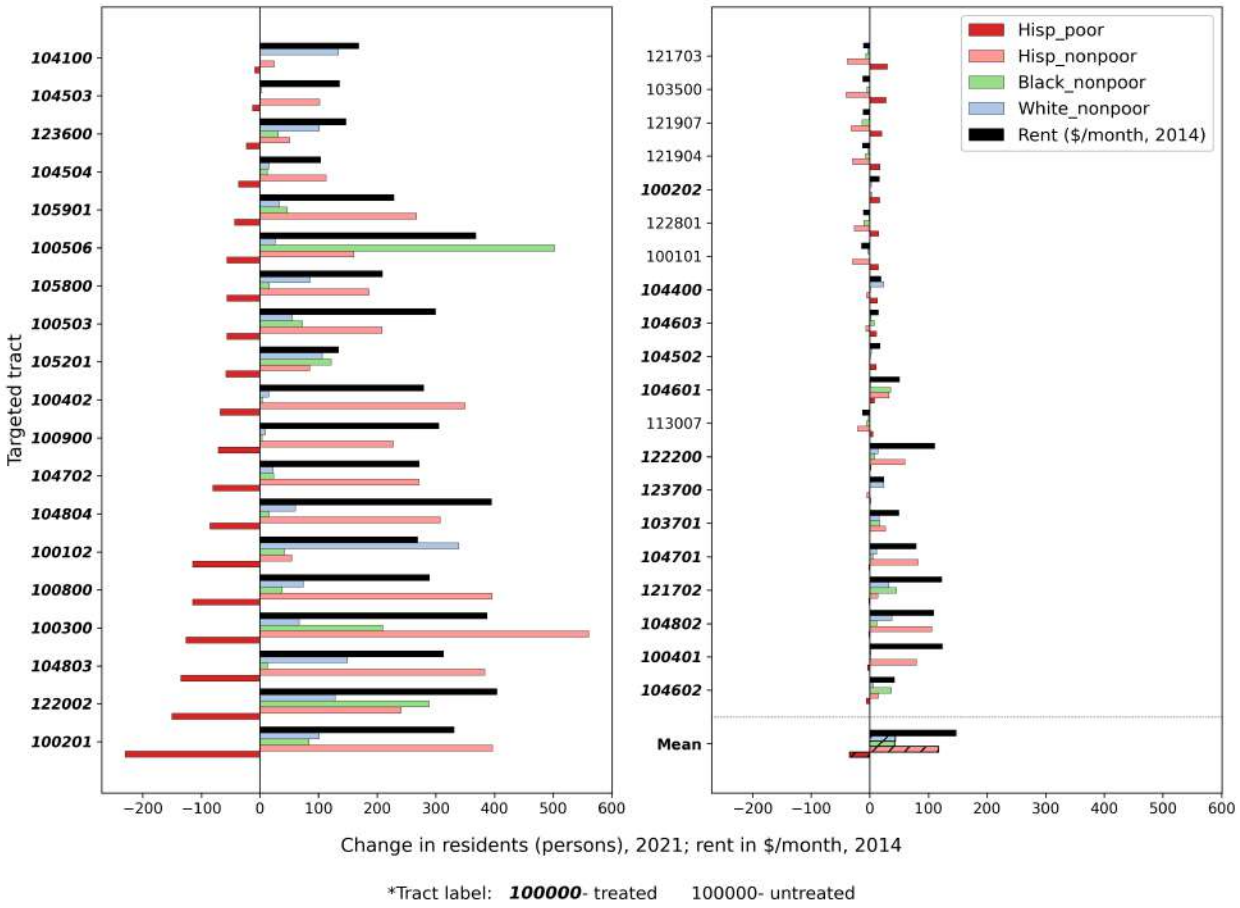


Figure 17: Targeted Removal: Change in Residents and Rent by Target Tract

Notes: Each cluster of bars shows the change in the number of residents by group in a target tract in 2021, with the change in the 2014 equilibrium monthly rent in black. Tracts are sorted by the size of the poor Hispanic net outflow. The bottom cluster of the right panel shows the mean across the target tracts. Treated-tract labels appear in bold italic.

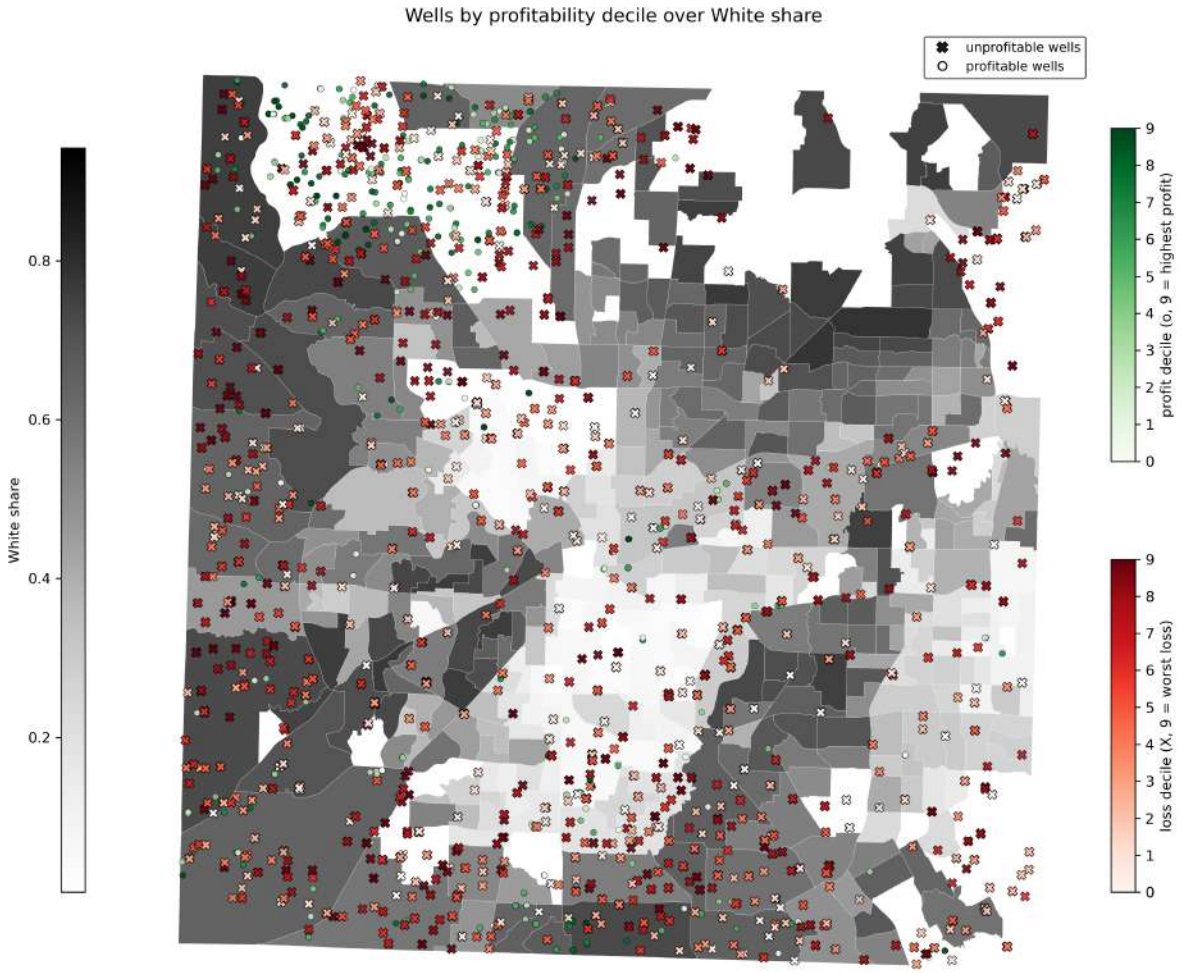


Figure 18: Well Profitability and Neighborhood Demographic Composition

Notes: Census tracts are shaded by the White population share. Circles denote profitable wells and crosses denote under-performing wells. Among profitable wells, darker green indicates a higher realized-profit decile. Among under-performing wells, darker red indicates a larger realized loss.